CRITICAL ROLE OF SUPEROXIDE PRODUCTION IN THE PATHOGENESIS OF AUTOIMMUNE DIABETES

by

Terri Christine Thayer

B.A. in Biology, Alfred University, 2005

Submitted to the Graduate Faculty of

The School of Medicine in partial fulfillment

of the requirements for the degree of

Doctor of Philosophy

University of Pittsburgh

2010

UNIVERSITY OF PITTSBURGH

FACULTY OF SCHOOL OF MEDICINE

This dissertation was presented

by

Terri Christine Thayer

It was defended on

October 13, 2010

and approved by

Bruce Freeman, Ph.D.
Professor and Chair of Pharmacology and Chemical Biology

Jay Kolls, M.D.
Professor of Genetics and Pediatrics, Louisiana State University School of Medicine
Adjunct Professor of Immunology and Pediatrics, University of Pittsburgh School of Medicine

William Ridgway, M.D.
Professor and Director of Immunology, Allergy and Rheumatology, University of Cincinnati College of Medicine

Massimo Trucco, M.D.
Professor of Pediatrics, Epidemiology, Genetics, and Immunology

Clayton E. Mathews, Ph.D, Chair
Associate Professor of Pathology, Immunology and Laboratory Medicine, University of Florida College of Medicine

Copyright © by Terri C. Thayer

2010

CRITICAL ROLE OF SUPEROXIDE PRODUCTION IN THE INITIATION AND PATHOGENESIS OF AUTOIMMUNE DIABETES

Terri C. Thayer, PhD

University of Pittsburgh, 2010

Type 1 diabetes (T1D), a disease characterized by the autoimmune-mediated destruction of the insulin-secreting beta cells of the pancreas, affects approximately 1% of the US population, with an incidence that is increasing at a rate of 3% per year. Beta cell killing is accomplished through various immune-mediated mechanisms, with the production of reactive oxygen species (ROS) contributing to both inflammation and cell death. While previous reports suggested that antioxidant scavenging protected beta cells against ROS-mediated damage, islet-specific over-expression of antioxidants was not fully protective. As systemic elevation in free radical defenses had a positive impact on islet survival, I hypothesize that control of oxidative stress at the level of the immune system will regulate proinflammatory responses.

Genetic studies using the ALR mouse have provided strong support for my hypothesis. ALR-derived diabetes resistance and reduced oxidative burst from neutrophils and macrophages, as well as elevated Superoxide Dismutase 1 (SOD1) activity all map to the *Suppressor of superoxide production (Susp)* locus on Chr. 3. NAPDH oxidase (NOX) function from ALR cells could be rescued with inhibition of SOD1, demonstrating that dissipation was modifying immune effector function. Elevated SOD1 activity was associated with increased dimer stability, suggesting a post-translational modification is enhancing dimerization.

Introduction of *Susp* into the NOD background was highly protective against T1D. This resistance is linked to the loss of T lymphocyte diabetogenic potential. The loss of T cell

ROS in T1D protection was confirmed using NOX-deficient NOD mice. T cell lineage commitment and proinflammatory cytokine synthesis were dependent on ROS signaling. Macrophages and T cells from NOD-*Ncf1*^{m1J} mice exhibited a skewed cytokine response, with increased synthesis of IL-17 and IL-10, as opposed to the predominant IFN-γ production typically observed from NOD lymphocytes.

Genome-wide analyses were performed to fine map *Susp* in order to define the mechanism leading to altered SOD1 activity. Positional cloning experiments mapped *Susp* between *D3Mit180* (34.4 Mbp) and *D3Mit223* (34.8 Mbp) on Chr. 3. This mapping defines a novel candidate region involved in the regulation of SOD1 activity and dimerization stability, resulting in reduced superoxide release via NADPH oxidase activity.

TABLE OF CONTENTS

PREFACE ..... **XVI**

1.0 INTRODUCTION **1**

1.1 TYPE 1 DIABETES **2**

1.1.1 Autoimmune pathogenesis **2**

1.1.2 Mouse Model: Non-obese Diabetic **3**

1.1.3 Innate Immune System **4**

1.1.4 Adaptive immune effectors **5**

1.1.5 Genetics of T1D **12**

1.2 REACTIVE OXYGEN SPECIES **15**

1.2.1 NADPH oxidase **16**

1.2.2 ROS and inflammation **19**

1.2.3 ROS as signaling molecules **21**

1.2.4 Antioxidant therapy for T1D protection **24**

1.2.5 The ALR Mouse **25**

2.0 ALR-DERIVED CHROMOSOME 3 *SUPPRESSOR OF SUPEROXIDE PRODUCTION* DOMINANTLY PREVENTS TYPE 1 DIABETES AND INSULITIS **28**

2.1 ABSTRACT **28**

2.2 INTRODUCTION **30**

2.3 METHODS 31

2.3.1 Animals 31

2.3.2 Materials 32

2.3.3 Gene expression analysis 33

2.3.4 Sequencing of *Sod1* 33

2.3.5 Assessment of SOD1 activity 34

2.3.6 Evaluation of SOD1 stability 35

2.3.7 Cytochrome c measurement of oxidative burst 35

2.3.8 Measurement of oxygen consumption 36

2.3.9 Spontaneous incidence 36

2.3.10 Islet isolation and culture with cytokines 37

2.3.11 Transfer of AI4 splenocytes 37

2.3.12 Flow cytometric analysis of oxidative burst 37

2.3.13 Determination of anti-CD3 induced ROS generation in purified $CD4^+$ T cells 38

2.3.14 Adoptive transfer of purified T cells from NOD and NOD-*Susp* 38

2.3.15 Flow cytometry 39

2.3.16 Statistics 39

2.4 RESULTS 40

2.4.1 No difference in ALR SOD1 cDNA, expression, or content; however increase dimer stability is linked with elevated antioxidant activity and maps to the *Susp* interval. 40

2.4.2 Elevated SOD1 is reducing superoxide release after stimulation of bone marrow populations. 42

2.4.3 ALR Chr. 3 genomic contributions dominantly protect from overt diabetes and insulitis. 44

2.4.4 NOD-*Susp* islets are not fully protected from proinflammatory-mediated damage 45

2.4.5 NOD-*Susp* mice exhibit ALR-like elevation in SOD1 activity and reduction of NOX oxidative burst. 48

2.4.6 $CD4^+$ and $CD8^+$ T cells from NOD-*Susp* lose diabetogenic potential 48

2.5 DISCUSSION 51

3.0 SUPEROXIDE PRODUCTION IS CRITICAL FOR THE INDUCTION OF AUTOREACTIVITY AND T1D 55

3.1 ABSTRACT 55

3.2 INTRODUCTION 56

3.3 METHODS 58

3.3.1 Animals 58

3.3.2 Materials 59

3.3.3 Construction of the B6-$H2^{g7}$-$Ncf1^{m1J}$ and NOD.$Ncf1^{m1J}$ mouse strains . 59

3.3.4 Measurement of superoxide production 60

3.3.5 Measurement of oxygen consumption 60

3.3.6 Western immunoblotting 61

3.3.7 Spontaneous incidence 61

3.3.8 Islet isolation and culture with cytokines 62

3.3.9 Transfer of AI4 splenocytes 62

3.3.10 Transfer of BDC-2.5 T cell clones 62

3.3.11 Adoptive transfer 63

3.3.12 Antibody depletion studies 63

3.3.13 Flow cytometry 64

3.3.14 Statistics 64

3.4 RESULTS 64

3.4.1 *Ncf1* mutation ablates NOX superoxide production from bone marrow populations 64

3.4.2 *Ncf1* mutation ablates respiratory burst from T cells 68

3.4.3 Genetic ablation of NOX activity protects NOD congenic mice from T1D onset 69

3.4.4 Islets from NOD-*Ncf1*^{m1J} mice exhibit no enhanced protection against proinflammatory cytokine toxicity 71

3.4.5 NOD-*Ncf1*^{m1J} mice are fully susceptible to AI4 T cell transfer 73

3.4.6 NOD-*Ncf1*^{m1J} mice are resistant to BDC-2.5 T cell transfer 73

3.4.7 Macrophages are essential while neutrophils superfluous for type 1 diabetes pathogenesis 75

3.4.8 Delayed transfer of diabetes with NOD-*Ncf1*^{m1J} splenocytes and purified CD4^{+} and CD8^{+} T cells 77

3.5 DISCUSSION 79

4.0 NADPH OXIDASE DEFICIENCY REGULATES T HELPER LINEAGE COMMITMENT AND AUTOIMMUNITY 83

4.1 ABSTRACT 83

4.2 INTRODUCTION 84

4.3 METHODS 86

4.3.1 Animals 86

4.3.2 Materials 86

4.3.3 Flow cytometry 87

4.3.4 Measurement of intracellular ROS by flow cytometry 87

4.3.5 Isolation of mouse bone marrow-derived macrophages 88

4.3.6 Plate bound anti-CD3 and anti-CD28 activation of purified $CD4^+$ T cell and cell lysates 88

4.3.7 Cytokine measurements by ELISA and Luminex 89

4.3.8 qRT-PCR 89

4.3.9 Immunization of mice, antigen-recall and criss-cross assays 89

4.3.10 Intracellular cytokine staining 90

4.3.11 Western immunoblotting 91

4.3.12 Induction of EAE 91

4.3.13 Statistical analysis 91

4.4 RESULTS 92

4.4.1 NOD-*Ncf1*^{m1J} T cells exhibit a skewed cytokine response from Th1- to a Th17-like phenotype 92

4.4.2 NOD.*Ncf1*^{m1J} macrophages exhibit a decrease in pro-inflammatory cytokine and chemokine synthesis after innate immune activation 98

4.4.3 Modulation of superoxide alters Th17 and Th1 cytokine responses after immunization 101

4.4.4 NOD and NOD.*Ncf1*^{m1J} mice do not differ in levels of T Regulatory (Treg) Cells 103

4.4.5 NOD.*Ncf1*^{m1J} mice exhibit enhanced sensitivity to MOG_{35-55}-induced Experimental Allergic Encephalomyelitis (EAE) 104

4.5 DISCUSSION 105

5.0 FINE MAPPING OF ALR-DERIVED *SUPPRESSOR OF SUPEROXIDE PRODUCTION* LOCUS ON CHROMOSOME 3 110

5.1 ABSTRACT 110

5.2 INTRODUCTION 111

5.3 METHODS 113

5.3.1 Animals 113

5.3.2 Materials 114

5.3.3 Assessment of SOD1 activity 114

5.3.4 Flow cytometric analysis of oxidative burst 114

5.3.5 Genome Wide Scan using single nucleotide polymorphisms 115

5.3.6 Candidate gene expression analysis 115

5.3.7 Cytochrome c measurement of oxidative burst 116

5.3.8 Statistics 116

5.4 RESULTS 116

5.4.1 Genetic analysis and fine mapping of *Susp* locus on Chr. 3 116

5.4.2 Evaluation of genes within the *Susp* interval 123

5.4.3 Assessment of respiratory burst in $SOD^{-/-}$ mice 124

5.5 DISCUSSION 125

6.0 CONCLUSION AND SIGNIFICANCE 128

BIBLIOGRAPHY 132

LIST OF TABLES

Table 1. NOD-*Ncf1m1J* mice exhibit enhanced susceptibility to EAE 104

Table 2: Linkage of SNP and microsatellites in [ALRx(ALRxCAST)F1]BC1 mice 120

LIST OF FIGURES

Figure 1. Free Radical Production is an important contributor to beta cell death 21

Figure 2: Increased dimer stability is a feature of the ALR SOD1 isoform 41

Figure 3: Elevated SOD1 activity is reducing release of superoxide by stimulated bone marrow cells in ALR 44

Figure 4: ALR Chr. 3 genome dominantly protects from T1D and insulitis 45

Figure 5: Susceptibility of islets to proinflammatory mediators 47

Figure 6: NOD-*Susp* congenic mice exhibit reduced oxidative burst..... 48

Figure 7: NOD-*Susp* immune system fails to transfer T1D to immune deficient hosts..... 50

Figure 8: *Ncf1*^{m1J} mutation decreases the respiratory burst. 67

Figure 9: *Ncf1*^{m1J} mutation decreases the respiratory burst capacity splenic T cells without decreasing the percentage of cells..... 68

Figure 10: NOD-*Ncf1*^{m1J} mice resist spontaneous diabetes 70

Figure 11: Cultured islets from NOD.*Rag* and NOD-*Ncf1*^{m1J} mice were treated with cytokines IFN-γ, IL-1β, and TNF-α. 72

Figure 12: AI4 transgenic T cells, but not BDC-2.5 cells are able to induce diabetes in NOX-deficient mice..... 74

Figure 13 Macrophages but not neutrophils are critical for type 1 diabetes induction..... 76

Figure 14: The NOX-deficient NOD-*Ncf1*^{m1J} immune system has a reduced capacity to transfer type 1 diabetes to immune deficient hosts. 78

Figure 15: Anti-CD3 and anti-CD28 stimulation of NOD-*Ncf1*^{m1J} T cells exhibits a decrease in Th1 cytokine profile concomitant with an increase in Th17 cytokine synthesis 95

Figure 16: NOD-*Ncf1*^{m1J} naïve CD4^{+}CD62L^{+} T cells exhibit a Th17 cytokine profile after polyclonal stimulation..... 96

Figure 17: NOD-*Ncf1*^{m1J} T cells do not express Th1 lineage-specific transcription factors upon polyclonal stimulation..... 97

Figure 18: NOD.*Ncf1*^{m1J} macrophages exhibit a skewed Th1 to Th17 pro-inflammatory cytokine response after LPS-stimulation. 100

Figure 19: NOD-*Ncf1*^{m1J} mice exhibit both Th17 and Th1 T cell responses after HEL immunization 102

Figure 20: NOD mice with *Ncf1*^{m1J} mutation do not have increased numbers of Treg cells 103

Figure 21: Fine Mapping of NOD-*Susp* and ALR.NODc3 recombinant congenic mice 118

Figure 22: Diversity array of Single Nucleotide Polymorphisms (SNP) across Chr. 3 comparing ALR to CAST and NOD. 119

Figure 23: Phenotypic profile of CAST mice 120

Figure 24: Map position of ALR-derived *Susp* locus on Chr. 3 123

Figure 25: Superoxide release after KCN inhibition of SOD1 and PMA stimulation..... 124

Figure 26: Schematic of proposed model of *Susp* contributions to free radical dissipation, redox signaling, and immune cell function. 127

PREFACE

The completion of this dissertation would not have been possible if not for many people in my life. First off, I want to thank my family, Mom, Dad, Joe, and Scott. These are the people that have always supported, encouraged, and believed in me and my goals, pushing me to exceed my potential. I am always amazed and challenged at their generosity and how easily they sacrifice for others. Special thanks to my grandma, Christine Jerome, whose ever growing pride has encouraged me to do more.

It has been a blessing to have a partner to share in this accomplishment. My husband Dan is a constant source of love, compassion, support, and patience. From driving me to work and doctor's appointments, giving chocolate when it was needed, to providing a listening ear and excellent editing/proof reading assistance, Dan has been there every step of the way through my accomplishments and struggles. His help and "jokes" have made life that much more enjoyable. I can't imagine a day without being by his side and look forward to all the adventures we will share in the future.

I also have to thank my best friend, Aaron Gusdon. Aaron was a constant support and resource in the lab, teaching me everything I know about biochemistry and molecular biology, assisting in experiments and data discussion. We also had a lot of fun working together, always finding something to laugh about. We have far too much in common. He and I could talk about

everything from science and medicine, to TV and music. Aaron is a brilliant scientist and will be an amazing physician in the near future.

There probably isn't enough I can do to thank my mentor, Dr. Clayton Mathews. He took a chance on me, welcoming me to his lab in Pittsburgh and then in Florida. He has provided me with the education and the laboratory skills to advance this research, always pushing me to be better. These projects also would not be possible without my other mentors, Dr. Jon Piganelli and Dr. Hubert Tse. I wouldn't have been at Pitt if not for Dr. Piganelli. He interviewed me when I applied and showed me what Pitt had to offer in the areas of Immunology and Diabetes research. Once there, he always looked out for me, providing guidance and support. He has been an amazing teacher. I worked very closely with Hubert, as he was willing to let this naïve girl help out on a project. He taught me pretty much every immunological technique; always patient teaching me along the way. Not only have I been lucky to have had such great teachers but also great friends.

I would like to acknowledge the members of the Mathews Lab: Jeff Baust, Jing Chen, Vadim Pliner, Mani Annamalai, Yaíma Luzardo Lightfoot, and Meredith Campbell. They have all provided expert technical assistance in various ways, as well as providing a wonderful environment to work in every day. Yaíma has been the other grad student, able to share in the joys and grief of still being in school. She also has cute puppies we can talk about everyday. Meredith was an undergraduate student at UF that worked under my direction. She provided excellent assistance in genotyping and phenotyping with the large quantity of backcross mice. It's been a joy to watch her learn and blossom in the lab. I wish her all the best at medical school and know she will successfully change medicine for the better.

Lastly and most importantly, I'd like to thank my thesis committee members, Dr. Mathews, Dr. Bruce Freeman, Dr. Jay Kolls, Dr. Bill Ridgway, and Dr. Massimo Trucco. They have taken the responsibility to encourage, critique, and support my work. They have all served as amazing resources to strengthen and enrich the quality of my research in the areas of biochemistry, genetics, immunology, diabetes, and medicine. For this I am extremely grateful.

1.0 INTRODUCTION

The pancreas has important functions in the digestive and endocrine systems through the release of digestive enzymes and hormones, respectively. The hormone synthesizing cells, including insulin-producing beta cells, are organized within the islets of Langerhans along with glucagon-producing alpha cells, somatostatin-secreting delta, and pancreatic polypeptide-secreting gamma cells. Human islets are composed predominantly of alpha and beta cells, in similar number, whereas rodent islets contain mostly beta cells. The main function of the pancreatic islets is the regulation of blood glucose, and insulin plays a major role in this process. Insulin, a 6 Kd hormone composed of two chains linked by disulfide bridges, is secreted in response to rising concentrations of glucose in the blood. As glucose concentrations rise in the blood, they also increase in the interstitial fluid, leading to glucose transport into the beta cells via Glucose Transporter 2 (Glut2). Catabolism of glucose metabolism inside the beta cell increases the ATP/ADP ratio. To adjust to this increase in ATP, potassium channels close, depolarizing the plasma membrane and in turn opening calcium channels. Calcium flux then allows for the fusion of secretory granules with the plasma membrane, releasing insulin into circulation (1-3). Once in circulation, insulin signals for the uptake of glucose by muscle and fat cells. The binding of insulin to the insulin receptor initiates a signal cascade, which includes translocation of Glucose Transporter 4 (Glut4) to the membrane of muscle cells and adipocytes to facilitate glucose uptake. In conditions where there is a lack of insulin or improper signaling

from the insulin receptor, glucose uptake and metabolism are not regulated, resulting in hyperglycemia and overt diabetes.

1.1 TYPE 1 DIABETES

1.1.1 Autoimmune pathogenesis

Diabetes Mellitus is a collection of syndromes characterized by the inability to regulate blood glucose, resulting from any dysfunction in insulin processing, secretion, and/or signaling. Type 1A Diabetes (T1D), or juvenile diabetes, is an autoimmune disease characterized by the targeted destruction of insulin-producing beta cells, resulting in hyperglycemia, other metabolic disturbances, and dependency on exogenous insulin (4). In animal models, leukocytic infiltration of the pancreatic islets is witnessed as part of the early stages of disease (5-7). Present within the insulitic infiltration are macrophages, dendritic cells, T cell subsets and B cells; these cell types are implicated in the autoimmune process and associated complications in varying capacity.

Critical information has been derived from the study of organs procured from deceased human T1D patients. The insulitic infiltrates of cadaveric pancreata demonstrate the presence of $CD8^+$ cytotoxic T lymphocytes, macrophages, B cells, and $CD4^+$ helper T cells (7). In recent onset cases in which insulitis was present, infiltrates affected insulin-positive islets as opposed to insulin-deficient endocrine clusters (8). Analysis of beta and alpha cells shows only significant decreases of beta cells, with persisting insulitis and increased expression of MHC I and Fas (9). These data support the hypothesis that specific immune reactivity to beta cell antigens is central

to diabetes progression. However, even with newer programs, such as the Network for Pancreatic Organ Donors with Diabetes (nPOD), human samples have been scarce; therefore, much of the knowledge delineating the pathogenesis of T1D has been extrapolated from studies using NOD mice.

1.1.2 Mouse Model: Non-obese Diabetic

Animal models have been fundamental to T1D research. Mouse models, specifically the autoimmune diabetes-prone Non-obese Diabetic (NOD) mouse, have played an increasing role in the discovery of disease mechanisms, identification of autoantigens, and the development of a better understanding of the genetic pathogenesis of T1D.

The NOD strain was originally outbred from the Jc1:ICR mouse line during the selection of a cataract-prone strain with high fasting blood glucose. During this process, a female mouse spontaneously developed diabetes. Inbreeding of the offspring proceeded, developing a sub-line that developed a spontaneous diabetic condition (10, 11). Diabetes onset in NOD female mice manifests between 12-24 weeks of age, with approximately 80% of the females developing the disease. The NOD mouse strain is an extremely important animal model for T1D research, as this mouse stands as a surrogate for studies that are too invasive for clinical research.

With its pathogenic and genetic similarities to the human condition, the NOD is a useful tool to study the etiology, pathology, and progression of disease. While the NOD model is not without fault (12-14), the NOD is particularly useful in that it facilitates the isolation, study, and manipulation of specific genes, polymorphisms, and other genetic factors to identify not only how a specific gene may function deleteriously, but also to understand how specific

combinations of normal alleles result in immune dysregulation and autoimmune disease (12, 15-17).

1.1.3 Innate Immune System

The first line of defense against infection is provided by cells of the innate immune system, based on pattern recognition. Neutrophils, members of the polymorphonuclear (PMN) cell family that are distinguished by multi-lobed nuclei, are early responders to infection, as they are rapidly mobilized and activated (18). Following chemotactic signals, including interleukin (IL)-8 and interferon (IFN)-γ, neutrophils migrate to the site of inflammation within the first hour of infection, making them early contributors to acute inflammation and host defense responses (19-21). Antimicrobial functions of these cells involve phagocytosis followed by the release of reactive oxygen species (ROS) and hydrolytic enzymes (22). Macrophages are also phagocytes; however, they also serve as important antigen presenting cells (APC). Macrophages, along with dendritic cells (DC) and B cells, present antigen to and recruit adaptive immune lymphocytes. Through the secretion of cytokines and chemokines, these cells regulate the inflammatory processes (23-25).

Innate immune cells, including DC and macrophages, are critical for initiating the process of beta cell death during T1D. DC and macrophages are found in insulitic infiltrates and are implicated in driving early autoreactive immune responses (26). The depletion of macrophages protects NOD mice from T1D and insulitis (27). T cells from a macrophage-deficient environment lack diabetogenic potential, yet islet reactivity is restored when macrophages are replenished (28), demonstrating an essential role of macrophages in T1D development and pathogenesis. As well, DCs are critical for the initiation of T cell responses or induction of

tolerance, depending on the DC subset and T cell requirement (29-31). Antigen presentation by DC and macrophages provides antigen-specific activation of T cells (32, 33). The activation status of the APC, ROS signaling, and cytokine/chemokine milieu at the site of infection are all proposed to dictate signaling and differentiation of T cells. These factors determine the type of response: effector, pathogenic, or tolerogenic (33, 34). Activated T cell effectors produce proinflammatory cytokines, which may also facilitate further recruitment and activation of macrophages and neutrophils. These cytokines stimulate ROS production by macrophages, leading to the amplification of the inflammatory response subsequently mediated by adaptive immune cells (35, 36). Therefore, complex interplay of the innate and adaptive immune systems can promote either pathogenic or tolerogenic responses. These interactions are potential targets for therapies aimed at preventing T1D. It has been proposed that T1D in the mouse and human develops due to a break in or lack of tolerance resulting from poor APC function. Clinical trials are currently underway to investigate the safety and potential of DC therapy to promote tolerance or enhanced regulation of self-reactive T cells in human cohorts (37).

1.1.4 Adaptive immune effectors

Adaptive immune cells, specifically T lymphocytes, are implicated as the final effectors of beta cell death resulting in overt diabetes. T cells recognize specific peptide antigens when presented in the context of Major Histocompatibility Complex (MHC) molecules. This recognition is mediated by the T cell receptor (TCR). TCR chains are generated through the recombination of T cell receptor genes using variable alleles, creating an estimated 10^9 possible rearrangements for the TCR during T cell development in the thymus. This process of TCR gene recombination generates the immensely diverse repertoire needed to recognize and protect from

the variety of infections an individual may encounter. However, with great diversity comes the potential for recognition of self-peptides. During the maturation of T cells in the thymus, each cell undergoes positive and negative selection to MHC and antigen. Defects in negative selection are proposed to provide significant contributions to T1D susceptibility and development (38-40). Over 5,000 self-peptides are presented in the thymus, contributing to selection. The autoimmune regulator (AIRE) controls the wide range of genes expressed in the thymus (36, 39) and mutations in AIRE are associated with various autoimmune conditions, including T1D (39-41). Antigen is presented in the thymus and periphery in association with MHC. Polymorphisms in MHC are strongly associated with susceptibility in human and murine autoimmunity. As MHC molecules are important for T cell development and activation, the susceptibility or resistance alleles are proposed to influence thymic selection as well as tolerance in the periphery (36).

T cell activation occurs in response to specific antigen presentation and co-stimulation through the engagement of MHC/TCR and B7/CD28, respectively. Autoreactive responses of $CD4^+$ and $CD8^+$ T cells to islet antigen have been implicated in the pathogenesis of diabetes in humans and NOD mouse models. Diabetic patients and first-degree relatives are screened for autoantibodies against islet beta cell antigens, including insulin, glutamic acid decarboxylase (GAD) 65, islet cell antigen (ICA) 69, and insulinoma-associated-2 (IA-2A). The diabetogenic potential of these antigens has been established in NOD mice. T cells from NOD mice respond to GAD65 (42, 43), demonstrating immune recognition and activation. The injection of GAD65 peptides can alter disease, depending on the site and timing of injection (44). Vaccination with GAD65 peptides, proteins, and DNA encoding GAD65 reduces T1D incidence in NOD mice (45, 46). However, GAD65-deficient NOD mice are not protected from disease, and NOD mice

over-expressing GAD65 in the pancreatic islets do not exhibit exacerbated disease (reviewed in (47)). These data demonstrate the diabetogenic potential of GAD65, yet expression and reactivity is not essential, suggesting that it is one of several autoantigens.

Insulin has also been studied and described as a significant autoantigen in T1D (reviewed in (48)). T cells are present in islet infiltrates in the NOD and have been shown to react to the insulin B-chain (49). Expression of insulin B-chain in the thymus can reduce T1D incidence (50), demonstrating a role for islet antigen expression during negative selection. Additionally, knockout of *Ins2* on a mixed 129/B6 background, which has a protective $H2^b$ MHC allele, was sufficient to induce anti-insulin autoimmunity (51). Similarly, human patients with the susceptibility allele in the variable number tandem repeat (VNTR) element of the insulin gene promoter show decreased expression of insulin in the thymus and increased susceptibility to T1D (52, 53). These data demonstrate both the importance of thymic selection and that a defect in elimination of autoreactive TCR contributes to T1D. Increased thymic expression of insulin mRNA was linked with individuals that had protective alleles at the INS locus (52, 54). Using genetically manipulated NOD mice, insulin expression in the thymus has been both increased and deleted, resulting in altered T cell insulin autoreactivity, demonstrating that the natural levels of thymic insulin expression are important in the development of the TCR repertoire. Altered thymic INS expression in patients or animals models with T1D likely results in changes in the deletion of insulin-specific autoreactive T cells (55-57). The specific knock out of insulin expression in the thymus induced diabetes in NOD background as early as 3 weeks of age, demonstrating a critical loss of tolerance resulting from a lack of negative selection (51). PTPN22, a negative regulator of T cell activation (58, 59), is associated with T1D (60, 61), as well as other autoimmune diseases (61, 62). Studies using NOD congenics for PTPN22

orthologue, *Ptpn8*, showed modified incidence of T1D, demonstrating a role for PTPN22 in human and murine T1D (16).

The recruitment and activation of T cells is dependent on the presentation of antigen/MHC complexes by APC. Through the use of NOD TCR transgenic mice, the importance of antigen/MHC presentation to islet-specific T cells in the pancreatic lymph nodes (PLN) has been demonstrated (63). It is proposed that initial beta cell damage releases autoantigens, which are then processed and presented to T cells in the PLN (64). Antigen is proposed to be available between 15 and 18 days of age in the NOD (63, 64), which was associated with an increase in activated T cells (65). Early removal of PLNs can protect from T1D development, whereas late removal does not alter the course of T1D (65), suggesting the importance of early recruitment and priming of diabetogenic T cells in the PLNs. Islets express lymphocyte alpha4beta7 integrin and endothelial mucosal addressin cell adhesion molecule-1 (MAdCAM-1) which are both important for lymphocyte trafficking to mucosal lymphoid tissues, including the pancreas (66). The blockade of beta7 integrin or MAdCAM-1 with monoclonal antibodies significantly protected NOD mice from diabetes onset and insulitis, demonstrating a tissue-specific role for alpha4beta7 and MAdCAM-1 for lymphocyte migration to the pancreas (67).

After activation and homing to the site of inflammation, the pancreatic islets, effector T cells amplify the immune response and mediate beta cell killing through various mechanisms. $CD8^+$ T cell destruction of islets has been implicated in providing early release of antigen to prime and activate $CD4^+$ T cells (68). $CD8^+$ Cytotoxic T cells (CTL) are present in pancreatic islets of both patients as well as NOD mice (69) and contribute to beta cell killing. NOD mice deficient in perforin or Fas are both protected from T1D development, demonstrating that these

are two pathways by which CTLs mediate beta cell death (70, 71). $CD8^+$ T cells from NOD mice transgenic for the 8.3-TCRβ chain with or without perforin can kill target cells that express Fas (72). In addition, islet grafts lacking Fas are also destroyed in NOD hosts (73). T cells from 8.3-NOD lacking perforin and/or Fas were able to mediate beta cell killing (74), demonstrating that CTLs have multiple cytotoxic mechanisms in their arsenal and will use any and all means necessary to accomplish beta cell killing.

$CD4^+$ T cells are involved in diabetes through the recruitment of $CD8^+$ T cells and B cells, as well as cytokine production. The accumulation of $CD8^+$ T cells in NOD islets requires $CD4^+$ T cells in 8.3-NOD mice (75). Likewise, the adoptive transfer of $CD8^+$ T cells alone does not transfer disease. The transfer of $CD4^+$ T cells from pre-diabetic donors is slower than transfer with diabetic donor cells, and pre-diabetic $CD4^+$ T cells do not transfer disease when recipients are treated with anti-CD8-depleting antibodies (76). These data highlight a role for exposure to beta cell antigen for diabetogenic potential, as well as the necessity of $CD4^+$ and $CD8^+$ T cells for disease initiation. Priming of $CD8^+$ T cells is provided by professional APC and not the beta cell. NOD mice deficient in Class I MHC on APC do not develop diabetes, and insulitis does not progress (77). B cells are recruited and activated to produce antibodies. They also serve as important APC (reviewed in (78)). The role of antibodies in the pathogenesis of T1D is not clear; titers are used to evaluate risk (79). Autoreactive B cells are hypothesized to present beta cell antigens to $CD4^+$ T cells (15).

The presentation of islet antigen to $CD4^+$ T cells elicits cytokine responses. The balance between $CD4^+$ T cell subsets has been suggested to be important for maintaining equilibrium between tolerance and autoimmunity. A primarily IFN-γ, Th1 proinflammatory response is pathogenic in T1D, while polarizing with IL-4 and IL-10 to a Th2 phenotype was protective (80-

82). Also, TGF-β expression was found to skew APC and T cells, promoting a Th2 phenotype and protecting against T1D (83). IL-10 was initially described as a regulatory cytokine, inhibiting IFN-γ (84, 85) and TNF-α production and activity (86), as well as antigen presentation (87) and monocyte cytokine production (88). IL-10 inhibits macrophage function by decreasing cytokine synthesis and nitric oxide (NO) production (85). Additionally, IL-10 exposure greatly affected the ability of macrophages to induce a Th1 response, suggesting IL-10 inhibition of macrophage APC function was indirectly suppressing Th1 function (85, 89).

Natural Killer (NK) T cells are thought to provide a regulatory role and modify T helper responses. NOD mice are shown to have a defect in NK T cells (90); transfer of NK T cells from (NOD x BALB)F1 donors can prevent T1D (91). Defects in NK T cell numbers are correlated with decreased IL-4 production. NOD mice compared to B6-$H2^{g7}$ mice show reduced IL-4 synthesis after anti-CD3 stimulation (91, 92), suggesting that NK T cells contribute to cytokine responses. IL-4 expression protected NOD yet enhanced T cell autoreactivity in BDC2.5-NOD mice (93). Treatment with recombinant IL-10 prevented disease when given systemically but was not protective when expressed in islets (94). These discrepancies may be due to redundancy and compensatory roles of these cytokines, as well as tissue- and antigen-specific influences on T cell function. Therapies to modulate T cell function, either by modifying activation or inducing regulation, have so far failed to translate to human trials (reviewed in (95)). Difficulties in translating therapies from mouse to man, including evaluation of biomarkers, dosage, and timeframe of administration, still need to be overcome. An important strategy for bridging the gap between mouse and human disease is the use of genetic tools to identify pathways and mutations that influence immune regulation, peripheral tolerance, and disease susceptibility.

B cells are important contributors to T1D development, producting islet-specific autoantibodies (96) and serving as potent APC. Genetic ablation of immunoglobulin in NOD-*Igμ*^{null} protects mice from T1D (97-99). However, while autoantibodies can induce beta cell damage *in vitro*, antibody administration fails to induce T1D in NOD-*Igμ*^{null} mice (100). B cells, expressing Class II MHC, are important APC, presenting antigen to CD4^{+} T cells. The importance of this interaction is highlighted in NOD-*Igμ*^{null} mice: CD4^{+} T cell reactivity to islet antigen is diminished when B cells are absent (100, 101). Specific knockout of MHC II from B cells alone also provides significant protection from T1D onset, further demonstrating an essential role for B cells as APC, initiating the aberrant T lymphocyte responses that mediate beta cell killing (102).

Selection mechanisms serve to delete or anergize B cells that recognize self-peptide; however, defects in selection may allow for the persistence of autoreactive B lymphocytes in the periphery. Genetic linkages have associated B cell defects with T1D susceptibility in the NOD mouse model. B cells from NOD mice are found to be hyperactive and resistant to activation-induced cell death (103). The Chromosome (Chr.) 4 linkage *Idd9/11* locus is associated with the decreased tolerance of NOD B cells (104). Identifying genetic control and, subsequently, pathways associated with B cell anergy may outline therapeutic targets for down-regulating autoimmune activation.

While T cells are implicated as the final effectors mediating beta cell destruction, antigen presentation is required for lymphocyte activation, and defects in APC function and tolerance induction are associated with diabetes susceptibility. Therefore, targeting APC function to promote tolerance and enhance regulation is a potential approach for T1D therapy. In fact, as mentioned above, clinical trials focusing on DC therapy are currently underway. B cells also

represent an essential pathogenic arm in autoimmunity. Targeting B cell depletion through the use of anti-CD20 rituximab antibodies is also in early trials. A potential drawback to rituximab therapy is the inability of the antibody to deplete marginal zone (MZ) B cells. In NOD mice there is an expansion of MZ B cells around the time of T1D onset and an accumulation of MZ-like B cells in the pancreatic lymph node (105), suggesting a pathogenic role in T1D. Additionally, MZ B cells are capable of presenting islet autoantigen to T cells (105), suggesting they serve as important APC. Defining signaling differences associated with the *Idd9/11* linkage may provide insight into the role of B cell anergy in T1D susceptibility/resistance. Targeting APC function of MZ B cells may provide the additional immune regulation required to delay or prevent the onset of T1D. Therefore, evaluating genes associated with risk in the NOD may also delineate the pathways associated with modified B cell anergy, T cell function, and T1D susceptibility.

1.1.5 Genetics of T1D

Type 1 diabetes is a polygenic disease, with over 50 genetic linkages associated with susceptibility or resistance. However, the linkage to HLA Class II [termed *Insulin-Dependent Diabetes Mellitus 1 (IDDM1*)] is by far the dominant susceptibility locus (106). DQB alleles with Ser, Ala, or Val at amino acid residue 57 are associated with T1D susceptibility, while those alleles containing an Asp residue are considered protective. It is believed that the non-Asp-containing alleles cause a local rearrangement within the peptide-binding site, altering the peptide-binding specificity (107). This mutation changes peptide alignment, altering T cell recognition and thymic selection (108). Likewise, susceptibility has been linked to specific

HLA-A and HLA-B Class I alleles (109); however, little is known about the role of the disease-associated variants in T1D.

Additionally, several non-HLA linkages have been identified. Genome-wide association studies (GWAS) have repeatedly associated INS [*IDDM2*], PTPN22 [*IDDM5*], and Cytotoxic T-Lymphocyte Antigen 4 (CTLA4) [*IDDM12*] with T1D (106). The INS locus contains a variable number of tandem repeats (VNTR) in the 5'-flanking region. VNTR class I alleles with 26 to 63 repeats are associated with recessive susceptibility, while the dominantly protective class III alleles have significantly more repeats. The allelic effects on insulin gene transcription can be measured both *in vitro* and *in vivo*. Class III alleles are proposed to induce higher thymic insulin expression and enhanced deletion of insulin reactive T cells (110).

In the late 1980s, the first genome-wide screens of the NOD mouse strain were executed with the goal of identifying disease susceptibility/resistance loci or *Idd (insulin dependent diabetes)* (17, 111). Over 30 linkages have been mapped in the mouse; however, only a few of the genes responsible have been identified. Similar to the human condition, the most significant associations are with the MHC alleles (17, 111-113). The NOD MHC class II molecules, I-A^{g7} (*H2-Aa*^{g7}), as well as the absence of *H2-Ea* expression, are critical for T1D development (95, 114). The *H2*^{g7} MHC haplotype of the NOD allele shares homology with the human T1D susceptibility HLA-DQB1 locus. DQB alleles with Ser, Ala, or Val at position 57 are associated with T1D susceptibility, and the NOD *H2-A*^{g7} also contains a non-aspartic residue at position 57 (115-117). Congenic replacement of the NOD *H2*^{g7} MHC haplotype with an alternative MHC haplotype, including the *H2*^{b} of C57BL/6 (B6), prevents insulitis and overt diabetes development in NOD congenic animals (114). These data demonstrate that alleles encoded within *H2*^{g7} are critical for T1D. However, the introduction of *H2*^{g7} on a B6 background does not induce T1D,

demonstrating that MHC alone is not sufficient to cause disease (114). Likewise, in human populations only a minority of individuals with risk-associated HLA alleles develop diabetes. Transgenic mice have also been instrumental in demonstrating the diabetogenic potential of human HLA genes (118). NOD mice transgenically expressing human risk HLA alleles, such as HLA-DR3 or DQ8, develop T1D. Susceptibility, however, was modulated with the co-expression of HLA-DR4 or DQ6 protective alleles, correlating with human epidemiological data (119, 120) and confirming the effect of HLA alleles on T1D susceptibility.

Additionally, NOD mice expressing HLA-A*0201 and a deletion of the murine MHC class I genes (NOD.HHD) have an accelerated form of T1D (121, 122). Class I alleles are associated with T1D in the mouse (123). A polymorphism found in the alloxan resistant (ALR) strain and the diabetes-resistant cataract Shionogi (CTS) strain creates a unique allele *H2-D*^{dx}. Introducing this allele to the NOD background significantly reduces T1D (124). Likewise, introduction of the MHC class I allele *H-2K*^{wm7} to the NOD background confers some protection (123). Analysis of the *H-2K*^{wm7} MHC molecule defined a single peptide specificity (125). This suggests that protection is afforded by the presentation of non-diabetogenic antigens rather than beta cell-specific antigen, due to higher affinity for a particular MHC allele. Other associated genes have been mapped in the NOD and associated with T1D susceptibility and resistance. A linkage on Chr. 1 mapped to the gene *Beta 2 microglobulin* (*B2m*), an important component of the HLA/MHC. Allele-associated risk was confirmed using transgenic rescue, demonstrating that the NOD allele provides dominant susceptibility (126).

Other polymorphisms have been associated with T1D in human patients and animal models, including mutations in *Nramp1*. While the polymorphism in the mouse is not identical to that in the human, the resulting sequence variations in both reduce expression and function of

the enzyme. Using NOD models, including a novel RNA interference transgenic NOD for *Nramp1*, it was demonstrated that knockdown of *Nramp1* was protective from T1D (127) and that the role of this enzyme was to alter processing and presentation of pancreatic islet antigens (128). Another important mutation associated with risk in human and mouse is a single nucleotide polymorphism in *mt-ND2* and *mt-Nd2*, respectively. In both the human and mouse there is a C to A nucleotide substitution, resulting in a leucine to methionine amino acid substitution (129, 130), a mutation differentiating the NOD and ALR mouse strains. The protective allele present in the ALR mitochondrial genome suppresses mitochondrial ROS production (131, 132). This reduction in mitochondrial ROS has been highly correlated with enhanced protection against beta cell apoptosis (133, 134), highlighting an important role for ROS regulation in T1D resistance.

1.2 REACTIVE OXYGEN SPECIES

Free radicals, including reactive oxygen species (ROS), contain a reactive unpaired electron. ROS, like superoxide and hydrogen peroxide, are continuously generated in the cell through various mechanisms. Imbalances in free radical production and dissipation can contribute to oxidative stress. Oxidative stress can alter or damage DNA, lipids, and proteins, contributing to disruption of cellular function and cell death (135-137). In situations where excessive free radical production is warranted, such as at the site of inflammation, these molecules are important for anti-microbial responses but have been implicated in tissue injury. However, persistent elevation in ROS production and insufficient dissipation have been implicated in inflammation and pathogenesis of chronic conditions, including rheumatoid

arthritis, autoimmunity, ischemia, myocardial infarction, and other age-related diseases (138). While the toxic effects of free radicals are well recognized, ROS are also likely participants in basic cellular functions. Transcription factors are regulated by redox status, demonstrating a role for free radicals in regulating gene expression (139). Therefore, proper regulation of immune responses and free radical production is critical for sufficient pathogen clearance, as well as avoidance of chronic inflammatory conditions.

1.2.1 NADPH oxidase

There are several sources of intracellular ROS production, with major contributions provided by cell respiration in the mitochrondria and Nicotinamide Adenine Dinucleotide Phosphate (NADPH) oxidase complexes (NOX). Professional phagocytes, including neutrophils and macrophages, are important contributors to innate immunity and early host responses to infection. The primary anti-microbial defenses utilized by neutrophils are phagocytosis and the production of free radicals. Neutrophils produce ROS, specifically superoxide, via the enzymatic NOX complex, which is critical for phagocytosis and pathogen clearance (140, 141). NOX is an enzyme complex of six subunits. There are two trans-membrane proteins, p22phox and gp91phox, which constitute the catalytic component cytochrome b558 (142, 143). The other subunits p47phox, p67phox, p40phox and a GTPase, such as Rac, are localized in the cytoplasm during the inactivated state (142). Physical separation of these subunits provides important spatial regulation of activity and free radical production by preventing any basal free radical production by NOX (143, 144).

PMN exist in three different states, resting, primed, and activated, that are determined by the presence of external stimuli (145-147). Resting cells are quiescent, present in circulation,

with a round morphology. Proinflammatory stimuli induce morphological changes and adhesion to the endothelium. These primed PMN follow chemotactic gradients to the site of inflammation, where they become activated (145-149). Rapid priming stimuli, including PAF, C5a, and lysophosphatidylcholine (LPC), induce effects within 3-5 minutes, whereas long-acting agents like lipopolysaccharide (LPS), IFN-γ and TNF-α can take hours. In some cases, the binding of stimulus agents to G-protein-coupled receptors primes the oxidase. The recognition of activating agents, including formyl-Met-Leu-Phe (fMLP), OpZ, and phorbol 12-myristate 13-acetate (PMA), induces the assembly of all NOX subunits, fully activating PMN and superoxide production (150-152). Agonist binding to the receptor starts signaling cascades in which the activation of phospholipases is mediated by a G protein and PtdInsP2 is broken down into DAG and Insp3. Insp3 binds intracellular calcium (Ca^{2+}) stores. The subsequent release of Ca^{2+}, along with DAG, activates Protein Kinase C (PKC).

Activated PKC catalyses the phosphorylation of the NOX cytosolic subunits, including p47phox, p67phox and p40phox, exposing unique binding domains. p47phox contains four domains: the N-terminus, internal SH3 domain, auto-inhibitory domain, and proline-rich C-terminus (153-158). The N-terminus phox homology domain targets p47phox to the plasma membrane upon activation; however, during the resting state the SH3 domain binds the auto-inhibitory domain (159-162). This interaction obscures the translocation domain, providing localization in the cytoplasm when not activated. Phosphorylation of p47phox removes the inhibition. This initiates translocation to the plasma or vesicle membrane and binding to the transmembrane subunit p22phox. This interaction facilitates binding of p40phox and p67phox to cytochrome b558 and the formation of the active complex (163, 164). The transfer of electrons from NADPH across the membrane to molecular oxygen results in the reduction of oxygen into

superoxide (143, 145). The produced superoxide can be dismutated into hydrogen peroxide by enzymes of the superoxide dismutase (SOD) family. Degranulation releases myeloperoxidases, which catalyze the reaction of hydrogen peroxide with chloride anions to generate hypochlorous acid. This can be followed by *N*-chlorination of nitrogen-containing compounds, producing chloramines. All of these products contribute to free radical-mediated antimicrobial killing (141, 144), which could result in oxidative stress in situations where the production is excessive.

The production of superoxide and subsequent free radical products is critical for pathogen clearance. The necessity of respiratory burst elicited by neutrophils and macrophages is highlighted by the rare condition Chronic Granulomatous Disease (CGD). Patients with CGD present with chronic, recurring bacterial and fungal infections as well as formation of granulomas in multiple tissues (165). An inherited disorder, CGD was linked to defective neutrophil and macrophage respiratory burst caused by mutations in genes encoding NOX subunits, including gp91phox, p22phox, p67phox, and p47phox. Mutations in gp91phox, which are X-linked (166, 167), are found in roughly two-thirds of CGD patients, with various types of mutations being detected (165, 168). Missense, nonsense and splicing mutants have been described, contributing to a variety of structural and/or functional changes in gp91phox. Mutations in the phenylalanine residues result in the absence of cytochrome b558 (166). Carriers of gp91phox mutations also exhibit decreased activity and defective microbial defenses (169). Mutations in the p47phox subunit are found in about 25% of CGD cases, with the predominant mutation resulting in an early stop codon, disrupting binding and activation (168). Retroviral vectors have been used in the gp91phox mutant mouse model of CGD to restore NOX function, eradicate infections, and eliminate the granulomas (170). Clearly, NOX superoxide production is important for proper acute responses and pathogen clearance.

1.2.2 ROS and inflammation

NOX function is needed to control infection, however too much or dysregulated production can increase risk of tissue damage. Increased free radical production, insufficient dissipation, and uncontrolled ROS production have all been implicated in inflammation and pathogenesis of chronic conditions and autoimmunity.

Study of genes linked to arthritis susceptibility in rats identified *Ncf1 (Neutrophil cytosolic factor 1*), encoding the p47phox subunit of NOX, which was surprisingly associated with defective neutrophil respiratory burst (171). Contrary to the hypothesis that ROS is proinflammatory in arthritis, *Ncf1* mutant animals lacking superoxide production showed enhanced arthritis and encephalomyelitis, whereas activating NOX ameliorated arthritis (172). These data contradicted earlier reports showing *Ncf1* knockout mice to be resistant to myelin oligodendrocytic glycoprotein (MOG) 35-55 peptide-induced experimental allergic encephalomyelitis (EAE) (173). Also, *Ncf1* mouse mutants with deficient superoxide production demonstrate increased susceptibility to and severity of collagen-induced arthritis (CIA) and EAE (172). It is important to note that the EAE-inducing agents in the rat and mouse studies differ by the use of native myelin proteins and myelin protein-derived peptides, respectively. This dramatic difference in susceptibility may highlight a potential role for ROS in antigen processing and presentation. Oloffsson, Holmdahl *et. al.* show that adoptive transfer of arthritogenic, mitogen-activated spleen cells only transferred disease when the donor was NOX-intact, suggesting that NOX function is important for priming pathogenic $CD4^+$ T cell responses (171). The authors suggest that ROS may be important for T cell and macrophage apoptosis or inhibitory signals, which are lost in the absence of NOX function, leading to the increased inflammatory response.

Free radical production is proposed to be an important contributor to beta cell death in various capacities **(Figure 1)**. As beta cells have low free radical defenses, they are sensitive to fluctuations in redox balance (174, 175). NOX free radical production by cells of the innate immune system, including neutrophils and macrophages, can have direct cytotoxic effects on the beta cell. During antigen presentation, free radicals are hypothesized to be important intracellular and intercellular signaling molecules (140, 176, 177). T cell ROS production is important during signaling and directing lineage development and cytokine synthesis. Cytokine and chemokine signaling further recruits and activates immune cells, amplifying inflammation (34, 36). Cytokines can then increase free radical production in the beta cell, contributing to beta cell death. Specifically, cytokines, including IL-1β and IFN-γ, induce elevated iNOS expression and NO production, contributing to beta cell apoptosis (73, 178). Recent work suggests that NOX complex subunits are expressed in beta cells and produce superoxide upon stimulation; however, a role during the inflammatory process and beta cell killing is not yet determined.

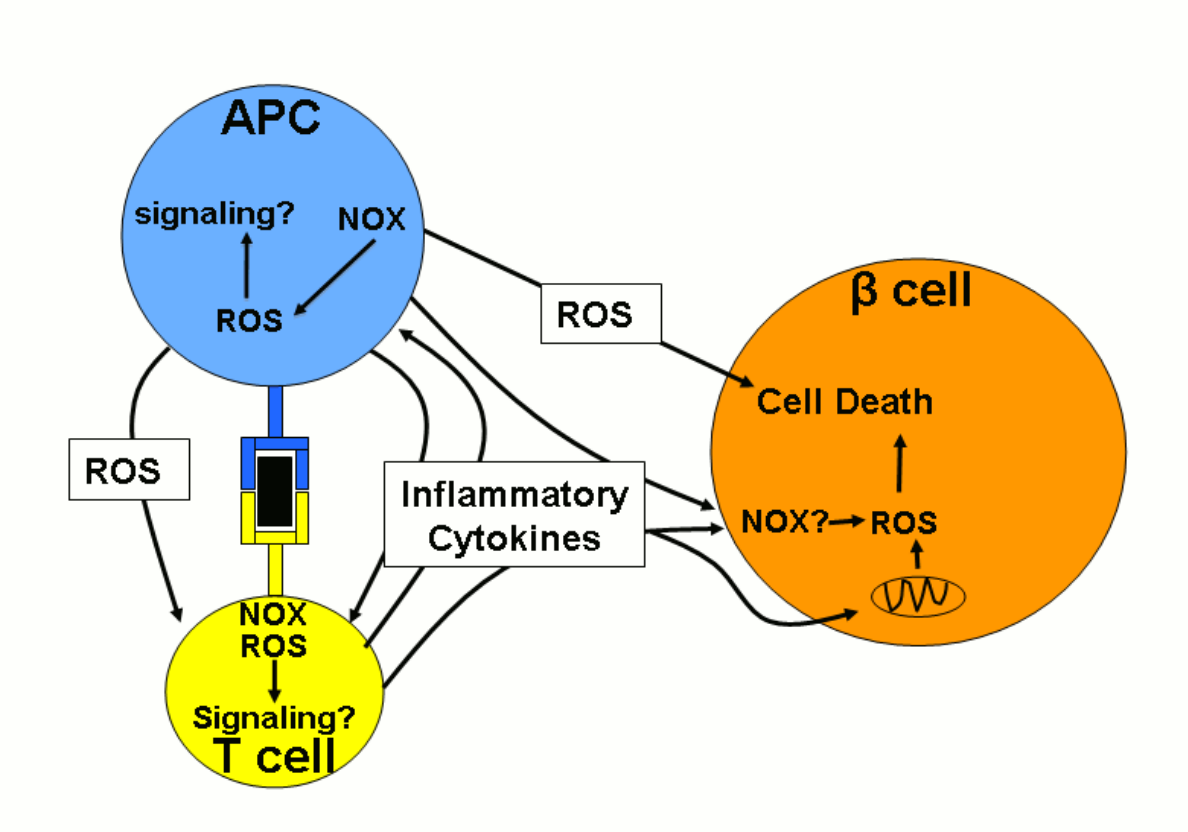

Figure 1. Free Radical Production is an important contributor to beta cell death. Cells of the innate immune system, including neutrophils and macrophages, produce superoxide via NOX and these free radicals can have direct cytotoxic affects on the beta cell. Free radicals produced during antigen presentation influence cytokine production and can cross cell membranes, participating during intercellular signaling. Intracellular T cell ROS is proposed to contribute to directing lineage development and cytokine production. Cytokine activity upregulates free radical production in the beta cell, contributing to beta cell death.

1.2.3 ROS as signaling molecules

The literature has recently been shifting focus from implicating ROS as damaging byproducts of cellular function to describing an essential role for free radicals as secondary messengers during signal transduction and signal amplification. ROS signaling is now implicated in the function of immune cells, including T lymphocytes (176). Redox status

systems, including NADPH, thioredoxin, and glutathione, are implicated in contributing to intercellular and intracellular T cell signaling (176). While mitochondria are considered the major source of free radicals (179), reports suggest that T cells express NOX-like molecules (180-182). Though the finding is controversial, T cell production of superoxide by a NOX enzyme is also reported. Previous work with gp91phox knockout mice has not demonstrated a clear role for NOX ROS production by T cells (181, 183). The introduction of a dominant negative Rac1 eliminated T cell ROS production (182); however, gp91phox deficiency did not fully ablate free radical production (181). In the T1D-prone NOD mice, polyclonal activation of T cells via anti-CD3 crosslinking stimulation elicits free radical production. The introduction of a p47phox mutation in NOD congenic mice ablates ROS production from $CD4^+$ T lymphocytes ((184) & Chapter 4). The introduction of this mutation has profound effects on macrophage and T cell function, as well as diabetes susceptibility with NOX-deficient immune cells ((184) & Chapter 4).

Modulation of ROS has been associated with regulation of Ras/Raf, Protein Kinase C and MAP kinase cascade pathways (185). It has previously been shown that depletion of APC intracellular glutathione shifts T helper polarization (186), demonstrating a role for ROS during antigen presentation and cytokine production. Hydrogen peroxide, a dismutation product of superoxide, is produced during oxidative burst and is proposed to play a role in lymphocyte antigen receptor activation (187-190). With similarities to calcium, hydrogen peroxide can easily diffuse inside a cell and between cells because it is electrically neutral (189, 191). Peroxides facilitate the oxidation of proteins, specifically cysteine residues (192, 193). Important targets of peroxide oxidation are transcription factors like p53, Jun, and NF-κB subunit p50, and this regulates transcriptional activity (139, 194).

Redox status and ROS production are associated with immune activation and the recruitment of lymphocytes. NOX function has been linked to altered T cell migration. The blockade of ROS production inhibits AP-1 activation and IL-8 synthesis (195), which are important contributors to chemotactic signals (19). Additionally, the upregulation of SOD and catalase in endothelial cells reduced monocyte chemoattractant protein-1 (MCP-1) induction (196). ROS production is proposed to be involved in the signaling between macrophages and lymphocytes (32, 197). As close contact is achieved at the immunological synapse during antigen presentation, free radicals are hypothesized to leave the oxidizing environment in the macrophage, diffusing to the lymphocyte (32, 198). Increases in hydrogen peroxide shift the antigen-specific dose response during B cell activation, suggesting that low-affinity BCR can be activated when redox status is shifted (189, 199). Macrophage-produced ROS is also suggested to pass to T lymphocytes. Proinflammatory third signals require ROS production to elicit APC cytokine production and lymphocyte effector function (200-202). This is achieved through regulation of transduction pathways and transcription factors that are affected by redox status, including NF-κB, STAT, and AP-1 (185, 203-205). ROS scavenging was found to suppress TCR-induced transcription of NF-κB and AP-1 (176, 206). Upregulation of these genes is associated with transient ROS fluxes. These responses are dependent on immune-derived signals. Blocking these innate-derived signals with catalytic antioxidants resulted in antigen-specific hyporesponsiveness, decreasing T cell proliferation and cytokine synthesis (202). These alterations to redox balance, using catalytic antioxidants or metalloporphyrin-based superoxide dismutase mimics, also had profound effects on diabetes development and transfer, associated with modified lymphocyte reactivity (202, 207-210).

Intracellular T cell ROS production is also critical during signal transduction and lineage commitment. In T cells, the engagement of CD28 stimulates rapid production of ROS that is required for NF-B activation and IL-2 expression (211), processes important for cell function, survival and proliferation. Additionally, reports suggest that activation-induced cell death (AICD) of T cells requires free radicals, as antioxidants inhibit AICD in T cell lines and primary cells after exposure to various stimuli (212-216). Cell death of naïve thymic T cells was abolished during hypoxic conditions (217). Furthermore, reductions in oxygen concentrations skewed CTL development and cytokine production (218). These data suggest that oxygen levels and oxygen-derived radicals are important for T cell survival and differentiation.

1.2.4 Antioxidant therapy for T1D protection

As oxidative stress is associated with exacerbated inflammation and beta cell death, free radical scavengers and antioxidants have been proposed as potential therapeutics for diabetes. It has been previously reported that antioxidants were able to delay and prevent the transfer of T1D by diabetogenic T cells (207, 210), suggesting that scavenging ROS interfered with proinflammatory autoimmune initiation. Several reports showed that the modification of antioxidant activity was able to reduce or prevent IL-1β-induced beta cell damage (219, 220). Beta cell over-expression of SOD1 reduced damage induced by the diabetogenic drugs alloxan and streptozotocin (221). Glutathione, SOD1, and thioredoxin (TRX) have been shown to block pro-apoptotic pathways involving apoptosis signal-regulating kinase, AP-1 and NF-κB (222, 223). Recombinant TRX also protected islets from TNF- and Fas-induced apoptosis (224); transgenic over-expression of TRX, specifically in the beta cells of NOD mice, significantly reduced incidence of T1D (225). Additionally, administration of the metalloporphyrin-based

SOD mimetic was able to protect mice from T1D induction by diabetogenic T cell clones (210). These data demonstrate a role for antioxidants in regulating apoptosis and immune-mediated beta cell death. Likewise, modifying redox balance attenuates immune cell activity; as systemic administration reduces inflammation, antioxidant therapy may also serve to skew pathogenic immune responses. Therefore, therapeutic manipulation of ROS in beta cells or cells of the immune system could have dramatic effects on T1D onset.

1.2.5 The ALR Mouse

The Alloxan Resistant (ALR) mouse strain, selected for resistance to alloxan-induced diabetes, is very useful for the study of redox balance, free radical dissipation, and resistance to autoimmunity. Alloxan is selectively taken up by beta cells through GLUT2. Once inside beta cells, alloxan decomposes and generates free radicals, inducing cell death. The ALR strain was outbred from the Jc1:ICR swiss progenitors from which the NOD strain was also derived. The NOD and ALR are closely related, with over 85% genetic identity between the strains, including almost all *Idd* loci (133). Analyses of *IL-2, β2m,* (112) and MHC class II alleles (226) revealed identical sequences comparing NOD and ALR. Though closely related to the NOD, the ALR mouse strain resists spontaneous and induced forms of diabetes. ALR islets also exhibit exquisite resistance to cytotoxic T cells and proinflammatory cytokines. Not surprisingly, the ALR demonstrates heightened free radical defenses with elevated activity of superoxide dismutase (SOD), glutathione peroxidase, and glutathione reductase, which also extends to the pancreatic islets (227-229). Additionally, cellular sources of free radical production, including mitochondria respiration, iNOS activity, and cytosolic NOX function, are impaired in the ALR, producing significantly lower amounts of ROS (17, 128, 131, 133, 228, 230). As the ALR is

distinguished by heightened antioxidant defenses and decreased free radical production, these characteristics are proposed to be critical in ALR-derived protection. Investigating the genetics of ALR compared to the T1D-prone NOD provides a unique analysis to describe protective mechanisms involved in the activation of autoreactive effectors and beta cell killing.

Genetic analyses identified ALR-derived protective loci on Chr. 3, 8 and 17, as well as a single nucleotide polymorphism in the mitochondrial genome. The peak linkage on Chr. 17 mapped to the MHC. It is important to note that ALR and NOD differ at the distal end of the MHC complex, encoding *H2-D*^{dx} and *H2-D*^{b}, respectively (112). The mitochondrial linkage is associated with the single nucleotide polymorphism in *mt-Nd2*, representing the only genetic difference in the mitochondrial genome between ALR and NOD. As previously discussed, the ALR-derived allele is associated with reduced mitochondrial ROS production, which has been highly correlated with enhanced protection against beta cell apoptosis (133). The linkage mapping to Chr. 8, termed *Idd22*, has not been mapped in other genome-wide association studies using other outcross partners, suggesting that the protective loci may be unique to the ALR strain. *Idd22* has been associated with ALR-derived resistance to both spontaneous T1D and alloxan-induced ROS-mediated diabetes (112, 133).

The locus on Chr. 3 overlapped with an independently mapped locus, *Suppressor of Superoxide Production (Susp)*, that was associated with both reduced superoxide production by NOX and heightened SOD1 activity (230). The mapping of an *Idd* to Chr. 3 is not surprising, as multiple linkages have been mapped to this chromosome via backcrosses of NOD with B10, B6, or NON mouse strains. These linkages have been designated as *Idd3, 10, 17, 18*. However, the IL-2 allele, the candidate for *Idd3*, is identical in ALR and NOD (112), and the diagnostic markers for *Idd10, 17,* and *18* are non-polymorphic comparing the strains, suggesting that the

ALR-derived locus on Chr. 3 may be novel rather than resulting from alleles at *Idd3*, *10*, *17*, or *18*. These data suggest that *Susp* phenotypic contributions may be involved in ALR-derived T1D resistance.

2.0 ALR-DERIVED CHROMOSOME 3 *SUPPRESSOR OF SUPEROXIDE PRODUCTION* DOMINANTLY PREVENTS TYPE 1 DIABETES AND INSULITIS

2.1 ABSTRACT

Free radicals are involved during various stages of autoreactivity and beta cell destruction. In addition to contributing to beta cell killing, reactive oxygen species (ROS) are important signaling molecules during the initiation of proinflammatory effectors. The Alloxan Resistant (ALR) mouse is uniquely resilient to oxidative stress, exhibiting elevated antioxidant defenses and reduced production of ROS. We have previously associated increased superoxide dismutase 1 (SOD1) activity with suppressed superoxide production (*Susp)* by neutrophils and macrophages. The ALR *Susp* locus overlapped with a previously identified ALR-derived T1D protective locus on Chromosome (Chr) 3, suggesting elevated SOD1 and reduced NADPH oxidase (NOX) function contribute to diabetes resistance. The role of SOD1 regulation and free radical scavenging were studied to determine the impact of the ALR-derived Chr. 3 loci on beta cell survival and diabetogenicity of T lymphocyte effectors.

To determine the role of *Susp* in T1D-prone model, the ALR-derived *Susp* locus on Chr. 3 was congenically introduced to the NOD background (NOD-*Susp*). NOD-*Susp* mice exhibited ALR-like activities of both SOD1 and NOX confirming the previous mapping of *Susp* to Chr. 3. Additionally, elevated SOD1 activity was associated with increased stability of SOD1 dimer in

NOD-*Susp* mice. The association of SOD1 with NOX function was confirmed by assaying respiratory burst in the presence of a SOD1 inhibitor, potassium cyanide. Inhibition of SOD1 restored superoxide production by PMA-stimulated bone marrow cells isolated from ALR and NOD-*Susp* mice.

Congenic introduction of ALR Chr. 3 genome to an NOD background dominantly protected mice from diabetes onset and insulitis development. Cultured islets from the NOD-*Susp* congenic mice were assessed for viability after proinflammatory cytokine treatment and mice were challenged with adoptive transfer of splenocytes from NOD-AI4 transgenic mice. However, NOD-*Susp* islets did not exhibit full protection from cytokine-mediated death and mice were hyperglycemic after adoptive transfer of AI4 splenocytes, demonstrating susceptibility to inflammatory mediators. The diabetogenic potential of T cells purified from NOD and NOD-*Susp* donors was assessed via adoptive transfer to susceptible NOD-*Scid* recipients. Purified T cells from NOD-*Susp* donors failed to induce diabetes in NOD-*Scid* mice. Therefore, ALR Chr. 3 is providing significant modification to immune cell reactivity, reducing beta cell-specific effector function by T cells from NOD-*Susp* donors.

These data demonstrate that ALR Chr. 3 contributions provide significant resistance to diabetes. The protection provided is associated with the elevated SOD1 activity. However, this increased antioxidant scavenging did not provide enhanced beta cell survival. Rather, the immune system from NOD-*Susp* mice lost diabetogenic potential. We have previously shown that NOX function is important for immune cell diabetogenic reactivity. Taken together, these data suggest that antioxidant regulation of oxidative stress is a major modifier of immune effector function and diabetes development.

2.2 INTRODUCTION

Type 1 Diabetes (T1D) results from the autoimmune destruction of the insulin secreting pancreatic beta cells. Immune-mediated attack involves various mechanisms that induce beta cell death, including Fas/FasL engagement, proinflammatory cytokine synthesis, and production of free radicals (reviewed in (231)). Reactive oxygen species (ROS) production is involved during various stages of autoreactivity and beta cell destruction (Fig. 1). ROS not only serve as cytotoxic mediators, but also as critical signaling molecules during activation of innate and adaptive immune responses (140, 177, 202, 207, 208). However, the role of ROS production and antioxidant scavenging in the development of spontaneous T1D is ill-defined (133, 176).

The Alloxan resistant (ALR) mouse strain was selected based on resistance to alloxan-induced free radical-mediated diabetes. The NOD and ALR are closely related with over 85% genetic identity between the strains (133). Despite the high genetic similarity, the ALR is resistant to spontaneous diabetes and to adoptive transfer with diabetogenic T cells (232). ALR islets also exhibit exquisite resistance to cytotoxic T cells and proinflammatory cytokines (229, 232). Not surprisingly, the ALR demonstrates heightened free radical defenses with elevated activity of superoxide dismutase (SOD), glutathione peroxidase, and glutathione reductase (228, 229, 232). Systemic and constitutive elevations of SOD1 activity were associated with increased stability of SOD1 dimer. The ALR mouse represents a unique model to study the role of ROS scavenging as well as free radical production in the development of aberrant immune responses and T1D resistance (112, 133, 226, 233).

Genetic analyses identified ALR-derived protective loci on Chr. 3, 8 and 17 (112, 226, 230), as well as a single nucleotide polymorphism in the mitochondrial genome (129). The locus on Chr. 3 overlaps with an independently mapped locus, *Suppressor of Superoxide Production*

(Susp), controlling reduced superoxide production by NADPH oxidase (NOX) (230). This reduction in NOX function was associated with the systemic and constitutive elevation of SOD1 activity (230). These data suggest that *Susp* phenotypic contributions may be involved in ALR-derived T1D resistance. To study to role of *Susp* in T1D-prone model, NOD mice congenic for the *Susp* locus were developed. Congenic mice inherited ALR-like phenotypes of elevated SOD1 and reduced NOX function. Inhibition of SOD1 activity was able to restore superoxide production by PMA-stimulated ALR bone marrow cells, demonstrating that increased superoxide turnover was reducing the release of free radicals.

Here we show that ALR Chr. 3 contributions dominantly protected mice from T1D onset and invasive insulitis. Though completely protected from spontaneous T1D onset, NOD-*Susp* islets were not fully resistant to cytokine-induced death and congenic mice were equally susceptible as NOD cohorts to adoptive transfer with AI4 $CD8^+$ T cells, demonstrating that beta cells did not exhibit the same resistance to proinflammatory mediators. However, transfer of T cells from NOD-*Susp* donors failed to induce diabetes in susceptible NOD-*Scid* recipients, demonstrating a loss of diabetogenic potential. These data suggest that elevated free radical scavenging at the immune cell level is most effective to reduce beta cell-directed autoimmunity.

2.3 METHODS

2.3.1 Animals

The ALR-derived *Susp* locus was congenically introgressed into the NOD genome. In order to generate congenic mouse model female NOD mice were mated with male ALR mice,

and the subsequent F1 progeny were backcrossed to NOD. Selection for ALR contributing genome on Chr. 3 and elimination of contaminating ALR alleles elsewhere in the genome was achieved through PCR amplification of six microsatellite primer pairs on Chr. 3 and an additional 94 informative microsatellite primers spanning all chromosomes at each generation from N2 to N7 as previously described (132). Mice were backcrossed for a total of 10 generations, followed by intercrossing to select NOD mice with ALR homozygous *Susp* locus. The congenic mice used throughout this report are NOD.ALR-(*D3Mit221-D3Mit189*) [NOD-*Susp*] with a congenic segment of ALR genome spanning from *D3Mit221* (7.89 Mbp) to *D3Mit189* (100.78 Mbp).

ALR/LtJ, NOD/ShiLtJ, NOD.B6-*Ncf1*$^{m1J/m1J}$ [NOD-*Ncf1*^{m1J}], and NOD-*Susp* mice were bred and housed in the University of Florida facility under specific pathogen-free conditions. NOD.CB17-*Prkdc*^{scid}/J [NOD-*Scid*], NOD.129S7 (B6)-*Rag1*^{tm1Mom}/J [NOD-*Rag1*], NOD.Cg-*Rag1*^{tm1Mom}Tg (TcraAI4)1Dvs/DvsJ [NOD-AI4a] and NOD.Cg-*Rag1*^{tm1Mom}Tg (TcrbAI4)1Dvs/DvsJ [NOD-AI4b] were purchased from The Jackson Laboratory (Bar Harbor, ME) and bred in our mouse facility. F1 hybrid progeny from matings of NOD-AI4a with NOD-AI4b [NOD-AI4a/b] developed diabetes between 3-5 weeks of age. All mice were housed in specific pathogen-free facilities and approved by the Institution Animal Care and Use Committee of the University of Florida.

2.3.2 Materials

Riboflavin, TEMED, potassium cyanide (KCN), 5-(and-6)-chloromethyl-2’7’-dichlorodihydrofluorescein diacetate (CM-H_2DCFDA), and 4-alpha-phorbol-12-myristate-13-acetate (PMA) were purchased from Sigma-Aldrich (St. Louis, MO). Dihydrorhodamine 123

(DHR123) was purchased from Invitrogen (Carlsbad, CA) and Dithiotheitol (DTT) from Bio-Rad (Hercules, CA). Superoxide Dismutase activity assay kit was purchased from Cayman Chemical (Chantilly, Virginia). All DNA oligonucleotides were obtained from Integrated DNA Technologies, Inc. (Coralville, Iowa).

2.3.3 Gene expression analysis

RNA was purified from liver using TRIzol Reagent [Life Technologies (Rockville, MD)]. cDNA was generated using the SuperScript First-Strand Synthesis System [Life Technologies]. The primer set used to measure the relative expression of Sod1, Sod1.F - GCA AGC GGT GAA CCA GTT GT and Sod1.R - CCA ACA TGC CTC TCT TCA TCC] was validated before use by sequencing of the amplified PCR product to determine specificity. Amplification with a primer set specific for 18S rRNA, 18S.F - CCG CAG CTA GGA ATA ATG GAA T and 18S.R – CGA ACC TCC GAC TTT CGT TCT, was utilized for normalization. The tests were run using 3 pools of liver cDNA per group and fluorescence detected by an ABI Prism 7700, using SYBR Green JumpStart Taq Ready Mix (Sigma) for detection as per manufacture's protocol. Quantitative Real-Time PCR conditions were an initial 2 min denaturation step at 94°C, followed by 45 cycles of (94°C for 30 sec, 60°C for 30 sec, and 72°C for 60 sec), and then finally at 4°C hold.

2.3.4 Sequencing of *Sod1*

Total liver RNA was isolated and cDNA synthesized as above. PCR was used to amplify the SOD1 coding sequence using primers specific for SOD1 [Sod1-Seq.F: CTC TCT GGT CCC

TCC GG: Sod1-Seq.R: GTC CTT AGC CCA GTC AAA GG]. PCR conditions were 2 min initial denaturation step at 94°C, followed by 45 cycles of (94°C for 30 sec, 60°C for 30 sec, and 72°C for 60 sec), and then finally a 4°C hold. Sequencing was performed on an ABI 3100 using big dye chemistry (ABI (Carlsbad, CA)). Sequences were aligned and analyzed using the Sequencher software package.

2.3.5 Western blotting

Whole cell lysates were separated on a 4-20% gradient SDS-PAGE gel and transferred onto nitrocellulose membrane. The membranes were incubated overnight at 4°C with polyclonal anti-SOD1 antibody (Santa Cruz or Millipore) and exposed to the appropriate secondary antibody conjugated to horseradish peroxidase (Jackson ImmunoResearch or Santa Cruz). Chemiluminescence was detected with SuperSignal Chemiluminescent Substrate (Thermo Scientific).

2.3.6 Assessment of SOD1 activity

Liver and bone marrow homogenates were prepared in 20 mM HEPES buffer (pH 7.2) with 1 mM EGTA, 210 mM mannitol and 70 mM sucrose. Protein content was determined using Pierce BCA Protein Assay Kit (Thermo Scientific). SOD1 was extracted using ethanol:chloroform (62.5/37.5 v/v). After centrifugation at 3000 x *g* for 5 min, the aqueous layer containing SOD1 was collected. SOD1 activity was measured with Cayman Chemical

Superoxide Dismutase Assay Kit following manufacturer's protocol. Pretreatment of lysates with 2 mM KCN confirmed full inhibition of SOD1 activity.

2.3.7 Evaluation of SOD1 stability

Red blood cell lysates were prepared in 0.5 M potassium phosphate buffer (pH 7.8). Samples were treated with Dithiothreitol (DTT) for 2 hours at 37°C. Thermal stability was assessed by incubation of lysates at 75°C, 85°C, or 95°C for 5 min. DTT-treated, heated, and control lysates were then separated on a 12% non-denaturing acrylamide gel with a 5% stacker. The gel was then saturated in 2.45 mM Nitroblue Tetrazolium (NBT) for 20 min at room temperature followed by saturation with 28 μM Riboflavin with 25 mM TEMED in 36 mM potassium phosphate (pH 7.8) for 15 min at room temperature. Gels were illuminated under fluorescent light until full contrast was obtained (234).

2.3.8 Cytochrome c measurement of oxidative burst

Bone marrow was collected from age-matched female mice and red blood cells were removed on a Histopaque-1119 gradient as previously described (230). $1x10^5$ cells were pretreated with 2 mM KCN or HBSS for 15 min at room temperature. Cells were then transferred to HBSS containing 145 μM cytochrome C and were stimulated with PMA (98 nM) at 37°C. Reduction of cytochrome C was measured at 550 nm at 1 min intervals for 45 min. The maximum rate of reduction was calculated by linear regression analysis. Purified bovine erythrocyte SOD1 (Cayman Chemical) (0.5 U/mL) was used to confirm specificity of superoxide production.

2.3.9 Measurement of oxygen consumption

Bone marrow was collected from age-matched female mice and red blood cells were removed on a Histopaque-1119 gradient as previously described (230). The Oxygraph-2K (Oroboros Instruments Innsbruck, Austria) was calibrated for basal oxygen levels with HBSS and after the addition of sodium hydrosulfite, following manufacturer's instructions. A total of $2x10^7$ cells were pretreated with 2 mM KCN or HBSS for 15 min at room temperature. Cells were resuspended in 2 mL HBSS and loaded into the chamber of the Oxygraph-2K at 37°C. Samples were stimulated with 1 µM PMA and oxygen concentration and rate of consumption were monitored for 30 min.

2.3.10 Spontaneous incidence

At 8 weeks of age, NOD-*Susp* female and male mice were enrolled and monitored for diabetes onset via weekly urinalysis testing using Diastix [Bayer (Elkhart, IN)] and compared with NOD-*Susp(F1)*, NOD-*Susp(NOD)* littermate controls, and NOD cohorts. Mice positive for glucosuria were monitored daily thereafter for hyperglycemia using One Touch Ultra 2 meters [Life Scan, Inc (Milpitas, CA)]. Any mouse with measured blood glucose levels on consecutive days >250 mg/dL were diagnosed with type 1 diabetes. To examine islet inflammation of non-diabetic females from each genotype at 30 weeks of age pancreata were fixed in 10% neutral buffered formalin, embedded in paraffin, stained with aldehyde fuchsin to identify granulated beta cells, and counter-stained with hematoxylin and eosin. Islets were scored over a range between 0 (no lesions) and 4.0 (end-stage insulitis) and a mean insulitis score calculated.

2.3.11 Islet isolation and culture with cytokines

Pancreatic islets from age-matched female NOD-*Rag1* and NOD-*Susp* mice were isolated (235) and cultured with IFN-γ, IL-1β, and TNF-α as previously described (232). Islet NO production was measured and cell viability was assessed via MTT assay as previously reported (228).

2.3.12 Transfer of AI4 splenocytes

At 3-4 weeks of age, NOD-AI4a/b donors were sacrificed and splenocytes were harvested. After the red blood cells were lysed with Gey's solution live cells were counted and diluted to a concentration of 10^8 cells per mL. A total of 2 x 10^7 cells in sterile PBS were injected via the tail vein into sub-lethally irradiated eight week old NOD and NOD-*Susp* females [dose of 7.5 Gy delivered using X-RAD 320 (Precision X-ray, North Branford, CT)] as previously described. Mice were monitored every other day for the onset of diabetes as described above.

2.3.13 Flow cytometric analysis of oxidative burst

Neutrophil and macrophage superoxide production were also assayed using a FACS assay, as previously described (230). Briefly, bone marrow was isolated and purified using a Histopaque-1119 gradient. Cells were labeled with PerCpCy5.5-labeled anti-Ly6g (Gr1) and APC-labeled anti-CD11b and then loaded with Dihydrorhodamine 123 (DHR 123) for 5 minutes at 37°C. Cells were subjected to flow cytometry prior to stimulation, and then at 5 minute

intervals after PMA [98 nM] stimulation. The ROS driven conversion of DHR 123 to rhodamine was measured using a BD Fortessa. Data were collected and analyzed with FACSDiva software (BD Biosciences).

2.3.14 Determination of anti-CD3 induced ROS generation in purified $CD4^+$ T cells

ROS generation was measured with the oxidation-sensitive dyes CM-H_2DCFDA as described previously (181) with the following modifications (Tse and Thayer, *In Press*). $CD4^+$ T cells were purified with a $CD4^+$ T cell isolation kit (Miltenyi Biotec) per the manufacture's guidelines. Purified 10^7 $CD4^+$ T cells were stained with CM-H_2DCFDA (Sigma) 2μM at 37°C for 30min, washed and then stained with hamster anti-mouse CD3 Ab (BD Pharmingen) at 10μg/ml for 25 min at 4°C. ROS generation was induced in 10^6 $CD4^+$ T cells by cross-linking the anti-CD3 antibodies with 5 μg/mL rabbit anti-hamster IgG (BD Pharmingen) at 37°C. Fluorescence was detected with a BD Fortessa at 0, 30, and 60 min after stimulation. ROS generation was determined by the increase in CM-H_2DCFDA fluorescence upon anti-CD3 stimulation over unstimulated control. The increase in dye oxidation was calculated as the percentage increase in mean fluorescence intensity (MFI) of anti-CD3 stimulated cells over unstimulated cells for each time point using the following equation:

$$([MFI(stim)-MFI(unstim)] / MFI(unstim)) \times 100.$$

2.3.15 Adoptive transfer of purified T cells from NOD and NOD-*Susp*

Eight week old, female NOD and NOD-*Susp* donors were used for adoptive transfer experiments. All donors were diabetes free at the time of sacrifice. Splenocytes were harvested

and red blood cells were lysed using Gey's solution. $CD4^+$ and $CD8^+$ T cells were purified by negative selection with magnetic beads according to the manufacturer's protocol using a $CD4^+$ T cell isolation kit or a $CD8^+$ T cell isolation kit (Miltenyi Biotec), respectively. Purity, over 96%, was confirmed by flow cytometric analysis. $CD4^+$ and $CD8^+$ T cells were mixed at a ratio of 3:1 and a total of 10^7 cells were transferred i.p. to 8 week old NOD-*Scid* recipients. Mice were monitored weekly for diabetes onset as described above. Engraftment of donor T cells into the T cell deficient NOD-Scid hosts was confirmed by flow cytometry 80 days post transfer.

2.3.16 Flow cytometry

Peripheral blood samples were lysed with Gey's solution twice and resuspended in 100 µl HBSS for staining. Gey's treated splenocytes, ficol separated bone marrow suspensions, or purified T cells were counted and resuspended in HBSS at 2 x 10^7 cells/mL. Approximately 10^6 cells were labeled with antibodies at the proper dilution. Fluorescence was measured using LSR Fortessa (BD Bioscience, San Jose, CA). Data were collected and analyzed using FACSDiva 6.0 software (BD Biosciences).

2.3.17 Statistics

GraphPad Prism (GraphPad Software, Inc, (La Jolla, CA)] was used for calculating statistical differences. Significance between mean values was determined using the Student's *t* test or One-way ANOVA, with $p < 0.05$ considered significant. Kaplan-Meier survival analysis was used to evaluate diabetes onset.

2.4 RESULTS

2.4.1 No difference in ALR SOD1 cDNA, expression, or content; however increase dimer stability is linked with elevated antioxidant activity and maps to the *Susp* interval.

It has previously been reported that ALR exhibits a constitutive and systemic elevation in the activity of SOD1 (112, 230), including that measured in liver **(Fig. 2A)**. However, sequencing of the cDNA did not identify any polymorphisms comparing ALR to control strains. Sod1 cDNA sequences from ALR, NOD, BALB, and B6 have been deposited in Genbank. Analysis of SOD1 mRNA expression and protein content also were not different in ALR **(Fig. 2B)**, suggesting post-translational modifications may be altering activity. Therefore, the stability of the enzyme under reducing conditions was evaluated. Red blood cell lysates were treated with DTT to disrupt the disulfide bridges required for dimerization or heated to 75°C, 85°C, or 95°C. SOD1 activity was visualized after treatment with NBT. While there was no enhanced thermal stability of SOD1 derived from ALR or NOD-*Susp* compared to NOD (data not shown), SOD1 from both ALR and NOD-*Susp* mice retained active SOD1 dimer after incubation with DTT **(Fig. 2C)**, demonstrating increased stability of the enzyme to disulfide reduction.

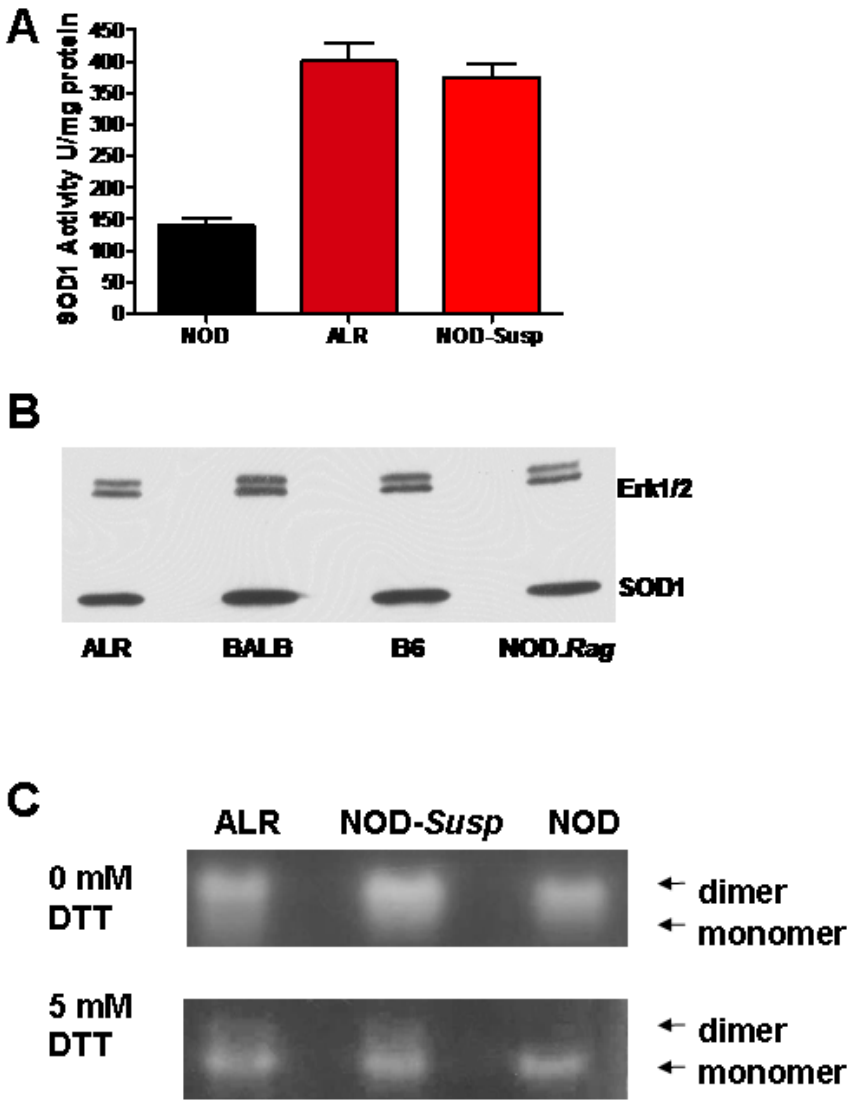

Figure 2: Increased dimer stability is a feature of the ALR SOD1 isoform. (A) Liver lysates SOD1 activities. (B) Western blot for SOD1 content. (C) SOD1 dimer stability after treatment with DTT was visualized on a 12% non-denaturing acrylamide gel stained with NBT and riboflavin.

2.4.2 Elevated SOD1 is reducing superoxide release after stimulation of bone marrow populations.

Previous reports evaluating increased free radical scavenging and decreased ROS production inherent to the ALR have associated elevated SOD1 activity with decreased oxidative burst by neutrophil and macrophage NADPH oxidase (230), however none of these reports have directly linked these two phenotypes. Similar to what we have measured in liver **(Fig. 2A)**, bone marrow cells from both ALR and NOD-*Susp* exhibited increased SOD1 activity compared to bone marrow cells isolated from NOD [$p<0.02$ **(Fig. 3A)]**. The difference in SOD1 activity was ablated at KCN concentrations above 2mM that completely inhibited SOD1 activity (data not shown). Oxidative burst was measured via cytochrome c reduction as well as oxygen consumption. NOD bone marrow cells stimulated with PMA exhibit a robust burst with significant increases in cytochrome c reduction and oxygen consumption **(Fig. 3B and 3C, respectively (black columns))**. After pre-treatment with the SOD1 inhibitor KCN (2mM) superoxide release from NOD cells was elevated as dismutation was blocked. These elevations are lost when purified SOD1 is added back, confirming specificity for superoxide production. After stimulation with PMA, ALR cells demonstrate no increase in superoxide release **(Fig. 3B)**, however, there was a significant increase in the oxygen consumed **(Fig. 3C)**. When SOD1 is inhibited with KCN, superoxide production is elevated after stimulation of bone marrow from ALR and NOD-*Susp* mice. Specificity is confirmed by adding back SOD1 and by using a NOD congenic with a mutation that ablates NOX function (NOD-*Ncf1*) (184). These data confirm that NOX function is likely intact in ALR monocytes and that the decreased secretion of superoxide in these cells from ALR mice results from elevated SOD1 activity and stability inherited with the Chr. 3 *Susp* locus.

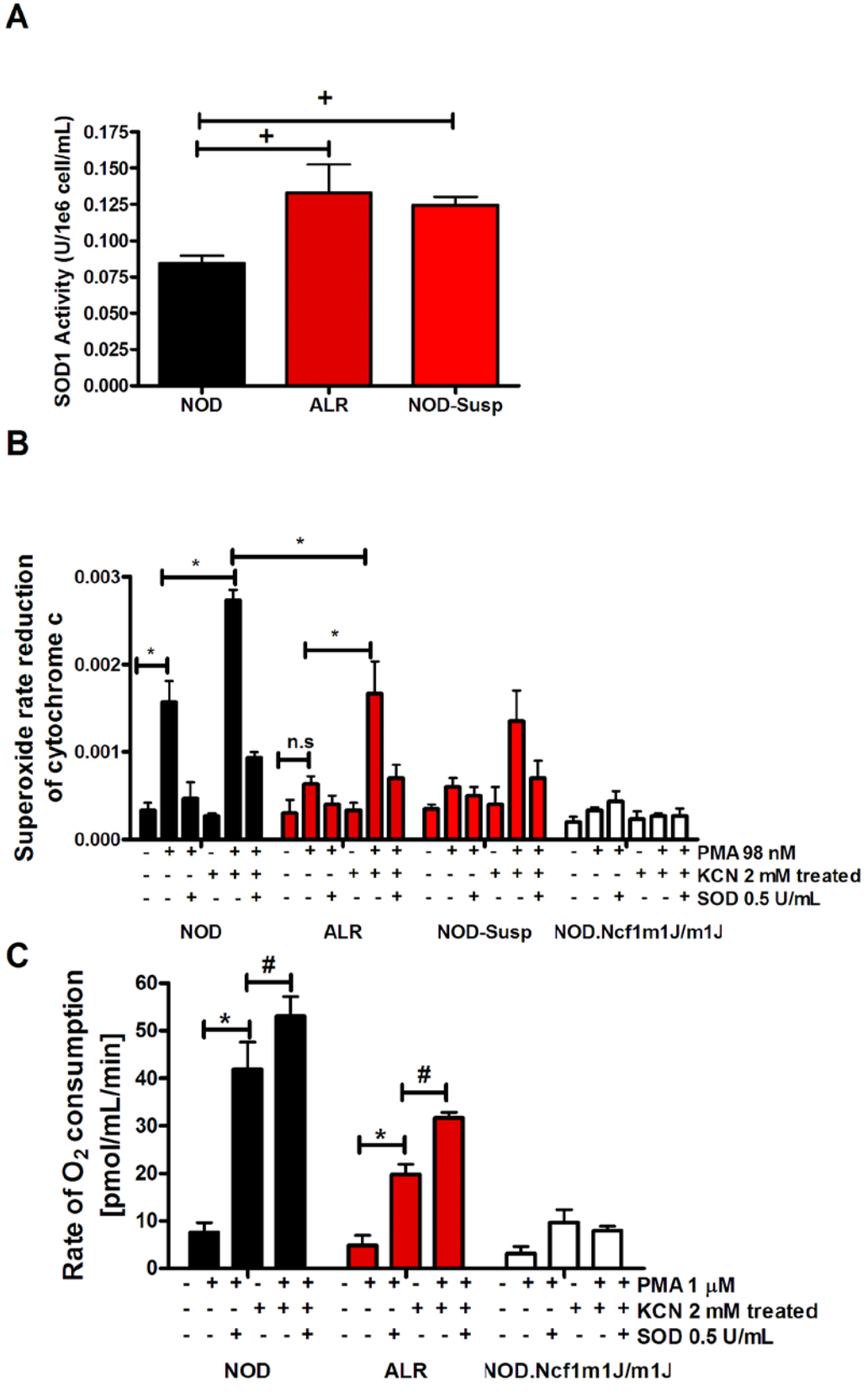
A
SOD1 Activity (U/1e6 cell/mL)
0.175
0.150
0.125
0.100
0.075
0.050
0.025
0.000
+
+
NOD
ALR
NOD-Susp
B
Superoxide rate reduction of cytochrome c
0.003
0.002
0.001
0.000
*
*
*
*
n.s
PMA 98 nM
KCN 2 mM treated
SOD 0.5 U/mL
NOD
ALR
NOD-Susp
NOD.Ncf1m1J/m1J
C
Rate of O_2 consumption [pmol/mL/min]
60
50
40
30
20
10
0
*
#
*
#
PMA 1 μM
KCN 2 mM treated
SOD 0.5 U/mL
NOD
ALR
NOD.Ncf1m1J/m1J

Figure 3: Elevated SOD1 activity is reducing release of superoxide by stimulated bone marrow cells in ALR. (A) Bone marrow lysates were assayed for SOD1 activity. Superoxide production was evaluated by measuring (B) rate reduction of cytochrome c and (C) oxygen consumption by PMA-stimulated bone marrow cells stimulated after inhibition of SOD1 with KCN. Data representative of 3 independent experiments performed in triplicate. +$p<0.02$, # $p<0.006$, or * $p< 0.0001$.

2.4.3 ALR Chr. 3 genomic contributions dominantly protect from overt diabetes and insulitis.

Cohorts of NOD-*Susp* mice heterozygous or ALR homozygous on Chr. 3 were evaluated for T1D onset compared to littermate controls that were homozygous for NOD genome throughout the *Susp* interval. *Susp* dominantly prevented both T1D and insulitis **(Fig. 4)**. NOD-*Susp* females homozygous or heterozygous for ALR genome on Chr. 3 were 100% diabetes free out to 35 weeks of age, compared to only 25% of littermate controls **(Fig. 4A)**. NOD-*Susp* males were also completely diabetes resistant (data not shown). Histological analysis of the mice that did not develop diabetes demonstrated no advancing insulitis in NOD-*Susp* congenic females compared to severe insulitis in the littermate controls **(Fig. 4B)**. Islets from NOD-*Susp* mice were also free of the accumulation of leukocytes compared to littermate controls that exhibited advanced insulitic infiltration **(Fig. 4C)**.

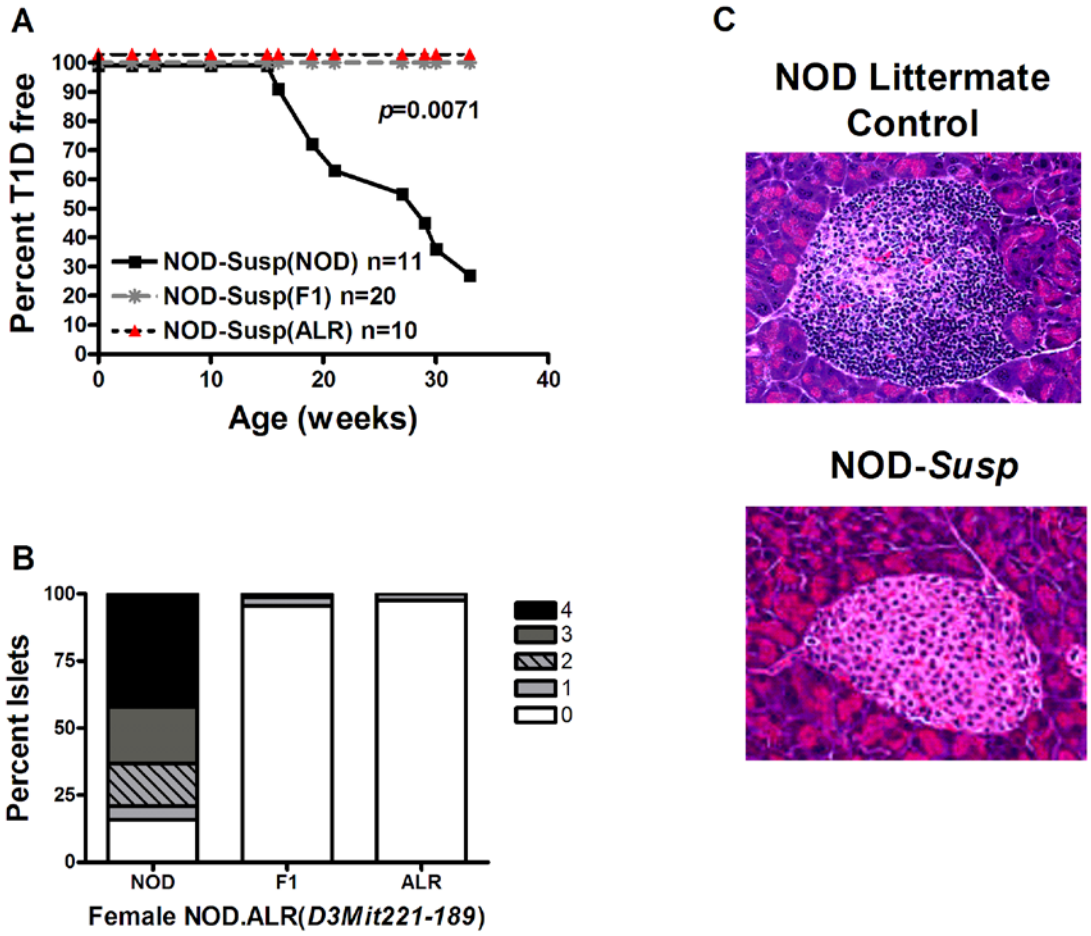

Figure 4: ALR Chr. 3 genome dominantly protects from T1D and insulitis. (A) Age-matched female NOD-*Susp(NOD)* littermate controls, NOD-*Susp(F1)*, and NOD-*Susp(ALR)* mice were monitored by glucosuria for the onset of spontaneous diabetes. (B) Insulitis scores in 40 week old non-diabetic mice. (C) Hemotoxylin and eosin staining of representative islets from mouse pancreata.

2.4.4 NOD-*Susp* islets are not fully protected from proinflammatory-mediated damage

To determine if diabetes resistance in NOD-*Susp* mice was conferred by enhanced pancreatic beta cell survival, islets from NOD.*Rag*, ALR, and NOD-*Susp* mice were isolated and treated with cytokines to evaluate cell viability and NO production. Treatment with proinflammatory cytokines significantly reduced cell viability of NOD.*Rag* and NOD-*Susp*

cultured islets compared to ALR **(Fig. 5A)**. NOD-*Susp* islets produced NO after treatment with cytokines **(Fig. 5B)**, demonstrating no change in the synthesis of reactive nitrogen species.

To evaluate if beta cells demonstrated advanced survival *in vivo* to lysis mediated by autoreactive $CD8^+$ T cells, sub-lethally irradiated NOD and NOD-*Susp* female mice were adoptively transferred with splenocytes from NOD-AI4a/b transgenic mice. There was no significant difference in the rate or overall incidence of diabetes **(Fig. 5C)** as 66% NOD and 50% NOD-*Susp* mice developed diabetes by 15 days after adoptive transfer.

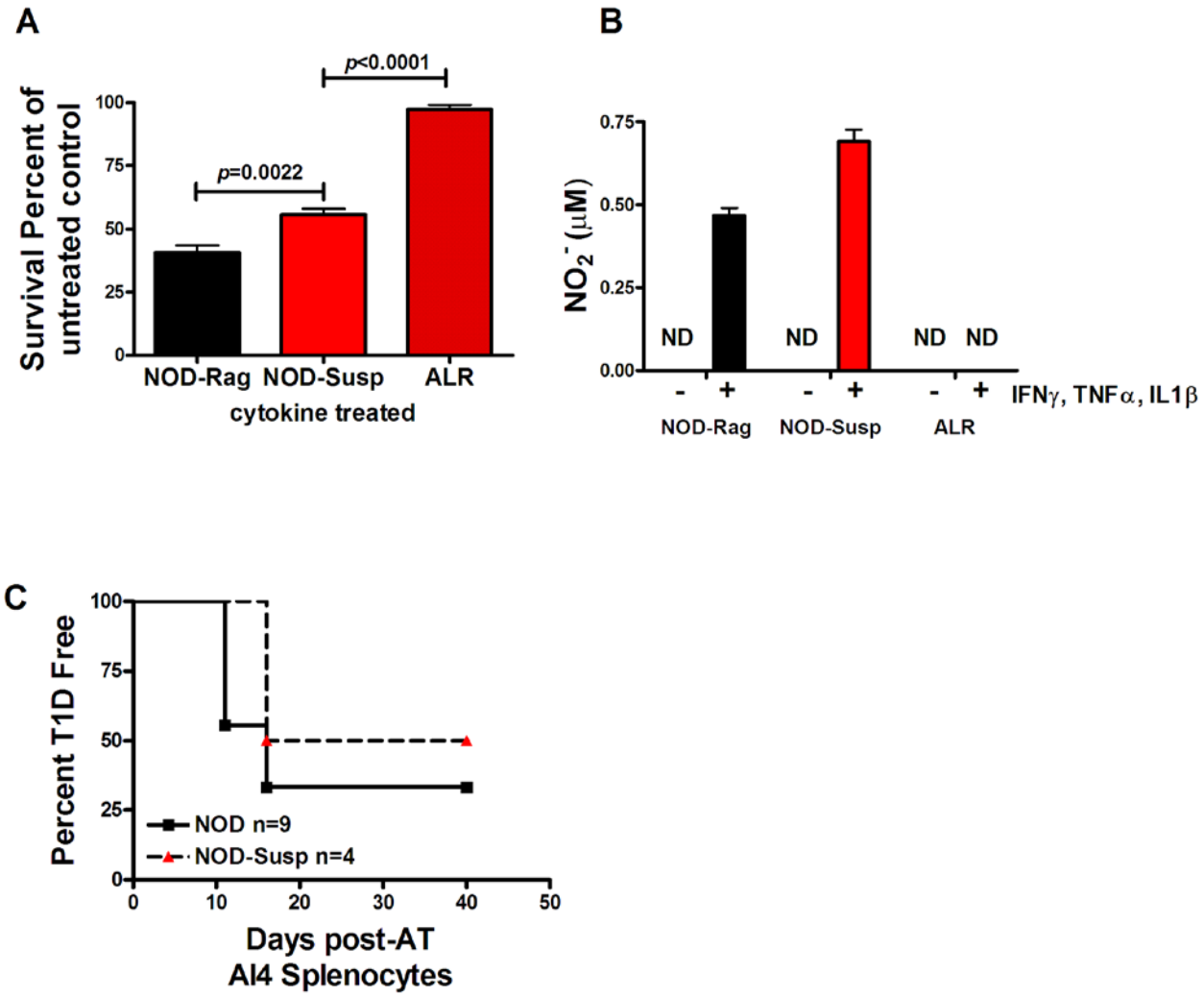

Figure 5: Susceptibility of islets to proinflammatory mediators. Cultured islets from NOD.*Rag*, NOD-*Susp*, and ALR mice were treated with cytokines, IFN-γ, IL-1β, and TNF-α. Islets susceptibility to (A) proinflammatory cytokine-mediated damage and (B) induced NO production after treatment. Data representative of 3 independent experiments performed in triplicate. (C) Splenocytes (2 x 10^7 cells) from NOD-AI4 donors were transferred to sub-lethally (7.5 Gy) irradiated NOD and NOD-*Susp* recipients. Mice were considered diabetic after 2 consecutive readings of blood glucose above 250 mg/dL. ND not detected

2.4.5 NOD-*Susp* mice exhibit ALR-like elevation in SOD1 activity and reduction of NOX oxidative burst.

NOD-*Susp* mice demonstrated elevated SOD1 activity (data not shown) similar to that of ALR, as well as reduced oxidative burst by stimulated macrophages **(Fig. 6)** and neutrophils (data not shown) as measured by superoxide-driven conversion of DHR123.

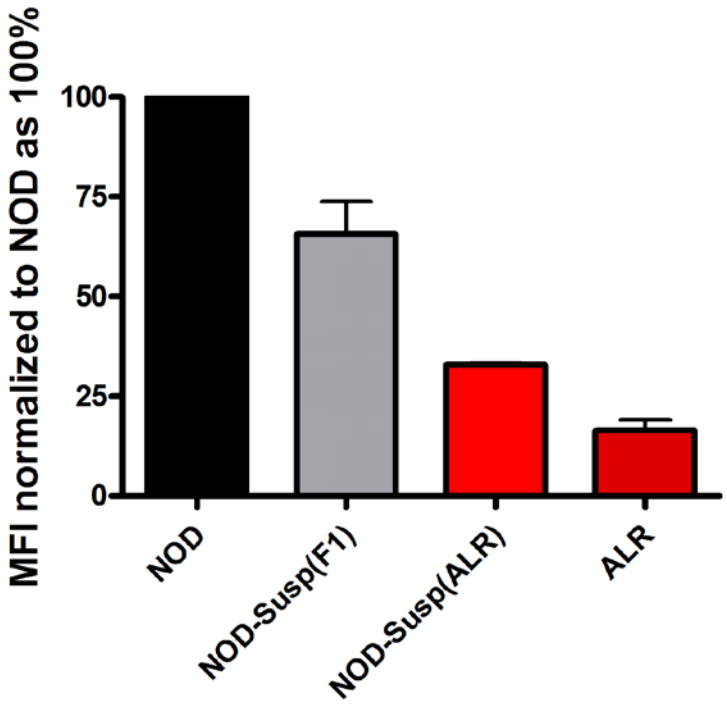

Figure 6: NOD-*Susp* congenic mice exhibit reduced oxidative burst. Macrophages collected from bone marrow were stimulated with PMA. ROS-driven conversion of DHR123 was monitored via flow cytometry.

2.4.6 $CD4^+$ and $CD8^+$ T cells from NOD-*Susp* lose diabetogenic potential

In addition to a defect in macrophage and neutrophil superoxide production, purified $CD4^+$ T cells from NOD-*Susp* mice failed to produce superoxide after TCR crosslinking **(Fig**

7A). Previous genetic studies observed a co-dominant inheritance, witnessed with intermediate SOD1 activity and respiratory burst from heterozygous mice. However, $CD4^+$ T cells exhibit a complete loss of stimulated ROS production, suggesting that the modest elevation of SOD1 dismutation is sufficient to eliminate superoxide produced. As enhanced beta cell protection was not providing full protection **(Fig. 5)** and T cells lacked superoxide production after TCR crosslinking **(Fig. 7A)**, the diabetogenic potential of the T cells was evaluated. Purified $CD4^+$ and $CD8^+$ T cells from NOD and NOD-*Susp* donors were adoptively transferred to NOD-*Scid* recipients. NOD-*Susp* T cells failed to induce diabetes as 100% of recipients were T1D-free, compared to 12% of controls **(Fig. 7B)**. Therefore, while *Susp* has a clear impact on myeloid cells, the role of this linkage in T1D resistance is due to a change in the autoreactive potential of T cells.

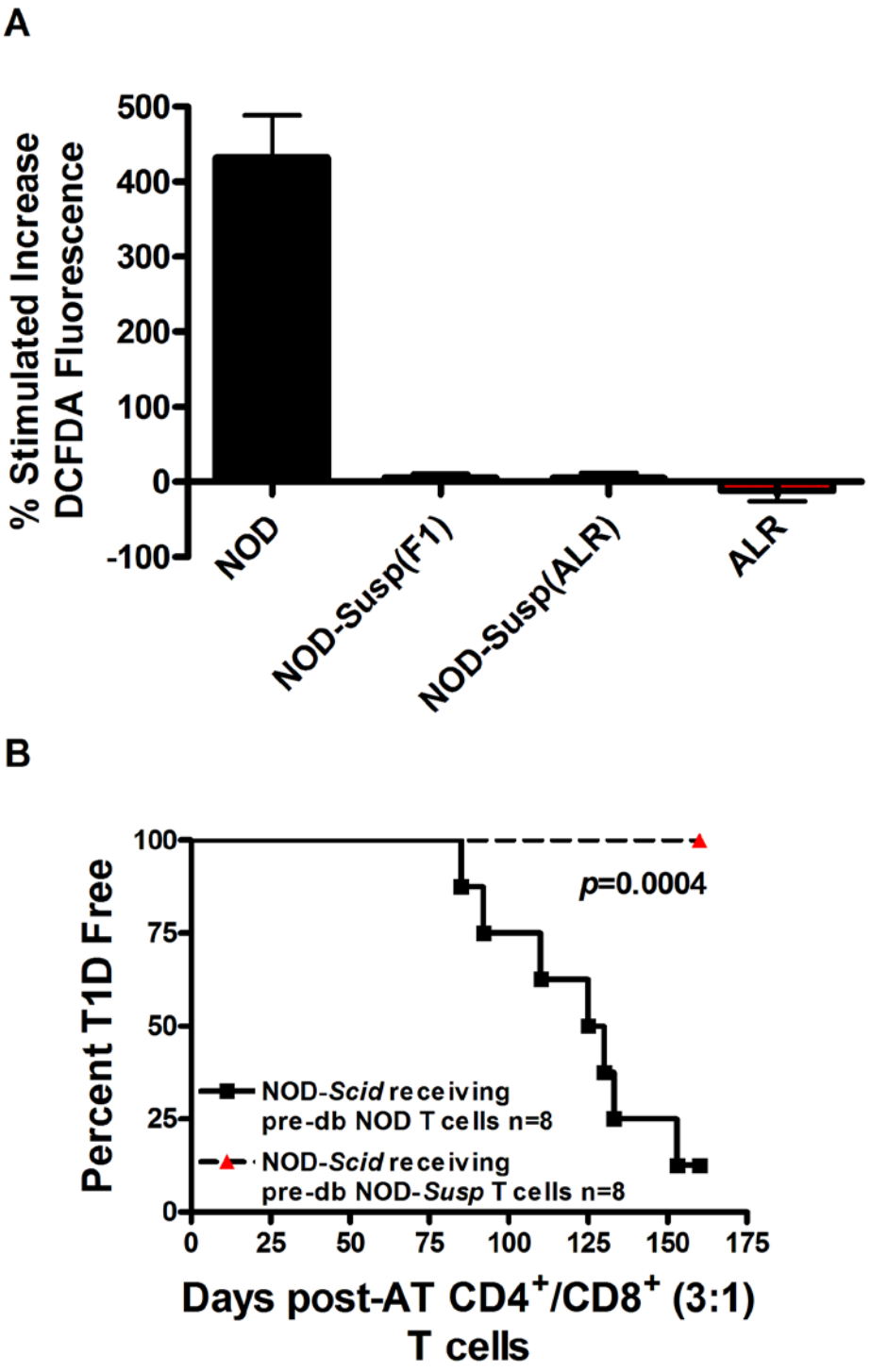

Figure 7: NOD-*Susp* immune system fails to transfer T1D to immune deficient hosts. T cell ROS production was measured by labeling purified $CD4^+$ T cells with CM-H_2DCFDA. Cells were activated by adding hamster anti-mouse CD3 and then cross-linked with rabbit anti-hamster IgG. Cells were analyzed at 0, 30, and

60min. (A) ROS generation was determined by the increase in CM-H_2DCFDA fluorescence upon anti-CD3 stimulation over unstimulated control. (B) Purified $CD4^+$ and $CD8^+$ T cells at a ratio of 3:1 (10^7 cells) from 8 week old prediabetic donor NOD and NOD-*Susp* female mice were transferred i.p. to NOD-*Scid* hosts.

2.5 DISCUSSION

The ALR mouse represents a unique model to study the impact of ROS scavenging as well as modulation of free radical production on type 1 diabetes development (227, 228, 232, 233). Elevated free radical defenses are linked with ALR islet resistance to free radical toxins, proinflammatory cytokines, and diabetogenic immune mediators. Specifically, ALR exhibits a constitutive and systemic elevation in SOD1 activity, despite no observed differences in SOD1 sequence, expression, or protein content **(Fig. 2)**. However, elevated SOD1 activity is associated with increased stability of the active homodimer. After treatment with DTT, ALR SOD1 dimers remain active compared to controls, where dimer activity is lost due to the disruption of the necessary disulfide bridges. This suggests that under stressful conditions, such as inflammation, ALR SOD1 stability may be enhanced resulting in continued SOD1 function.

Previous reports described an inverse correlation of elevated hepatic SOD1 activity with decreased oxidative burst by neutrophil and macrophage NADPH oxidase (112, 230). As increased SOD1 activity was also extended to bone marrow populations **(Fig. 3A)** we propose that increased superoxide dismutation was resulting in the suppression of superoxide production by immune cells, or at least in our ability to measure superoxide generation. After PMA stimulation, ALR bone marrow cells demonstrate no measurable increase in superoxide release, however, there is a significant increase in the oxygen consumed **(Fig. 3B and 3C)** suggesting

oxygen was being converted to superoxide. When SOD1 is inhibited with KCN, ALR superoxide production is elevated, demonstrating that NOX complex is functional in the ALR and that the reduction in superoxide being produced by the ALR cells results from the increased scavenging by SOD1. This heightened free radical dismutation significantly alters the function of both innate and adaptive immune cells.

Genetic segregation analyses localized *Susp* to Chr. 3 (112, 204). To study the role of elevated SOD1 and reduced NOX in a T1D-prone model, the ALR-derived *Susp* locus was congenically introduced on the NOD background. ALR genome on Chr. 3 was dominantly protective against T1D development as mice heterozygous and homozygous for *Susp* were 100% diabetes free, compared to littermate controls, which had an onset similar to that of NOD population **(Fig. 4A)**. Histological analysis of pancreata demonstrated little to no insulitis in congenic animals **(Fig. 4B-C)**, suggesting there is a loss in the accumulation of leukocytes at the site of inflammation associated with ALR Chr. 3 genome. The finding of an almost complete absence of insulitis was not expected, as the females of the parental ALR strain exhibit mild insulitis (112).

While the congenic segment is large, encompassing ~92 Mbp on Chr. 3, these results demonstrate that ALR alleles provide significant modifications to diabetes susceptibility. Within this region are several previously mapped loci including, *Idd3, 10, 17, 18.* However, the IL-2 allele, the candidate for *Idd3*, is identical in ALR and NOD (112), and the diagnostic markers for *Idd 10, 17,* and *18* are non-polymorphic comparing the strains, suggesting that the ALR-derived locus on Chr. 3 may be novel rather than resulting from alleles at *Idd3, 10, 17,* or *18*. Mice with smaller congenic segments will allow for further evaluation of T1D resistance provided by ALR-derived Chr. 3 alleles.

To isolate the mechanism of protection to either the islet or immune system, islet viability after cytokine treatment was assessed. While exhibiting slightly higher viability compared to NOD.*Rag* controls, NOD-*Susp* islets were not fully protected from cytokine-mediated damage as the ALR islets **(Fig. 5A** and (228, 232)**)**. Elevations in SOD1 activity are witnessed in pancreata of ALR mice and there are also decreases in other ROS and RNS sources. Unlike ALR, after cytokine treatment NOD-*Susp* islets produced large amounts of NO, a potent contributor to beta cell toxicity **(Fig. 5B)**.

Type 1 diabetes is considered a T cell mediated disease. In previous studies, ALR islets were demonstrated to resist destruction both *in vivo* and *in vitro* by autoreactive CD8 T cells (232). To determine if the *Susp* region was associated with enhanced beta cell resistance to autoreactive cytotoxic T lymphocytes we performed adoptive transfer experiments using splenocytes from NOD mice transgenic for the diabetogenic AI4 T cell receptor (236). *In vivo*, NOD-*Susp* islets did not demonstrate enhanced protection to inflammatory mediators as mice were susceptible to AI4 $CD8^+$ T cells **(Fig. 5C)**. Therefore, *Susp* does not provide obvious resistance to T1D at the level of the pancreatic islet, and similar to the majority of the linkages associated with T1D, likely contributes to diabetes resistance through the modification of cells of the immune system.

NOD-*Susp* congenic mice exhibited ALR-like elevation in SOD1 as well as decreased free radical production by immune cells, including neutrophils, macrophages **(Figs. 3 and 6)** and $CD4^+$ T cells **(Fig. 7A)**. Therefore, the beta cell reactivity of NOD-*Susp* T cells was assessed via adoptive transfer to T1D-prone NOD-*Scid* recipients. NOD-*Susp* immune cells failed to induce diabetes in a susceptible host demonstrating a loss of islet-directed autoreactivity **(Fig. 7B)**. Taken together these data suggest that the protective role of this Chr. 3 linkage is by modulating

immune cell reactivity responsible for the aberrant immune response associated with beta cell-directed autoimmunity.

Free radical signaling is an important regulator of immune cell activation and cytokine synthesis (202, 207, 208, 210). We have previously described a role for NOX superoxide production and antioxidant activity in directing proinflammatory cytokine production and diabetes susceptibility (202, 207, 208). Evidence in animal models demonstrates a protective role for antioxidants, protecting islets from apoptosis, rejection, and autoimmunity (222, 224, 225). However, transgenic over-expression of antioxidants in beta cells via the rat insulin promoter has been less efficacious in preventing spontaneous T1D development (225, 237, 238), whereas systemic elevation of antioxidants has been effective in delaying or reducing T1D (202, 210, 232, 239). This suggests mechanisms other than islet-specific ROS scavenging were conferring resistance. Specifically, modulation of immune reactivity most likely was accounting for decreased autoimmunity in these studies. Our data suggests that the protection afforded by elevated SOD1 is not by significant enhancement of beta cell survival, but rather by modifying T cell reactivity. The T1D protection witnessed in the NOD-*Susp* mice highlights an important role for antioxidant regulation of free radical signaling in immune cells and autoreactive T lymphocytes.

3.0 SUPEROXIDE PRODUCTION IS CRITICAL FOR THE INDUCTION OF AUTOREACTIVITY AND T1D

This manuscript has been submitted for publication to *Diabetes*.

3.1 ABSTRACT

The role of reactive oxygen species (ROS) and their scavenging in the pathogenesis of Type 1 Diabetes (T1D) have garnered considerable controversy. We previously linked decreased monocyte ROS with diabetes resistance in the ALR mouse, suggesting that free radical production by the immune system is important for diabetes. NOD-*Ncf1*^{m1J} mice with a genetic ablation of NOX activity had reduced and delayed T1D compared to NOD mice. To determine the required cellular sources of ROS we used antibody depletion and adoptive transfer experiments. After receiving treatment female mice were monitored for hyperglycemia and overt diabetes. Depletion of macrophages and neutrophils fully protected NOD mice from T1D. However, elimination of neutrophils alone showed no significant reduction or delay in incidence, demonstrating that neutrophils are dispensable for T1D progression. Induction of T1D in NOD-*Scid* mice by adoptive transfer with diabetic NOD-*Ncf1*^{m1J} splenocytes was significantly delayed compared to diabetic NOD splenocytes, suggesting macrophage ROS and modulation of effector responses are critical for T1D. The adaptive immune response was also altered by the absence of

NOX activity, as purified T cells from NOD-*Ncf1*^{m1J} mice failed to induce diabetes. These data demonstrate that the impaired autoreactive response of NOX-deficient NOD-*Ncf1*^{m1J} immune system results from an alteration in the APC-T cell axis rather than failure of neutrophils to act as effector cells.

3.2 INTRODUCTION

Destruction of pancreatic beta cells is mediated by aberrant immune responses to islet antigens leading to T1D. During the early stages of disease, an insulitic infiltrate consisting of macrophages, dendritic cells (DC), T cells, and B cells accumulates in the pancreas (5, 6). Effector mechanisms, including direct T cell cytotoxicity and indirect methods mediated by leukocytes, contribute to beta cell destruction and overt diabetes. Production of reactive oxygen species (ROS) has been proposed to be an important contributor to beta cell loss during T1D pathogenesis. Endogenous free radicals produced by the beta cell in response to cytokines are one source of cytotoxic ROS. IFN-γ in combination with IL-1β and TNF-α is cytotoxic to beta cells, due to increased production of nitric oxide and superoxide. However, the roles of cellular sources of ROS during the development of spontaneous T1D have not been fully defined (133, 176).

NADPH Oxidase (NOX), a multi-component enzymatic complex, is a major source of free radicals and is important for the effector function of neutrophils and macrophages (141-143). Islet-infiltrating macrophages release high levels of ROS, including superoxide via NOX. Defects in NOX function have been associated with increased susceptibility to autoimmunity in

experimental allergic encephalomyelitis and collagen-induced arthritis. In addition to contributing to toxicity, free radicals are also potent signaling molecules and are important in adaptive immune responses (140, 177, 202, 208). Recent work has demonstrated that exogenous as well as endogenous sources of ROS are involved in initiating and dictating cytokine responses of $CD4^+$ T cells (Tse and Thayer, *In Press*) (176, 187, 190, 202). Our findings in the ALR mouse suggest a role for increased free radical scavenging and reduced superoxide production in modifying diabetogenic reactivity of T cells. NOD mice containing the ALR-derived *Suppressor of superoxide production (Susp)* locus are protected from T1D and T cells lose diabetogenic effector capabilities when transferred to susceptible hosts. To study the role of superoxide production via NOX in a T1D-prone mouse model, independent of other ALR-derived phenotypes, a mutation in $p47^{phox}$ subunit was congenically introduced into the Non-obese diabetic (NOD) mouse (NOD-$Ncf1^{m1J}$).

Genetic ablation of NOX protects against T1D development, as NOD-$Ncf1^{m1J}$ mice have reduced incidence and delayed diabetes onset. To determine the innate immune cellular sources of ROS essential for T1D pathogenesis, we depleted neutrophils and macrophages from NOD mice. Here we show that macrophages are essential for T1D induction while neutrophils are dispensable. Additionally, NOD-$Ncf1^{m1J}$ mice were protected from T1D after adoptive transfer of BDC-2.5 T cells, demonstrating a requirement of NOX during $CD4^+$ T cell-mediated autoreactivity. NOX-deficient beta cells were not fully protected as NOD-$Ncf1^{m1J}$ islets were susceptible to cytokine mediated damage and mice developed diabetes induced by AI4 $CD8^+$ T cells. We have previously shown that NOX function is important for T helper cell lineage development and cytokine synthesis (202, 207, 208). Here we report the reduced diabetogenic capabilities of NOX-deficient leukocytes as purified splenocytes and T cells from NOD-$Ncf1^{m1J}$

mice had delayed transfer kinetics of T1D in contrast to NOD mice. Therefore, ROS production by macrophages and T cells is essential for the development and effector function of proinflammatory responses mediating beta cell destruction.

3.3 METHODS

3.3.1 Animals

NOD/ShiLtJ, NOD.B6-*Ncf1*$^{m1J/m1J}$ [NOD-*Ncf1*^{m1J}] mice were bred and housed in the University of Florida or the Children's Hospital of Pittsburgh facility under specific pathogen-free conditions. NOD.CB17-*Prkdc*^{scid}/J [NOD-*Scid*], C57BL/6-*Ncf1*^{m1J} [B6-*Ncf1*] and C57BL/6.NOD-(*D17Mit21-D17Mit10*)/LtJ [B6-*H2*^{g7}] mice were purchased from The Jackson Laboratory (Bar Harbor, ME). NOD.129S7 (B6)-*Rag1*^{tm1Mom}/J [NOD.*Rag*], NOD.Cg-*Rag1*^{tm1Mom}Tg (TcraAI4)1Dvs/DvsJ [NOD-AI4a] and NOD.Cg-*Rag1*^{tm1Mom}Tg (TcrbAI4)1Dvs/DvsJ [NOD-AI4b] were purchased from The Jackson Laboratory (Bar Harbor, ME) and bred in our mouse facility. F1 hybrid progeny from matings of NOD-AI4a with NOD-AI4b [NOD-AI4a/b] developed diabetes between 3-5 weeks of age. All mice were housed in specific pathogen-free facilities and approved by the Institution Animal Care and Use Committee at the University of Florida or the Children's Hospital of Pittsburgh.

3.3.2 Materials

Depleting antibodies anti-Gr1 [RB6-8C5] and anti-Ly6g [1A8] purchased from Bio X Cell (West Lebanon, NH) are both Rat IgG2 antibodies. Fluorescently labeled antibodies, Pacific blue labeled anti-CD11b (M1/70), APC labeled anti-F4/80 (BM8), and PE labeled anti-CD8 (53-6.7) were purchased from eBioscience (San Diego, CA). PE labeled anti-Ly6G (1A8), APC labeled anti-CD11b (M1/70) and FITC labeled anti-CD11c (HL3) were purchased from BD Pharmingen (San Jose, CA). Pacific blue labeled anti-CD4 (GK1.5) and APC/Cy7 labeled anti-B220 (RA3-6B2) were purchased from Biolegend (San Diego, CA).

3.3.3 Construction of the B6-*H2*^{g7}-*Ncf1*^{m1J} and NOD.*Ncf1*^{m1J} mouse strains

The spontaneous null allele *Ncf1*^{m1J} (Chromosome 5) was congenically introgressed into the NOD genome to ablate NOX superoxide production by first generating F2 mice from outcrosses of B6-*Ncf1*^{m1J} with B6-*H2*^{g7}. The subsequent B6.*H2*^{g7}-*Ncf1*^{m1J} mice were outcrossed and backcrossed to NOD for 10 generations. To eliminate contaminating chromosomal segments, genotyping was performed by PCR amplification of 94 polymorphic microsatellite primers (Invitrogen) covering all 19 autosomes for the first six generations as described previously. By N6 mice were homozygous for NOD genome at all loci save those in linkage with *Ncf1* on Chr. 5. From N6 until N10 genotyping was performed with markers on Chr. 5 allowing for mice with the smallest possible congenic segment to be bred. At N10 these marker-assisted or “speed” congenic mice were intercrossed to generate mice that were homozygous for the *Ncf1*^{m1J} allele.

DNA was obtained from murine tail biopsies as described previously. *Ncf1* exon 8-specific PCR primers (forward: 5'-biotin-TAG AAA GGG AAA GCC AGA AAG AAT-3', reverse: 5'-ACG CTT TGA TGG TTA CAT ACG GT-3') were used to distinguish single nucleotide polymorphisms between the wild type allele and a mutation in the splice site of exon 8 as previously described (172). DNA sequencing was performed using pyrosequencing (PSQ 96MA, Pyrosequencing, AB). The pyrosequencing primer (5'-ACG CTT TGA TGG TTA CAT ACG GT-3') was used for sequencing. Pyrosequence data were quantified and background corrected using PSQ 96MA version 2.0.2 software (Pyrosequencing, AB).

3.3.4 Measurement of superoxide production

Bone marrow was collected from age-matched NOD and NOD-*Ncf1*^{m1J} female mice and red blood cells were removed on a Histopaque-1119 gradient as previously described (230). In HBSS containing 145 μM cytochrome C, $1x10^5$ cells were stimulated with PMA (98 nM) at 37°C. Reduction of cytochrome C was measured at 550 nm at 1 min intervals for 45 min. The maximum rate of reduction was calculated by linear regression analysis. Purified SOD1 (0.5 U/mL) was used to confirm specificity of superoxide production.

3.3.5 Measurement of oxygen consumption

Bone marrow was collected from age-matched female mice and red blood cells were removed on a Histopaque-1119 gradient as previously described (230). The Oxygraph-2K (Oroboros Instruments Innsbruck, Austria) was calibrated for basal oxygen levels with HBSS and after the addition of sodium hydrosulfite, following manufacturer's instructions. A total of

$2x10^7$ cells were pretreated with 2 mM KCN or HBSS for 15 min at room temperature. Cells were resuspended in 2 mL HBSS and loaded into the chamber of the Oxygraph-2K at 37°C. Samples were stimulated with 1 µM PMA and oxygen concentration and rate of consumption were monitored for 30 min.

3.3.6 Western immunoblotting

Whole cell lysates were separated on a 4-20% gradient SDS-PAGE gel and transferred onto 0.45 µm charged PVDF membranes. The membranes were incubated overnight at 4°C with antibodies against Stat4, Stat1α, T-bet, Stat3, or β-actin and exposed to the appropriate secondary antibody conjugated to horseradish peroxidase (Jackson ImmunoResearch). Chemiluminescence was detected with ECL plus (Amersham Pharmacia). Image J software (National Institutes of Health) was used to generate densitometry data.

3.3.7 Spontaneous incidence

At 8 weeks of age, NOD and NOD-*Ncf1*^{m1J} female mice were enrolled and monitored for diabetes onset with weekly urinalysis using Diastix [Bayer (Elkhart, IN)]. Mice positive for glucosuria were monitored daily thereafter for hyperglycemia using One Touch Ultra 2 meters [Life Scan, Inc (Milpitas, CA)]. Any mouse with measured blood glucose levels on consecutive days >250 mg/dL were diagnosed with type 1 diabetes.

3.3.8 Islet isolation and culture with cytokines

Pancreatic islets from age-matched female NOD.*Rag* and NOD-*Ncf1*^{m1J} isolated (235) and cultured with IFN-γ, IL-1β, and TNF-α as previously described (232). Islet NO production was measured and cell viability was assessed via MTT assay as previously reported (228).

3.3.9 Transfer of AI4 splenocytes

At 3-4 weeks of age, NOD-AI4a/b donors were sacrificed and splenocytes were harvested. After the red blood cells were lysed with Gey's solution live cells were counted and diluted to a concentration of 10^8 cells per mL. A total of 2 x 10^7 cells in sterile PBS were injected via the tail vein into sub-lethally irradiated eight week old NOD and NOD-*Ncf1*^{m1J} females [dose of 7.5 Gy delivered using X-RAD 320 (Precision X-ray, North Branford, CT) as previously described. Mice were monitored every other day for the onset of diabetes as described above.

3.3.10 Transfer of BDC-2.5 T cell clones

Cultures of BDC-2.5 T cells were collected and expanded *in vitro* as previously described (210) for adoptive transfer experiments. NOD and NOD-*Ncf1*^{m1J} mice were injected i.p. with 10^7 BDC-2.5 T cells between 3-7 days of age. Mice were monitored daily by urinalysis, using Diastix, for the onset of diabetes.

3.3.11 Adoptive transfer

Diabetic (20 weeks old) or pre-diabetic (8 weeks old) NOD and NOD-*Ncf1*^{m1J} donors were used for adoptive transfer experiments. Splenocytes were harvested and red blood cells were lysed using Gey's solution. Splenocytes, 2 x 10^7 cells in PBS, were transferred i.p. to 8 week old NOD-*Scid* recipients. Additionally, $CD4^+$ and $CD8^+$ T cells were purified by negative selection with magnetic beads according to the manufacturer's protocol using a $CD4^+$ T cell isolation kit or a $CD8^+$ T cell isolation kit (Miltenyi Biotec), respectively. Purity, over 96%, was confirmed by flow cytometric analysis. $CD4^+$ and $CD8^+$ T cells were mixed at a ratio of 3:1 and 10^7 cells were transferred i.p. to 8 week old NOD-*Scid* recipients. Mice were monitored weekly for diabetes onset as described above. Engraftment of cells was confirmed by flow cytometry.

3.3.12 Antibody depletion studies

Depletion studies were initiated at 4 weeks of age and were carried out until the onset of T1D, as described above, or until 35 weeks of age. Female NOD mice were treated i.p. with antibody diluted in sterile PBS three times per week. The dose for either the anti-Gr-1 (RB6-8C5) or anti-Ly6g (1A8) depleting antibodies was 500 µg on Monday and Wednesday as well as 750 µg on Friday of each week (240). The volume of all injections was 100 µL. Depletion of macrophages and neutrophils in peripheral blood was confirmed monthly by flow cytometry. Bone marrow, splenocytes, and peripheral blood were analyzed via flow cytometry at sacrifice.

3.3.13 Flow cytometry

Peripheral blood samples were lysed with Gey's solution twice and resuspended in 100 µl HBSS for staining. Gey's treated splenocytes, ficol separated bone marrow suspensions, or purified T cells were counted and resuspended in HBSS at 2 x 10^7 cells/mL. Approximately 10^6 cells were labeled with antibodies at the proper dilution. Fluorescence was measured using LSR Fortessa (BD Bioscience, San Jose, CA) and analyzed using FACSDiva 6.0 software (BD Biosciences).

3.3.14 Statistics

GraphPad Prism (GraphPad Software, Inc, (La Jolla, CA)] was used for calculating statistical differences. Significance between mean values was determined using the Student's *t* test, with $p<0.05$ considered significant. Kaplan-Meier survival analysis was used to evaluate diabetes onset.

3.4 RESULTS

3.4.1 *Ncf1* mutation ablates NOX superoxide production from bone marrow populations

To study the role of ROS in the pathogenesis of T1D, we generated NOD mice with a genetic ablation of NOX superoxide production by congenic introduction of a mutant $p47^{phox}$ subunit (*Ncf1)* of NOX. PMA stimulation of NOD bone marrow cells exhibited elevated

superoxide production (p<0.0001), however there was no increase in superoxide production after PMA stimulation of cells isolated from NOD-*Ncf1*^{m1J} mice as measured by cytochrome c reduction (**Fig. 8A)** and oxygen consumption (**Fig. 8B**), confirming ablation of NOX function. Mice with the *Ncf1*^{m1J} mutation had equal numbers of neutrophils (Ly6G^{+}CD11b^{+}) **(Figure 8C)** and macrophages (Ly6G^{-}CD11b^{+}) **(Figure 8E)** when compared to *Ncf1* intact mice of the same strain, but NOD, NOD-*Ncf1*^{m1J}, and B6-*H2*^{g7} mice did exhibit reduced neutrophils when compared to B6 or ALR mice **(Figure 8C)**. Oxidation of DHR 123 to rhodamine was significantly absent in both neutrophils **(Figure 8D)** and macrophages **(Figure 8F)** from NOD-*Ncf1*^{m1J} and B6-*H2*^{g7}-*Ncf1*^{m1J} mice. NOD and B6-*H2*^{g7} derived neutrophils and macrophages exhibited a normal oxidative burst. The inability of neutrophils and macrophages to generate a sufficient respiratory burst in the NOD-*Ncf1*^{m1J} mice was due to the absence of the p47^{phox} protein. Immunoblot analysis of whole cell lysates from purified macrophage and neutrophil (data not shown) cell populations demonstrated that the Ncf1 protein was absent in both cell types **(Figure 8G)**.

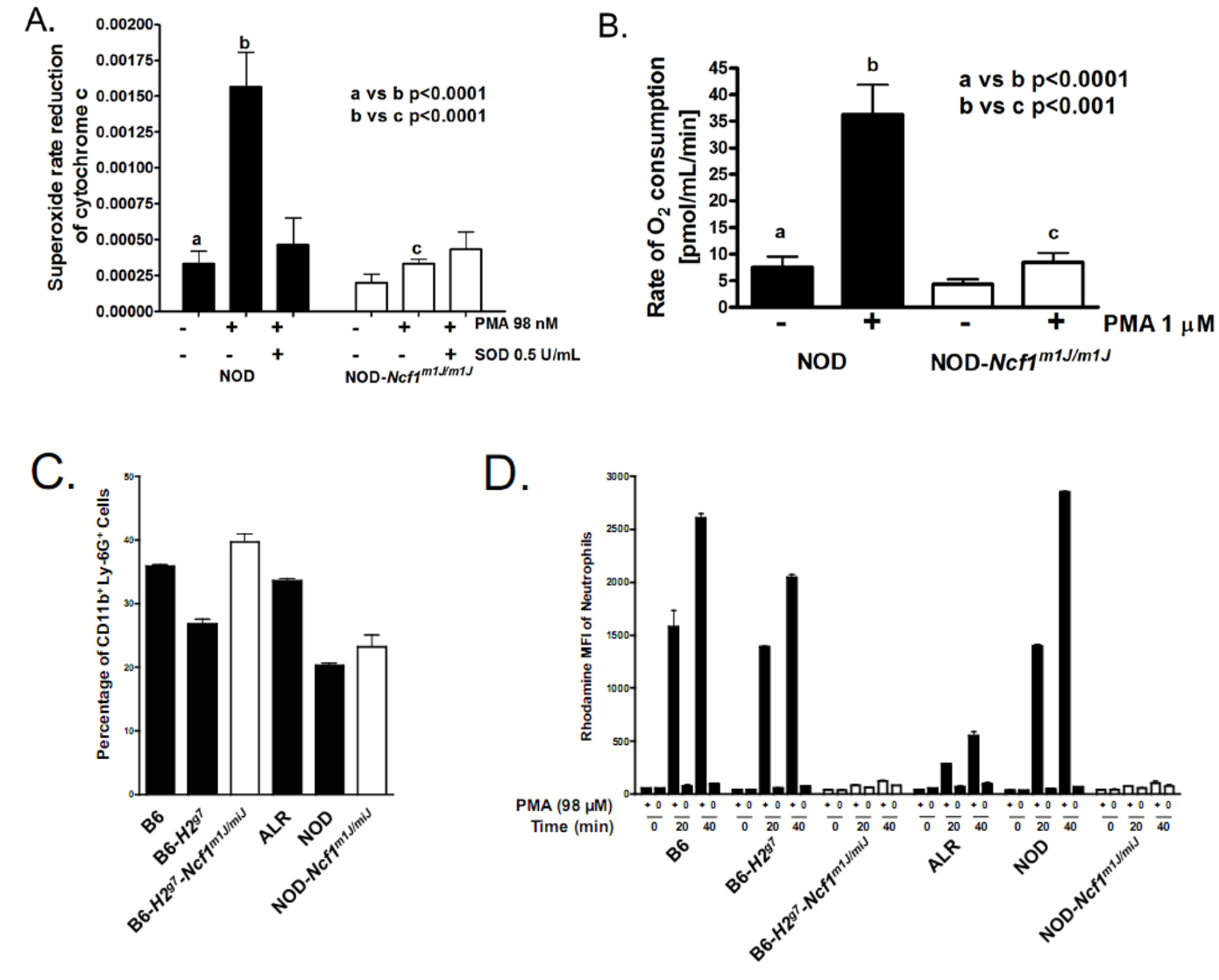
A.
Superoxide rate reduction of cytochrome c
0.00200
0.00175
0.00150
0.00125
0.00100
0.00075
0.00050
0.00025
0.00000
a
b
c
a vs b p<0.0001
b vs c p<0.0001
PMA 98 nM
SOD 0.5 U/mL
NOD
NOD-Ncf1m1J/m1J
B.
Rate of O2 consumption [pmol/mL/min]
45
40
35
30
25
20
15
10
5
0
a
b
c
a vs b p<0.0001
b vs c p<0.001
PMA 1 µM
NOD
NOD-Ncf1m1J/m1J
C.
Percentage of CD11b+Ly-6G+ Cells
50
40
30
20
10
0
B6
B6-H2g7
B6-H2g7-Ncf1m1J/m1J
ALR
NOD
NOD-Ncf1m1J/m1J
D.
Rhodamine MFI of Neutrophils
3000
2500
2000
1500
1000
500
0
PMA (98 µM)
Time (min)
0
20
40
B6
B6-H2g7
B6-H2g7-Ncf1m1J/m1J
ALR
NOD
NOD-Ncf1m1J/m1J

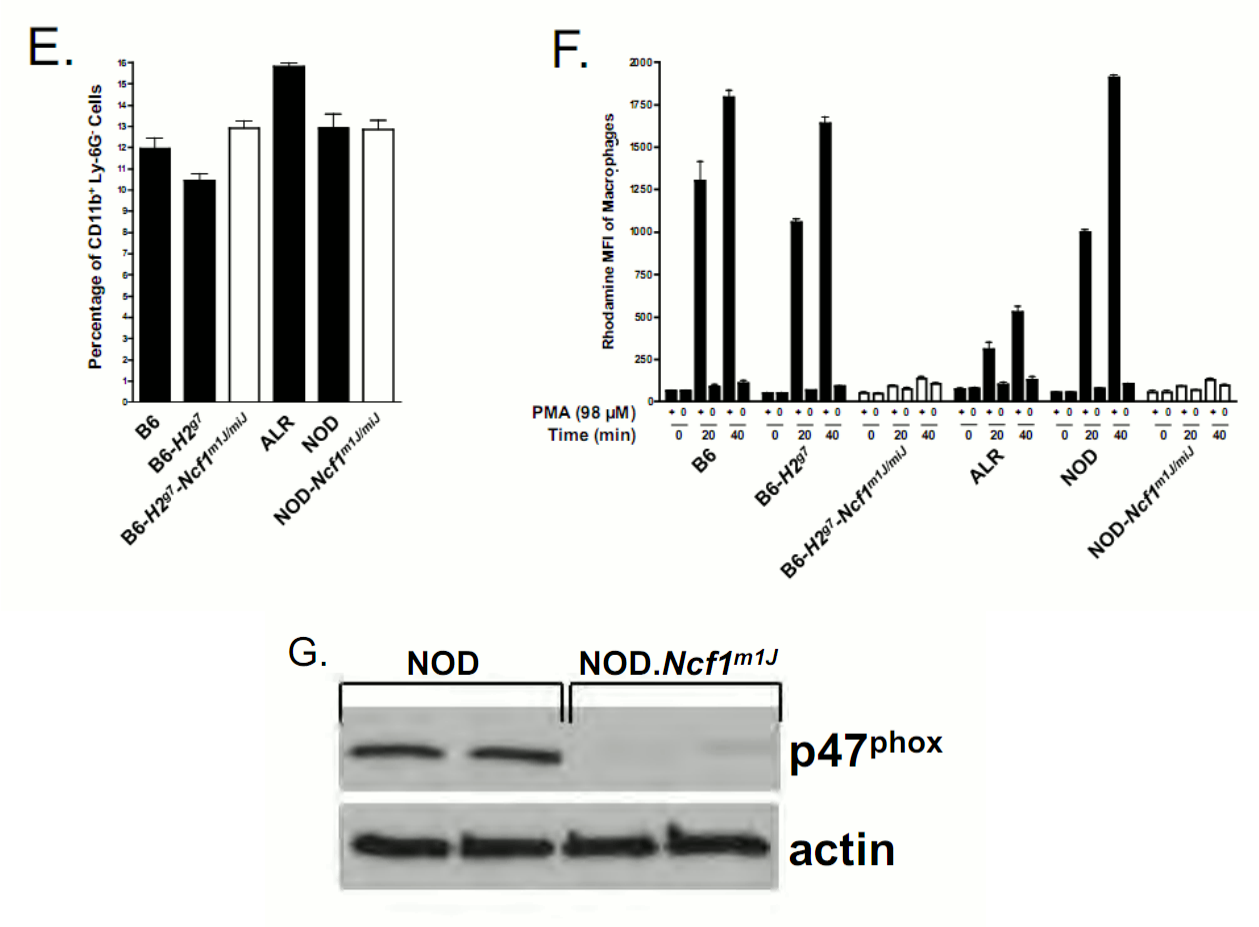

Figure 8: *Ncf1*^{m1J} mutation decreases the respiratory burst. Bone marrow from NOD and NOD-*Ncf1*^{m1J} mice was stimulated with PMA (98 nM). (A) Superoxide production was evaluated by measuring rate reduction of cytochrome C . Purified SOD1 (0.5 U/mL) was added to confirm production of superoxide. (B) Oxygen consumption was measured with an oxygen electrode for 30 mins. Results are from 5 independent experiments. The percentage of bone marrow neutrophils (C) and macrophages (E) from C57BL/6.H2^{g7}, C57BL/6.H2^{g7}.*Ncf1*^{m1J}, C57BL/6, ALR, NOD, and NOD.*Ncf1*^{m1J} mice was assessed by flow cytometry with gating for macrophage- (Ly6G^{-} CD11b^{+}) or neutrophil-specific (Ly6G^{+} CD11b^{+}) populations. The respiratory burst capacity of bone marrow neutrophils (D) and macrophages (F) was assessed by loading 5x10^{6} cells/mL with 0.99 M dihydrorhodamine and stimulated with 98 nM PMA for 40 minutes. The oxidation of dihydrorhodamine to rhodamine was assessed by flow cytometry with gating for macrophage- (Gr1^{-} CD11b^{+}) or neutrophil-specific (Gr1^{+} CD11b^{+}) populations. (G) Whole cell lysates of cell sorted macrophages were used in an immunoblot analysis for p47^{phox} and actin expression.

3.4.2 *Ncf1* mutation ablates respiratory burst from T cells

T cells express a $p47^{phox}$ containing NADPH oxidase and polyclonal anti-CD3 stimulation elicits ROS production from primary T cells (181). Targeted deletion of *Ncf1* eliminates T cell ROS production (181), therefore we tested if the $Ncf1^{m1J}$ allele also inhibited anti-CD3 stimulated ROS production from $CD4^+$ T cells in the NOD mouse. When purified $CD4^+$ T cells from NOD mice were incubated with anti-CD3 there was a significant increase in ROS production by these $CD4^+$ cells **(Figure 9A)**. In contrast, stimulation of NOD-$Ncf1^{m1J}$ $CD4^+$ T cells did not lead to an increase in oxidation of the fluorescent indicator **(Figure 9A)**. This lack of ROS production was not the result of low $CD4^+$ T cell numbers as no differences were observed when comparing NOD and NOD-$Ncf1^{m1J}$ T cells **(Figure 9B)**.

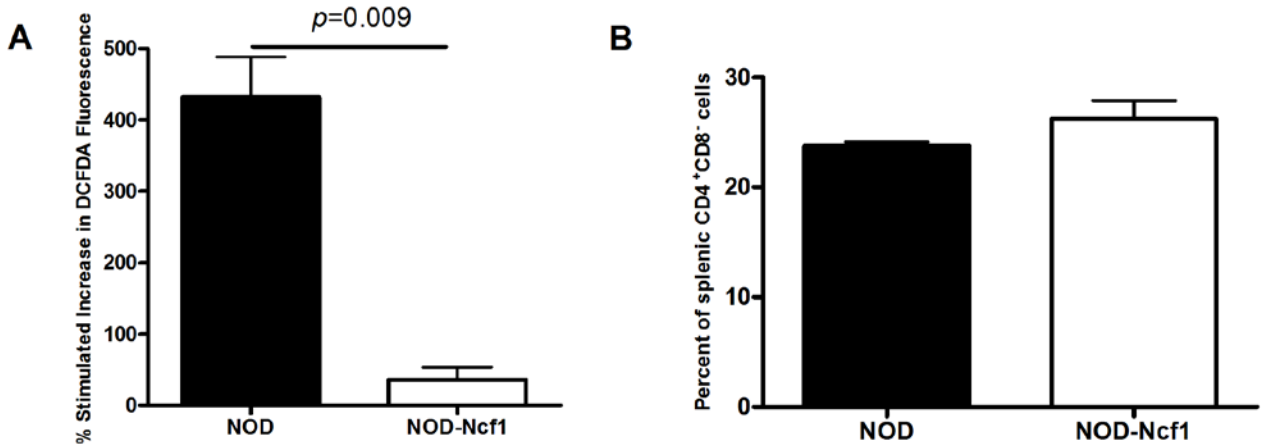

Figure 9: $Ncf1^{m1J}$ mutation decreases the respiratory burst capacity splenic T cells without decreasing the percentage of cells. T cell ROS production was measured in by labeling purified $CD4^+$ T cells with CM-H_2DCFDA. Cells were activated by adding hamster anti-mouse CD3 and then cross-linked with rabbit anti-hamster IgG. Cells were analyzed at 0, 30, and 60min. (A) ROS generation was determined by the increase in CM-H2DCFDA fluorescence upon anti-CD3 stimulation over unstimulated control. (B) The percentage of splenic $CD4^+$

T cells was assessed by flow cytometry by gating for $CD4^+$ T cell-specific populations ($CD3^+$ $CD4^+$ $CD8^-$). Results are representative of 3 independent experiments.

3.4.3 Genetic ablation of NOX activity protects NOD congenic mice from T1D onset

ROS synthesis is toxic to islet beta cells and also responsible for pathological complications associated with T1D, but whether ROS production is also necessary for initiating diabetogenesis and an autoimmune effector T cell response is not known. To address these questions, spontaneous diabetes incidence of female NOD-*Ncf1*^{m1J} mice in comparison to female NOD mice was determined. At 40 weeks of age, 65% of female NOD-*Ncf1*^{m1J} mice were euglycemic and diabetes-free, while only 15% of the age matched NOD females were euglycemic **(Figure 10A)**. Histological examination of pancreata from non-diabetic NOD mice at seven and twenty-two weeks demonstrated a significant increase in insulitis **(Figure 10B**, insulitis score: 0.55 ± 0.57 and 2.67 ± 0.68, respectively**)**. Immune infiltration into the islets did not advance with age in NOD-*Ncf1*^{m1J} female mice (insulitis score: 7wk, 0.62 ± 0.54 and 22 wk, 0.68 ± 0.62). While the insulitis scores from 7 wk old NOD and NOD-*Ncf1*^{m1J} mice did not differ, the insulitis was significantly increased (p<0.01) in 22 wk old NOD compared to age-matched NOD-*Ncf1*^{m1J} females. Representative histology is presented in **Figure 10C-2F**.

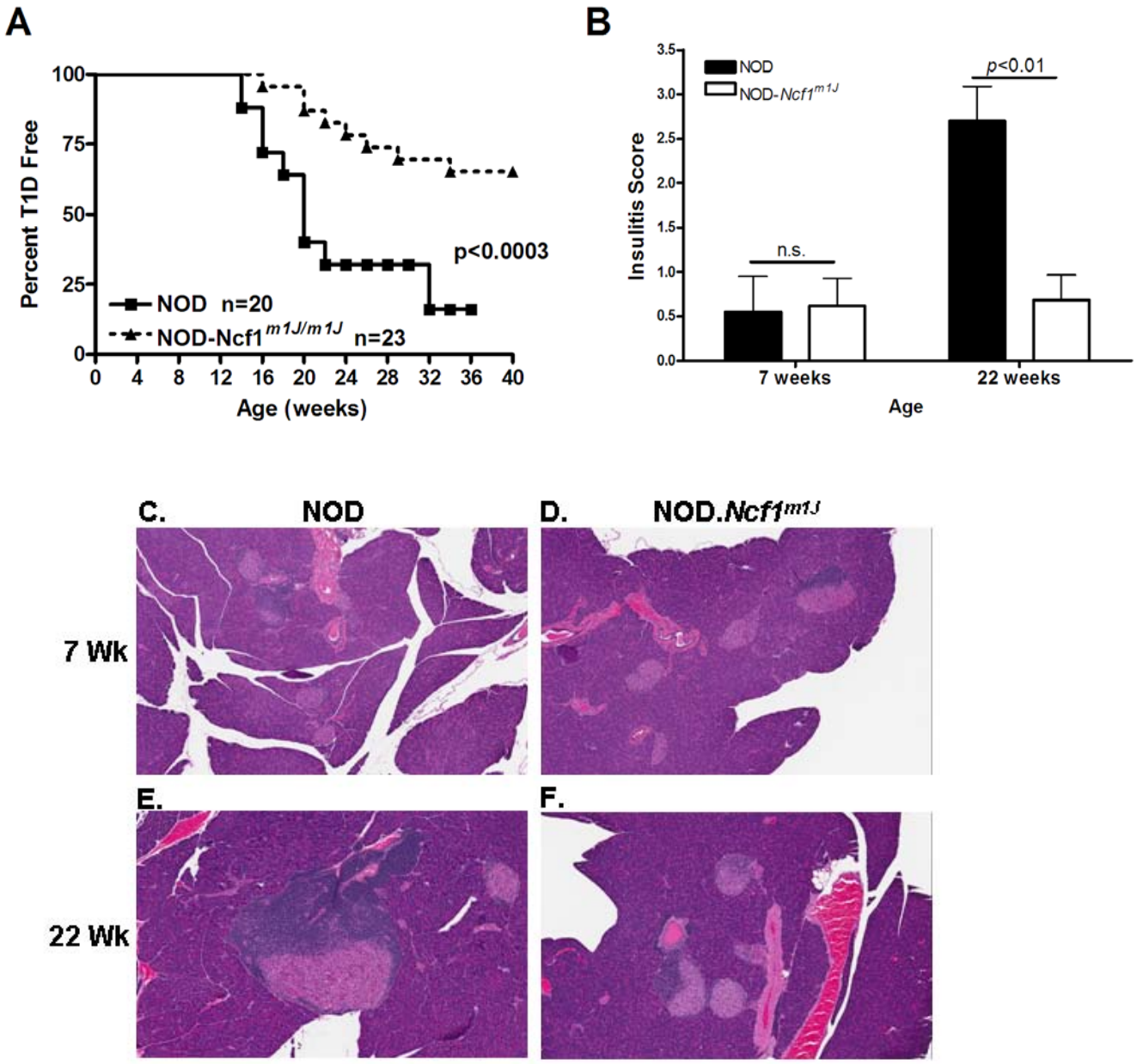

Figure 10: NOD-*Ncf1*^{m1J} mice resist spontaneous diabetes. (A) Kaplan-Meier survival curve of NOD (n=20) and NOD-*Ncf1*^{m1J} (n=20) age-matched female mice for spontaneous diabetes incidence. (B) Insulitis score of 7 and 22 week-old female NOD and NOD-*Ncf1*^{m1J} mice. Hemotoxylin and eosin staining of pancreatic sections from (C, E) 7 and 22 week-old female NOD and (D, F) NOD-*Ncf1*^{m1J} mice. Mice were diabetic after consecutive blood glucose readings of >300mg/dL.

3.4.4 Islets from NOD-*Ncf1*^{m1J} mice exhibit no enhanced protection against proinflammatory cytokine toxicity

To determine if the enhanced diabetes resistance in NOD-*Ncf1*^{m1J} mice was due to the inherent inability of islets to generate ROS to promote pancreatic beta cell destruction, islets from NOD.*Rag* and NOD-*Ncf1*^{m1J} mice were isolated and treated with cytokines to evaluate cell viability and NO production. Treatment with proinflammatory cytokines significantly reduced cell viability of NOD.*Rag* and NOD-*Ncf1*^{m1J} cultured islets **(Fig. 11A)**. NOX-deficient islets produced NO after treatment with cytokines **(Fig. 11B)**, demonstrating no change in the synthesis of reactive nitrogen species.

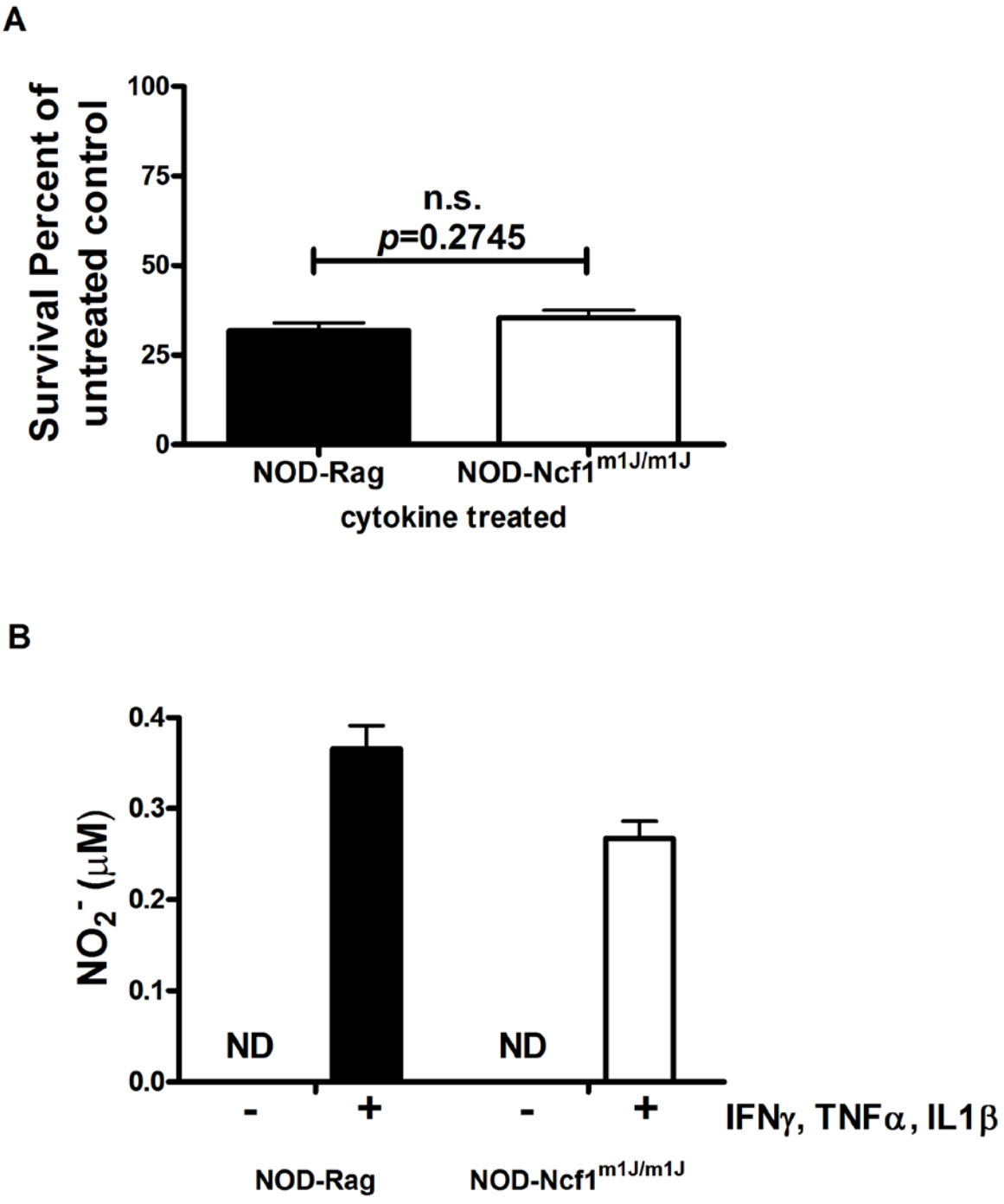

Figure 11: Cultured islets from NOD.*Rag* and NOD-*Ncf1*^{m1J} mice were treated with cytokines IFN-γ, IL-1β, and TNF-α. (A) Islets were susceptible to proinflammatory cytokine-mediated damage and (B) produced NO after treatment. Data representative of 3 independent experiments performed in triplicate.

3.4.5 NOD-*Ncf1*^{m1J} mice are susceptible to AI4 T cell transfer

Intracellular production of ROS within islet cells contributes to beta cell killing (178, 241-244), but whether the synthesis of ROS also functions as accessory molecules to facilitate T cell autoreactivity within the islet has not been well studied. Beta cells express a phagocytic-like NOX complex that can produce superoxide upon stimulation (242, 244). To determine if genetic ablation of NOX at the beta cell level would prevent diabetes induction with diabetogenic CD8^{+} T cells, we transferred highly pathogenic splenocytes from NOX-intact, NOD-AI4 transgenic donors to sub-lethally irradiated NOD and NOD-*Ncf1*^{m1J} female mice. There was no significant difference in the rate or overall incidence of diabetes **(Fig. 12A)** as 75% NOD and 75% NOD-*Ncf1*^{m1J} mice developed hyperglycemia 15 days after adoptive transfer.

3.4.6 NOD-*Ncf1*^{m1J} mice are resistant to BDC-2.5 T cell transfer

In addition to their function in perpetuating cytotoxic responses, macrophages also serve as vital antigen presenting cells. Depletion or inactivation of phagocytes and macrophages has prevented diabetes progression in mouse and rat models (27, 245-247) and recent reports suggest that macrophages are essential for T cell autoreactivity in the BDC-2.5 transfer models (24, 28, 248). To determine if the absence of phagocyte ROS production is essential for mediating type 1 diabetes resistance in the NOD-*Ncf1*^{m1J} mouse, we transferred BDC-2.5 T cells (210) to NOX deficient NOD-*Ncf1*^{m1J} mice. CD4^{+} T cells from BDC-2.5 transgenic mice were transferred into age-matched NOD and NOD-*Ncf1*^{m1J} female recipients. All NOD recipients developed diabetes 5 days post transfer, however; thirty days following, NOD-*Ncf1*^{m1J} mice had still not developed diabetes **(Fig. 12B)**.

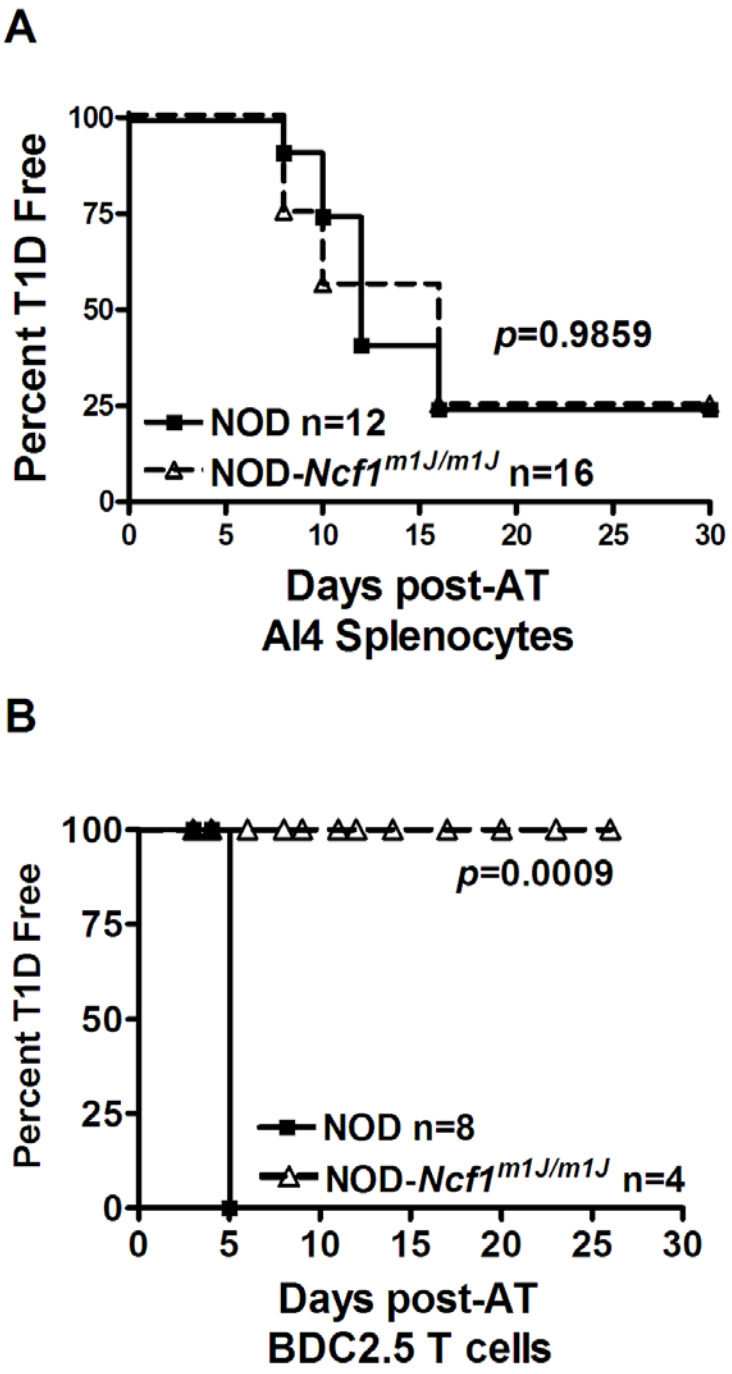

Figure 12: AI4 transgenic T cells, but not BDC-2.5 cells are able to induce diabetes in NOX-deficient mice. (A) Splenocytes (2 x 10^7 cells) from NOD-AI4 donors were transferred to sub-lethally (7.5 Gy) irradiated NOD and NOD-*Ncf1*^{m1J} recipients. (B) BDC-2.5 CD4$^+$ T cells were harvested, activated and transferred to age matched NOD and NOD-*Ncf1*^{m1J} recipients. Mice were monitored by glucosuria for the onset of diabetes. Mice were considered diabetic after 2 consecutive readings of blood glucose above 250 mg/dL.

3.4.7 Macrophages are essential while neutrophils are superfluous for type 1 diabetes pathogenesis

NOX respiratory burst is well described in neutrophils and macrophages and is an important mechanism by which these innate immune cells mediate killing (18, 141-143). Macrophages have previously been reported as critical to the development of spontaneous T1D, as specific depletion prevents T1D development (249-252); however direct assessment of neutrophils has not been investigated. To elucidate the involvement of neutrophils in type 1 diabetes pathogenesis, the use of Gr-1-specific monoclonal antibodies, RB6-8C5 and 1A8, were utilized for depletion studies. RB6-8C5 clone binds to Ly6G and Ly6C, while 1A8 is Ly6G specific. NOD female mice were treated with either RB6-8C5 antibodies to deplete macrophages and neutrophils, 1A8 antibodies to deplete only neutrophils (240). Depletion with RB6-8C5 provided 100% protection from diabetes development, while treatment with 1A8 only provided no protection from type 1 diabetes after 35 weeks as compared to control treated animals **(Fig. 13A)**. Weekly systemic administration of the antibodies began at 4 weeks of age, prior to advancing insulitis, and continued throughout the course of the study to maintain reduction of the target cell types. Peripheral blood samples were collected monthly and monitored via flow cytometry to determine depletion of macrophages ($CD11b^+F4/80^+$) and neutrophils ($CD11b^+Ly6G^+$). Over the course of the study, RB6-8C5 substantially depleted both macrophage and neutrophil populations **(Fig. 13B-D, center panel)** while 1A8 only depleted neutrophils with no significant affect on macrophage numbers **(Fig. 13B-D, right panel)**. $CD11b^+$ cells were gated and analyzed for F4/80 and Ly6G expression. Representative samples from 16 week old mice are shown in **Fig. 13D**. There were no changes in dendritic cell or lymphocyte populations from either treatment **(data not shown)**.

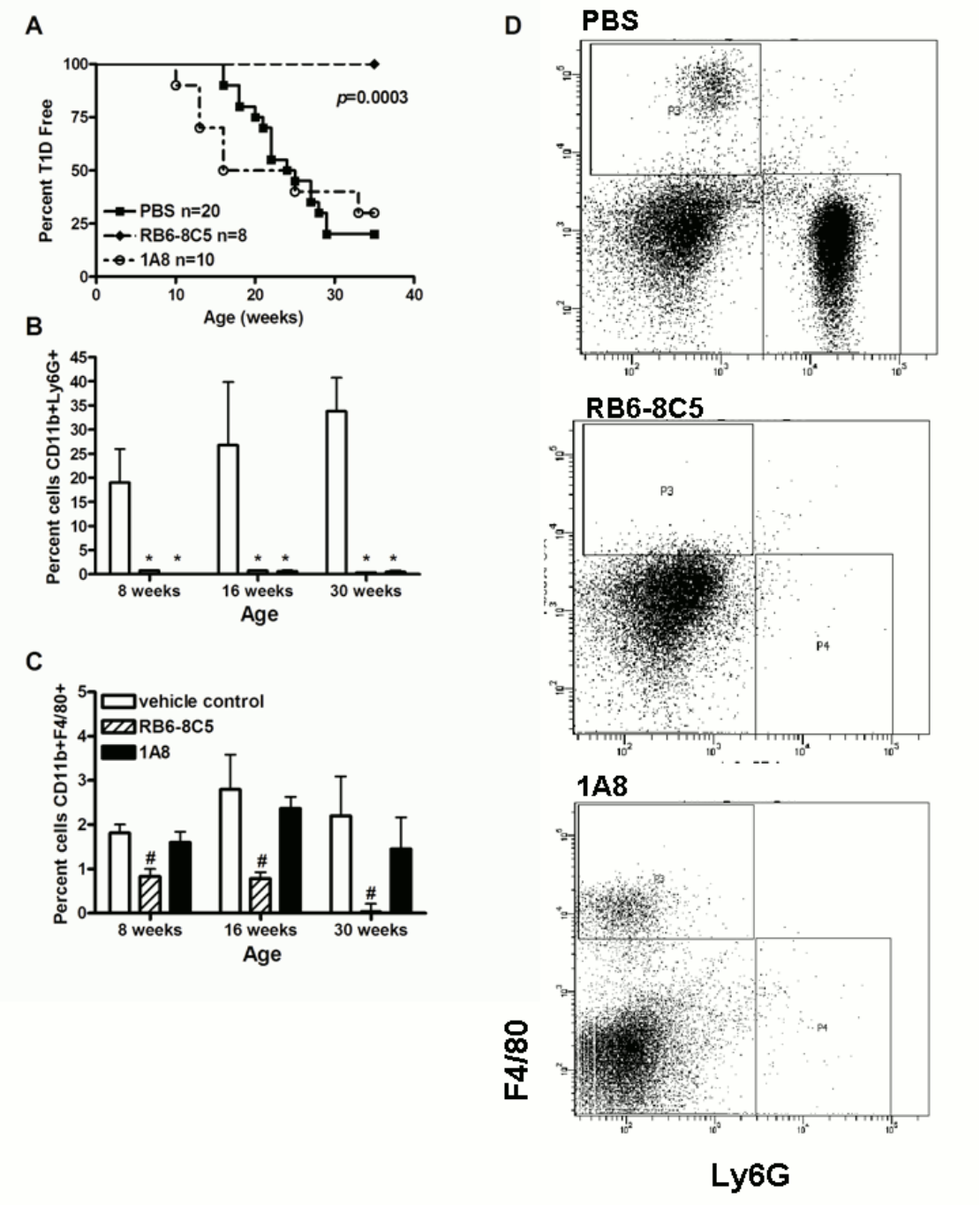

Figure 13 Macrophages but not neutrophils are critical for type 1 diabetes induction. (A) Age-matched NOD female mice were treated with 500 ug 2 days a week and 750 ug 1 day a week anti-Gr-1 RB6-8C5, 1 mg 3 days a week with anti-Gr-1 1A8, or PBS vehicle control starting at 4 weeks of age. Mice were monitored by glucosuria for the onset of diabetes and considered diabetic after 2 consecutive readings of blood glucose above 250 mg/dL. Peripheral blood was used to confirm depletion of (B) neutrophils ($CD11b^{+}Ly6G^{+}$) and (C) macrophages

($CD11b^+F4/80^+$) by flow cytometry. Blood samples were gated on $CD11b^+$ cells and analyzed for Ly6G and F4/80 expression (representative plot of treated mice at 16 weeks of age) (D). Statistical differences noted above signify: * $p< 0.0001$ or # $p<0.002$, respectively.

3.4.8 Delayed transfer of diabetes with NOD-*Ncf1*^{m1J} splenocytes and purified $CD4^+$ and $CD8^+$ T cells

To assess internal defects in the diabetogenicity of APC and T cells lacking intracellular superoxide production, whole splenocytes or purified T cells collected from diabetic and pre-diabetic female NOD and NOD-*Ncf1*^{m1J} donors were adoptively transferred into NOD-*Scid* recipients. Splenocytes from diabetic **(Figure 14A)** and prediabetic **(Figure 14B)** NOD-*Ncf1*^{m1J} mice exhibited delayed diabetes onset compared to NOD cells. As the phagocyte NADPH Oxidase is expressed in T cells and activated after T cell receptor stimulation, we also sought to determine if NOX-deficient T cells would lack the ability to transfer disease. To study potential defects specifically in NOX-deficient T cells, $CD4^+$ and $CD8^+$ T cells from donor animals were purified and adoptively transferred into NOX-intact NOD-*Scid* recipients. A significantly delayed transfer of disease was observed in hosts receiving NOD-*Ncf1*^{m1J} purified T cells **(Figure 14C)** compared to transfer with NOD donor T cells.

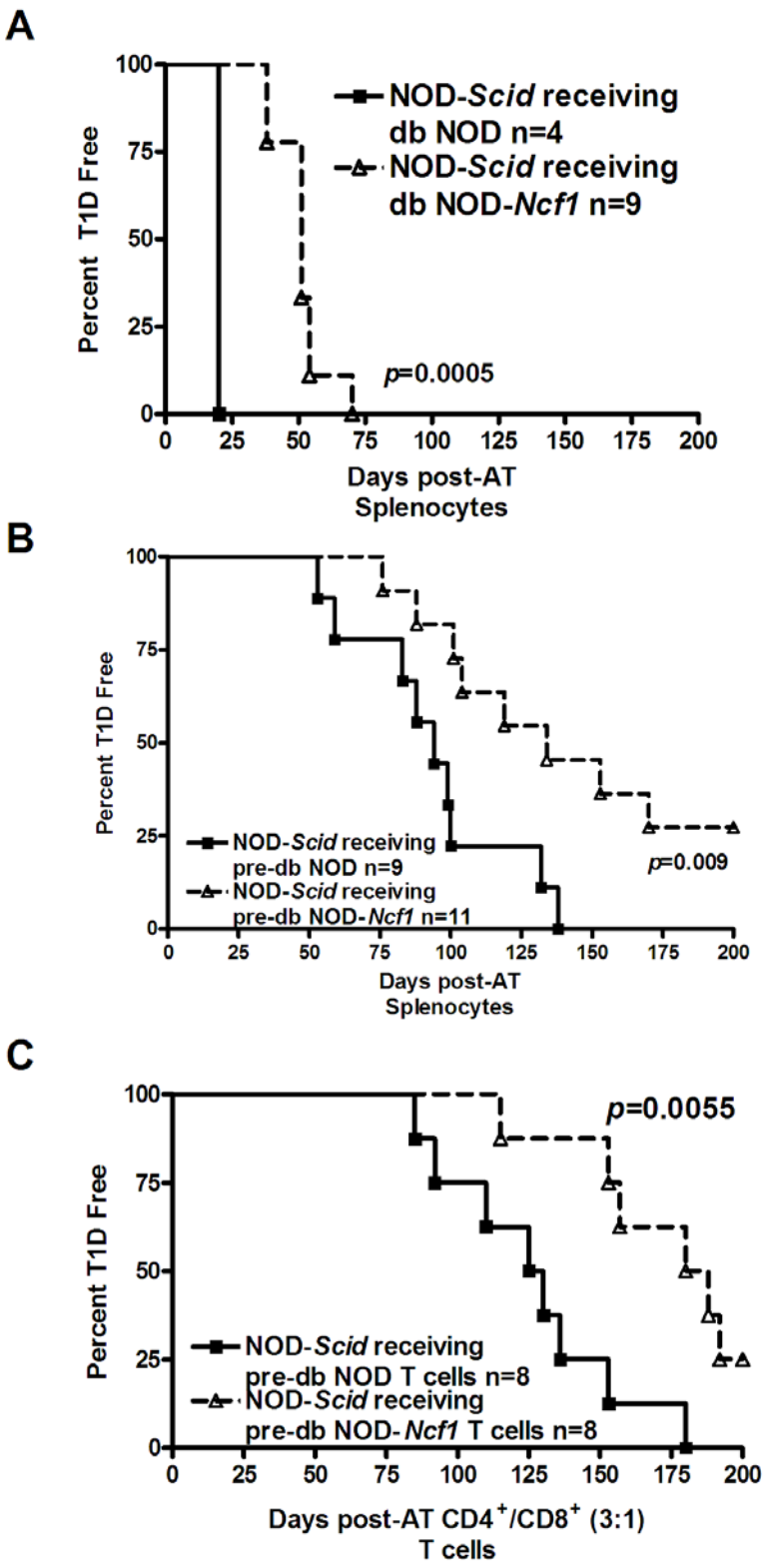

Figure 14: The NOX-deficient NOD-*Ncf1*^{m1J} immune system has a reduced capacity to transfer type 1 diabetes to immune deficient hosts. Splenocytes (2 x 10^7 cells) from (A) 20 week old diabetic or (B) 8 week old

prediabetic donor NOD and NOD-*Ncf1*^{m1J} female mice were transferred i.p. to NOD-*Scid* hosts. (C) A total of 10^7 purified $CD4^+$ and $CD8^+$ T cells at a ratio of 3:1 were transferred i.p. to NOD-*Scid* recipients. In all three transfer experiments mice were monitored by glucosuria for the onset of diabetes and confirmed by blood glucose measurement. Mice were considered diabetic after 2 consecutive readings of blood glucose above 250 mg/dL.

3.5 DISCUSSION

Free radical generation, either exogenous or endogenous to the beta cell, is thought to contribute to beta cell demise and diabetes (210, 227, 228, 232). Oxidative stress and the generation of free radicals are directly toxic to beta cells, but they also have a dual role as potent signaling molecules to induce pro-inflammatory cytokine synthesis that can also directly impact beta cell destruction. Genetic analyses investigating diabetes resistance in the ALR mouse linked increased free radical scavenging and decreased ROS production with T1D protection (112, 133, 230). NOD-*Ncf1*^{m1J} mice were generated to evaluate the role of superoxide production in the pathogenesis of T1D in the diabetes-prone NOD mouse model. Genetic ablation of NOX-mediated superoxide production (**Fig. 8-9**) was significantly protective when congenically introgressed into the NOD genetic background (**Fig. 10)**. Inhibition of NOX activity had a positive impact on diabetes development. NOD-*Ncf1*^{m1J} female mice exhibited a significant reduction (35% in NOD-*Ncf1*^{m1J} versus 85% in NOD; $P<0.0003$) and delay ($P<0.0001$) in autoimmune diabetes development compared to female NOD mice **(Fig. 10A)**. The delay in T1D was mirrored by a slower insulitis progression in NOD-*Ncf1*^{m1J} pancreata **(Fig. 10B)**. Insulitis scores for both NOD and NOD-*Ncf1*^{m1J} were equal at 7 weeks of age. A significant divergence ($P<0.01$) was observed comparing NOX deficient NOD mice at 22 weeks of age to non-diabetic wild-type NOD females. This lack of advance in insulitic damage signals

a delay in the switch from peripheral to invasive insulitis. Therefore, NOX activity and ROS production is important for T1D onset and it is required for insulitis progression.

Recent work suggests NOX complex subunits are expressed in beta cells and produce superoxide upon stimulation (242-244). In the absence of beta cell-specific ROS synthesis, NOD-*Ncf1*^{m1J} cultured islets were still susceptible to cytokine-mediated cell death **(Fig. 11A)** and capable of producing NO in response to cytokines **(Fig. 11B)**, demonstrating no defect in the production of reactive nitrogen species. NOD-*Ncf1*^{m1J} mice were equally susceptible as NOD mice to diabetes induction with AI4 splenocytes (**Fig. 12A)**, a highly diabetogenic CD8^{+} T cell. Pre-activated AI4 CD8 T^{+} cells are efficient effectors, capable of inducing T1D without leukocyte help (236, 253). These results demonstrate that NOX-deficient beta cells are susceptible to immune-mediated destruction.

Macrophage and neutrophil production of superoxide via NOX is an important mechanism employed during immune responses and is a significant source of ROS during inflammation. Macrophages have been shown to be important in the pathogenesis of T1D (24, 27, 28, 245, 246) however, neutrophils have not been as extensively studied. The contributions of ROS-producing innate immune cells to T1D pathogenesis were investigated with depleting antibodies specific for macrophages and neutrophils (RB6-8C5) or neutrophils alone (1A8) (240). When both macrophage and neutrophil populations were depleted, 100% of the animals were free of T1D out to 35 weeks; however, neutrophil depletion alone did not alter the course of T1D development **(Fig. 13)**. While neutrophils may be involved in beta cell killing and autoreactivity, effector contributions are not essential and may be redundant in the process of beta cell damage. Both neutrophils and macrophages exhibit important phagocytic and direct cytotoxic effector function, but macrophages are also involved in antigen presentation and

stimulation of T cells. The protection afforded by NOX inhibition may partially be explained at the macrophage level as observed with the adoptive transfer studies with BDC-2.5 $CD4^+$ T cells into NOD-*Ncf1*^{m1J} recipients **(Fig. 12B)**. Whereas AI4 $CD8^+$ T cells are preactivated in the host and can elicit beta cell-specific cytolytic effector function when transferred to a recipient, BDC-2.5 $CD4^+$ T cells require macrophages. Reports by Calderon *et al*. show that macrophages are essential for effector function and diabetes induction in BDC-2.5 transfer models (24, 248). Our data suggests that NOX-deficient macrophages are unable to mediate pancreatic beta cell destruction after adoptive transfer with BDC-2.5 T cells. Taken together, not only are macrophages required, but NOX-dependent ROS production by macrophages are likely essential for $CD4^+$ T cell effector function and autoreactivity.

Diabetogenic defects resulting from NOX ablation were assessed by adoptive transfer of whole splenocytes or purified T cells collected from diabetic and pre-diabetic female NOD and NOD-*Ncf1*^{m1J} donors. Adoptive transfer experiments demonstrated delayed transfer kinetics to NOX-intact hosts **(Fig 14A-C)**, suggesting a defect intrinsic to the NOX-deficient T cell. This delay occurred with the transfer of whole splenocytes and with purified $CD4^+$ and $CD8^+$ T cells, where antigen presentation would be in the context of a NOX-intact host APC. Transfer with splenocytes harvested from diabetic donors, where the islet-reactive population would be expanded and activated, was still delayed compared to control NOD donor cells. This finding demonstrates a fundamental defect in the ability of NOX-deficient leukocytes to respond and execute sufficient effector function. It also shows that ROS production by the T cell is essential for initiating islet-directed autoimmunity. Redox status and redox molecules are important contributors to transcriptional and post-transcriptional regulation of transcription factors and cytokine synthesis (139, 204, 254). Th_1 IFN-γ activity is implicated in the aberrant

autoreactivity mediating beta cell destruction (44, 255) and T1D, and deviations in the cytokine profile can be protective (80-82). We have previously shown that redox balance and superoxide production are critical in the initiation of a pathogenic cytokine response (184, 202, 207, 208, 256). The adoptive transfer experiments with pre-diabetic T cells alone demonstrated that in the absence of intrinsic ROS production there is decreased islet reactivity. Therefore, we propose that T1D is reduced and delayed by the *Ncf1*^{m1J} mutation as a result of inefficient Th_1 T cell activation and differentiation.

Our data describe a role for ROS produced by macrophages and T cells in the initiation of autoimmune diabetes. Macrophage ROS-mediated effector function is essential for $CD4^+$ T cell autoreactivity and T1D pathogenesis. Additionally, intracellular ROS produced by the T cell is important for executing efficient islet reactivity. The loss of ROS synthesis provided by the *Ncf1* mutation significantly alters effector function of macrophages and T cells. This demonstrates the importance of ROS-dependent mechanisms in controlling activation of autoimmune effectors and in turn mediating aberrant reactivity towards beta cells.

4.0 NADPH OXIDASE DEFICIENCY REGULATES T HELPER LINEAGE COMMITMENT AND AUTOIMMUNITY

This manuscript was accepted for publication in the *Journal of Immunology*. Dr. Hubert Tse (Department of Microbiology, University of Alabama) and Terri Thayer (Immunology Graduate Program) are co-first authors, having generated the majority of the data and prepared the manuscript.

4.1 ABSTRACT

Reactive oxygen species (ROS) are used by the immune system to eliminate infections; however they may also serve as signaling intermediates to coordinate the efforts of the innate and adaptive immune systems. In this study, we show that by eliminating macrophage and T cell superoxide production through the NADPH Oxidase (NOX), T cell polarization was altered. After stimulation with immobilized anti-CD3 and anti-CD28 or priming recall, T cells from NOX-deficient mice exhibited a skewed Th17 phenotype, whereas NOX-intact cells produced cytokines indicative of a Th1 response. These findings were corroborated *in vivo* by studying two different autoimmune diseases mediated by Th17 or Th1 pathogenic T cell responses. NOX-deficient Non-Obese Diabetic (NOD) mice were Th17 prone with a concomitant susceptibility to experimental allergic encephalomyelitis and significant protection against Type

1 Diabetes (T1D). These data validated the role of superoxide in shaping T helper responses and as a signaling intermediate to modulate Th17 and Th1 T cell responses.

4.2 INTRODUCTION

Type 1 diabetes (T1D) is an autoimmune disease with a prevalence of approximately 1% with an incidence that is increasing at a rate of 3% per year. While T1D is one of the most common chronic diseases of childhood, there is no cure for this disease and the pathogenic mechanisms of the human condition remain unidentified. Persistent evidence demonstrates that Th1 T cell responses and the synthesis of pro-inflammatory cytokines and reactive oxygen species (ROS) are essential for beta cell destruction in T1D (178, 210, 232, 248). The exact role of ROS in T1D appears to be complex, and whereas these molecules have been linked to beta cell killing, a role for these molecules at the level of the immune response has not been firmly established.

ROS are not only the first line of defense of innate immune effectors in response to invading pathogens, but they also function as both intra- and intercellular signaling molecules for the induction of pro-inflammatory cytokine synthesis. The combined action of innate immune-derived pro-inflammatory cytokines and ROS modulates adaptive immune function. A potential major source of ROS in immune signaling in both Antigen Presenting Cells (APC) and T lymphocytes is the NADPH Oxidase (NOX). Recent evidence has demonstrated, via the genetic ablation of an essential subunit of NOX, *Cybb* ($gp91^{phox}$), the importance of NOX activity in skewing T helper responses during the response to a fungal infection (257, 258). Whereas

extracellular ROS appears to control T cell reactivity, T lymphocytes do express a phagocyte-type NOX and this complex functions in T cells to produce ROS in response to stimulation via the T Cell Receptor (TCR) (181).

The absence of reactive oxygen species in T cells has also been demonstrated to be associated with an increase in the severity of antigen-induced experimental allergic encephalomyelitis (EAE) and collagen-induced arthritis (171, 172, 259, 260). In contrast, our previous genetic mapping studies using T1D-prone NOD with T1D-resistant ALR mice linked resistance against spontaneous autoimmune diabetes, reduced oxidative burst from neutrophils and macrophages, as well as elevated Superoxide Dismutase 1 (SOD1) activity to the *Suppressor of Superoxide Production* (*Susp*) locus on Chr. 3 (112, 230). Congenic replacement of Chr. 3 *Susp* locus in the NOD provided 100% protection from T1D and was associated with decreased autoreactivity of T lymphocytes (Chapter 2). To study the impact of ablated NOX activity on the development of spontaneous autoimmune diabetes, in the absence of high SOD1 activity, we generated NOD mice with a spontaneous mutation in the Neutrophil Cytosolic Factor 1 (*Ncf1*) gene (Chapter 3). The *Ncf1*^{m1J} mutation is a point mutation in exon 8 that results in an aberrant mRNA splicing event and terminal truncation of the p47^{phox} subunit, preventing NOX assembly and superoxide synthesis (171, 172, 259, 260). This mutation was also associated with reduced T1D incidence and inefficient diabetes transfer with NOX-deficient lymphocytes.

Here, we report a role for superoxide in modulating immune responses. NOX-deficiency altered redox-dependent innate immune cytokine synthesis, observed as reductions in TNF-α, IL-1β, and IL-12 p70 while IL-23, a cytokine necessary for driving Th17 differentiation (261), was elevated. In addition, polyclonal or antigen-induced activated T cells from NOD-*Ncf1*^{m1J} mice exhibited a decreased Th1 cytokine response, and instead demonstrated a cytokine profile

reminiscent of a Th17 response. These immune polarizations were strongly correlated with the immune responses in the whole animal as NOX-deficiency attenuated T1D while promoting development of the prototypical Th17 disease, EAE. These data demonstrate the importance of superoxide in shaping immune responses.

4.3 METHODS

4.3.1 Animals

NOD/ShiLtJ, ALR/LtJ, and NOD.B6-*Ncf1*^{m1J} (NOD-*Ncf1*^{m1J}) mice were bred and housed under specific pathogen-free conditions in the Animal Facility of the Rangos Research Center in the University of Pittsburgh. B6.NOD-(*D17Mit21-D17Mit10*) [B6-*H2*^{g7}], B6(Cg)-*Ncf1*^{m1J}/J (B6-*Ncf1*^{m1J}), and SJL/J mice were purchased from The Jackson Laboratory (Bar Harbor, ME). Female mice at 6 to 8 weeks of age were used in all experiments except for the EAE induction, where 6-week-old males were used.

4.3.2 Materials

Anti-IL-2 and anti-IFNγ antibody pairs for ELISAs, as well as CD3, CD4, CD8, CD90.2, Ly6g (Gr1), and CD11b fluorochrome-conjugated antibodies were purchased from Pharmingen (San Diego, CA). Hen egg lysozyme (HEL), anti-β-actin monoclonal antibody, CM-H_2DCFDA, and 4-alpha-phorbol-12-myristate-13-acetate (PMA) were purchased from Sigma (St. Louis,

MO). Dihydrorhodamine 123 (DHR123) was purchased from Invitrogen (Carlsbad, CA). Antibodies against $p47^{phox}$, the gene product of *Ncf1*, and phospho-Stat3 were purchased from Cell Signaling (Danvers, MA). Antibodies against Stat4 and T-bet were purchased from Santa Cruz Biotechnology (Santa Cruz, CA). The anti-Stat1α antibody was purchased from Zymed (San Francisco, CA).

4.3.3 Flow cytometry

Splenic leukocytes were harvested and washed twice in FACS buffer (1% BSA in PBS), counted, and resuspended in a final concentration of $2x10^7$ cells/mL in FACS buffer. One million cells were stained with directly fluorochrome-conjugated Abs purchased from either eBioscience or BD Biosciences. The antibodies [PE-labeled anti-Ly6g (Gr1), APC-labeled anti-CD11b, Pacific blue-labeled anti-CD4, APC-labeled anti-CD25, PE-labeled anti-FoxP3, FITC-labeled anti-CD8, PECy5-labeled anti-CD4, PE-labeled anti-CD62L, PerCpCy5.5-labeled anti-CD69, and APC-Cy7-labeled anti-CD44, FITC-labeled anti-IFNγ, and PE-labeled anti-IL-17A] were used at the appropriate dilution (10 µL of each Ab) and fluorescence was measured using a LSRII (BD Biosciences). Results were analyzed with Cellquest software (BD Biosciences).

4.3.4 Measurement of intracellular ROS by flow cytometry

Neutrophil and macrophage superoxide production were assayed using FACS as previously described (230). Briefly, bone marrow was isolated and purified using a Ficoll gradient. Cells were labeled with PE-labeled anti-Ly6g (Gr1) and APC-labeled anti-CD11b and then loaded with Dihydrorhodamine 123 (DHR 123) for 5 minutes at 37°C. Cells were subjected

to flow cytometry prior to stimulation, and then at 5-minute intervals after 98 nM PMA stimulation. The ROS driven conversion of DHR 123 to rhodamine was measured using a FACSCalibur. Ly6g and CD11b extracellular markers were used to discriminate neutrophils ($Ly6G^+$, $CD11b^+$) and macrophages ($Ly6G^-$, $CD11b^+$) from other bone marrow cells, and results were analyzed with Cellquest software (BD Biosciences).

4.3.5 Isolation of mouse bone marrow-derived macrophages

Bone marrow-derived macrophages were cultured as described previously (256) and plated on 6- and 24-well tissue culture plates and 100 mm petri dishes at concentrations of 4 x 10^6 cells/well, 10^6 cells/well, or 2.4 x 10^7 cells/dish, respectively. Macrophages were stimulated with 100 ng/mL of LPS from *E. coli* (055:B5) (Sigma Aldrich).

4.3.6 Plate bound anti-CD3 and anti-CD28 activation of purified $CD4^+$ T cell and cell lysates

Splenic $CD4^+$ T cells were purified by negative selection with a $CD4^+$ T cell isolation kit (Miltenyi Biotec) supplemented with biotinylated mouse anti-rat RT1B (OX-6) Ab. Naïve $CD4^+CD62L^+$ T cells were purified with a $CD4^+CD62L^+$ T cell Isolation kit (Miltenyi Biotec) by following manufacturer's protocol. $5x10^5$ purified splenic T cells were stimulated with anti-CD3ε and anti-CD28 Ab at concentrations of 0.1 µg/mL and 1 µg/mL, respectively, for 72 hr (256). Supernatants were harvested for cytokine analysis, T cell proliferation, and whole cell lysates were prepared as described previously (256).

4.3.7 Cytokine measurements by ELISA and Luminex

IL-2, IFNγ, IL-12 p70, IL-17, TNFα, and IL-1β were detected with DuoSet ELISA kits (R&D Systems) or with Ab pairs from BD Pharmingen. TGFβ was measured using a TGFβ Quantikine kit from R&D Systems. ELISA plates were read on a SpectraMax M2 microplate reader and analyzed using Softmax Pro v.5.0.1 (Molecular Devices Corp.). Additionally, cytokine levels in culture supernatants were quantified using the Bio-Plex™ multiplex suspension array system and a mouse cytokine/chemokine panel (Bio-Rad). The concentrations of each sample were determined using Bio-Plex Manager Version 3.0 software. NO_2^- was measured by the Greiss assay as described previously (256).

4.3.8 qRT-PCR

Bone marrow-derived macrophages were stimulated 4 hours with LPS. RNA was isolated with TRIzol and cDNA prepared by SuperScript III (Invitrogen). SYBR Green reagent (BioRad) was used for quantitative RT-PCR analyzed on a LightCycler 480 II (Roche) with forward and reverse primers specific for *Xbp1*, *Hspa5* (BIP), *Chop*, and *Actin* as adapted from (262).

4.3.9 Immunization of mice, antigen-recall and criss-cross assays

Mice were injected with 100 µg of HEL in CFA subcutaneously at the base of the tail. Seven days after immunization, mice were sacrificed and the inguinal and periaortic lymph node (LN) were harvested for *in vitro* antigen recall assays as described previously (202). Antigen-

recall assays were set up by stimulating LN single cell suspensions with 25 μg of HEL in complete DMEM and supernatants were harvested for cytokine analysis at 48, 72, and 96 hours. For antigen-recall criss-cross assays, LN single cell suspensions were split into two groups and used to purify T cell and antigen-presenting cells by negative selection. $CD4^+$ T cells were purified by negative selection with a $CD4^+$ T cell isolation kit (Miltenyi Biotec) supplemented with biotinylated mouse anti-rat RT1B (OX-6) Ab according to the manufacturer's protocol. Antigen-presenting cells were purified by negative selection with anti-CD4 and anti-CD8 antibodies conjugated to magnetic beads over a LS column (Miltenyi Biotec).

4.3.10 Intracellular cytokine staining

Intracellular IFN-γ and IL-17A was measured after polyclonal stimulation of naïve $CD4^+CD62L^+$ T cells. Stimulated cells were treated with GolgiStop for 5 hours at 37 ^oC in a 5% CO_2 humid air incubator with the aid of the murine BD intracellular cytokine staining kit (BD Biosciences) according to the manufacturer's protocol. After stimulation, cells were surface stained with PECy5-labeled anti-CD4, fixed in BD Cytofix/Cytoperm buffer, washed in BD Perm/Wash buffer, and then stained with FITC-labeled rat anti-IFN-γ (XMG1.2; BD Biosciences) and PE-labeled rat anti-IL-17A (TC11-18H10; BD Biosciences) and isotype controls according to the manufacturer's protocol. Cells were washed twice in BD Perm/Wash buffer, resuspended in FACS buffer, and stained cells were analyzed on a BD Fortessa. Results were analyzed with FACSDiva software (BD Biosciences).

4.3.11 Western immunoblotting

Whole cell lysates was separated on a 4-20% gradient SDS-PAGE gel and transferred onto 0.45 μm charged PVDF membranes. The membranes were incubated overnight at 4^{o}C with antibodies against Stat4, Stat1α, T-bet, Stat3, or β-actin and exposed to the appropriate secondary antibody conjugated to horseradish peroxidase (Jackson ImmunoResearch). Chemiluminescence was detected with ECL plus (Amersham Pharmacia). Image J software (National Institutes of Health) was used to generate densitometry data.

4.3.12 Induction of EAE

Eight week old SJL, NOD, and NOD-*Ncf1*^{m1J} were treated with 100μg MOG_{35-55} in CFA by subcutaneous injection in the base of tail. Mice were also treated i.p. with 200ng Pertussis toxin on day 0 and day 2. Mice were evaluated three days a week for symptoms following the standard five-point scale: 0, asymptomatic; 1, limp tail; 2, hind limb weakness/ incomplete limb paralysis; 3, complete hind leg paralysis; 4, complete hind and partial front leg paralysis; 5, moribund (263, 264).

4.3.13 Statistical analysis

Determination of the difference between mean values for each experimental group was assessed by the Student's *t* test, with $p<0.05$ considered significant. All experiments were performed at least three separate times with data obtained in triplicate wells in each experiment.

4.4 RESULTS

4.4.1 NOD-*Ncf1*^{m1J} T cells exhibit a skewed cytokine response from Th1- to a Th17-like phenotype

Recent evidence has demonstrated that T cells express a phagocyte type NADPH oxidase that is vital for TCR signaling upon CD3 and CD28 cross-linking (181), therefore, we hypothesized that NOX-deficient NOD mice would have decreased T cell receptor signaling and subsequent adaptive immune effector function. Immunoblot analysis of whole cell lysates from anti-CD3 and anti-CD28-stimulated NOD and NOD-*Ncf1*^{m1J} T cells demonstrated that only NOD-*Ncf1*^{m1J} T cells lacked p47^{phox} expression **(Figure 15A)** similar to bone marrow-derived macrophages **(Figure 8G)**. The *Ncf1* mutation in NOD T cells also had a profound effect on cytokine synthesis as plate-bound anti-CD3 and anti-CD28 cross-linking of purified NOD-*Ncf1*^{m1J} T cells exhibited a 3-fold decrease in proliferation, IL-2, and IFNγ secretion **(Figure 15B-D)** in comparison to NOD T cells. Interestingly, these polyclonal-stimulated T cells demonstrated a T cell response reminiscent of a Th17-like phenotype. NOD-*Ncf1*^{m1J} T cells synthesized 2-fold decrease in TNFα, 3-fold more IL-17, 40-fold increase in TGF-β, 2-fold increase in IL-10, equivalent IL-6 levels, 2-fold decrease in IL-4, and a 2.5-fold decrease in GM-CSF levels compared with NOD T cells upon polyclonal stimulation **(Figure 15E-K)**. Additionally, intracellular cytokine staining of polyclonal stimulated naïve CD4^{+}CD62L^{+} T cells **(Figure 16)** from NOD and NOD-*Ncf1*^{m1J} mice was performed. No differences were observed in naïve (CD4^{+}CD62L^{+}CD69^{-}CD44^{-}), effector (CD4^{+}CD62L^{-}CD69^{+}CD44^{+}), and memory (CD4^{+}CD62L^{-}CD69^{-}CD44^{+}) splenic CD4^{+} T cell subsets from 8-wk-old age-matched NOD and NOD-*Ncf1*^{m1J} female mice by flow cytometry (**Figure 16A**). Naïve NOD-stimulated T cells

exhibited a 1.5-fold increase in the percentage of $CD4^+$/IFN-γ^+ cells **(Figure 16B)**, whereas NOD-*Ncf1*^{m1J} T cells had a 5-fold increase in $CD4^+$/IL-$17A^+$ expressing cells **(Figure 16C)**.

The decrease in Th1 cytokine synthesis (IFNγ) from NOD-*Ncf1*^{m1J} T cells was due to the absence of Th1-specific transcription factor expression such as T-bet, Stat4, and Stat1α **(Figure 17A and 17B)**. The absence of these key transcription factors in activated NOD-*Ncf1*^{m1J} T cells was associated with the absence of Th1 cytokine synthesis and demonstrates an important role of superoxide in skewing T helper responses. Activation of Stat3, which is necessary for Th17 lineage commitment (265, 266), was assessed by immunoblot analysis in NOD and NOD-*Ncf1*^{m1J} T cells. Anti-CD3- and anti-CD28-stimulated NOD-*Ncf1*^{m1J} T cells demonstrated an increase in phosphorylated-Stat3 (Y705 and S727) in comparison with NOD T cells after stimulation for 48 and 72 hours **(Figure 17C-E)**.

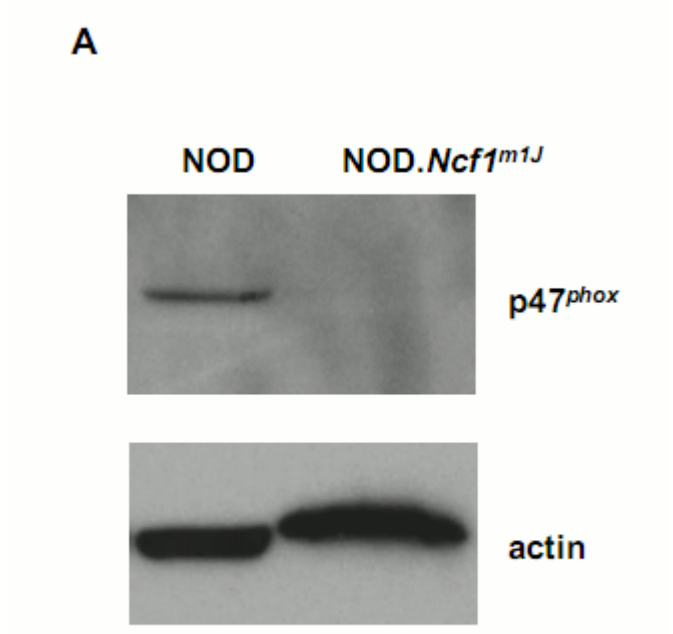

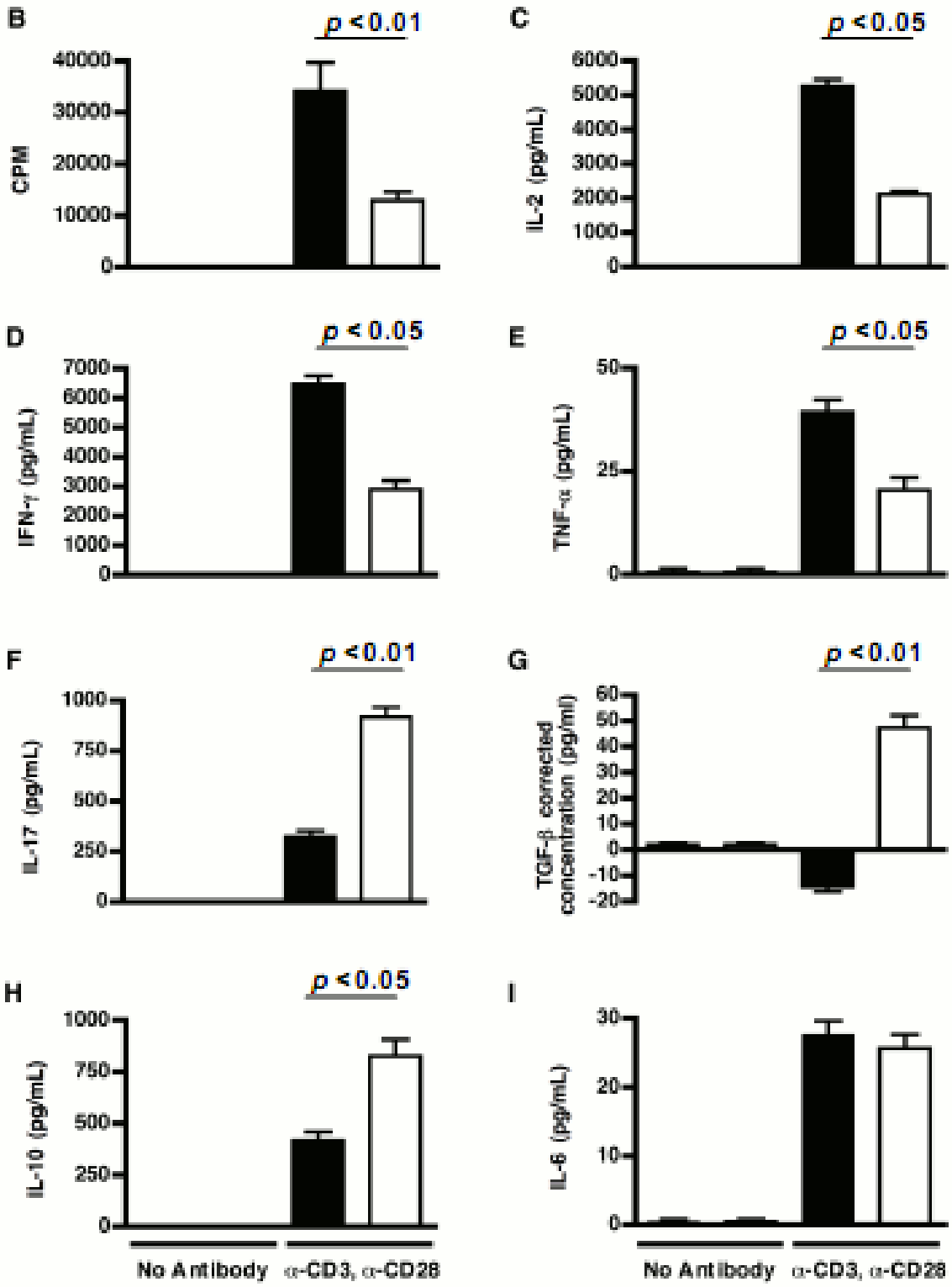
B
p < 0.01
CPM
40000
30000
20000
10000
0
C
p < 0.05
IL-2 (pg/mL)
6000
5000
4000
3000
2000
1000
0
D
p < 0.05
IFN-γ (pg/mL)
7000
6000
5000
4000
3000
2000
1000
0
E
p < 0.05
TNF-α (pg/mL)
50
25
0
F
p < 0.01
IL-17 (pg/mL)
1000
750
500
250
0
G
p < 0.01
TGF-β corrected concentration (pg/ml)
60
50
40
30
20
10
0
-10
-20
H
p < 0.05
IL-10 (pg/mL)
1000
750
500
250
0
No Antibody
α-CD3, α-CD28
I
IL-6 (pg/mL)
30
20
10
0
No Antibody
α-CD3, α-CD28

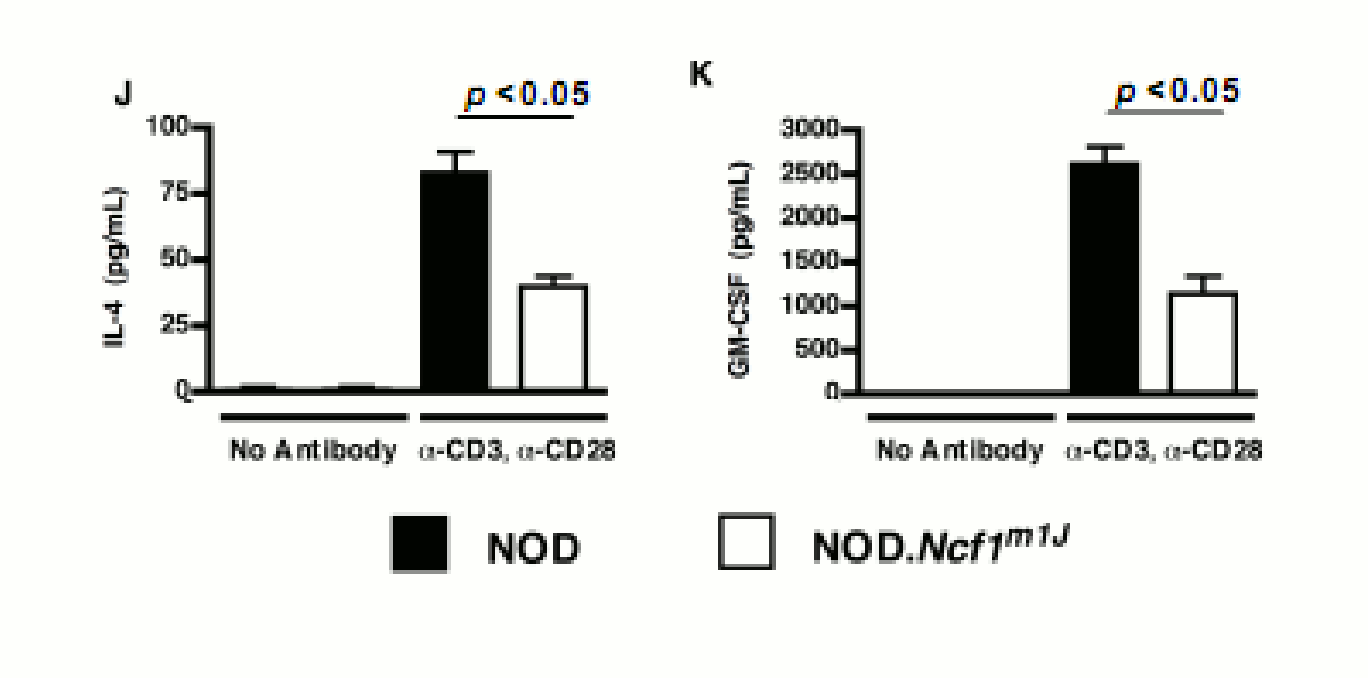

Figure 15: Anti-CD3 and anti-CD28 stimulation of NOD-*Ncf1*^{m1J} T cells exhibits a decrease in Th1 cytokine profile concomitant with an increase in Th17 cytokine synthesis. (A) Immunoblot analysis of p47phox expression in negatively selected and purified NOD and NOD-*Ncf1*^{m1J} T cells. (B-K) Proliferation and cytokine synthesis of purified NOD and NOD-*Ncf1*^{m1J} T cells ($2.5x10^5$ cells) after stimulation with polyclonal Abs for 72 hrs, as tested by cytokine-specific ELISAs and Luminex Bio-plex assay for cytokine synthesis. Proliferation was assessed by 3H-TdR incorporation. Results are representative of three independent experiments done in triplicate. n.m., Not measurable

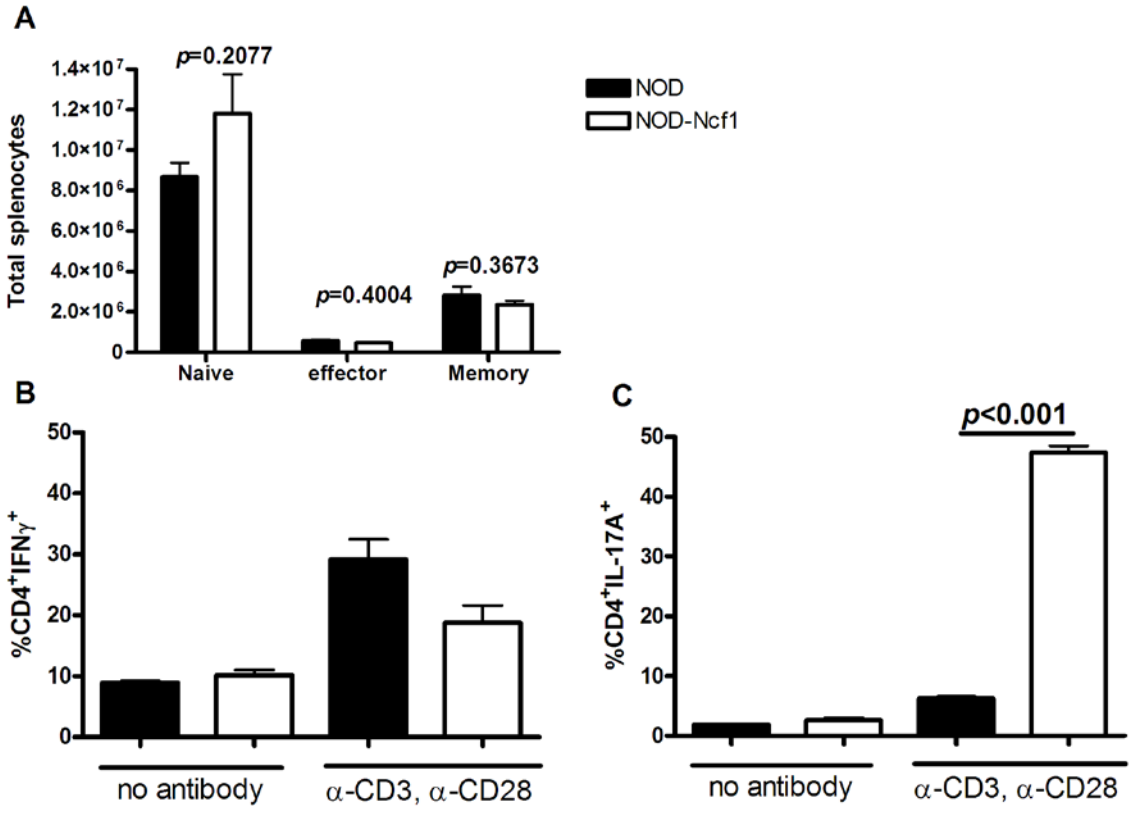

Figure 16: NOD-*Ncf1*^{m1J} naïve CD4$^+$CD62L$^+$ T cells exhibit a Th17 cytokine profile after polyclonal stimulation. (A) The percentages of splenic naïve (CD62L$^+$CD69$^-$CD44$^-$), effector (CD62L$^-$CD69$^+$CD44$^+$), and memory (CD62L$^-$CD69$^-$CD44$^+$) CD4$^+$ T cells were assessed by flow cytometry. Intracellular cytokine staining of (B) CD4$^+$/IFN-γ$^+$ and (C) CD4$^+$/IL-17A$^+$ after 72-h stimulation of purified naïve CD4$^+$CD62L$^+$ T cells from the spleen of NOD and NOD-*Ncf1*^{m1J} mice.

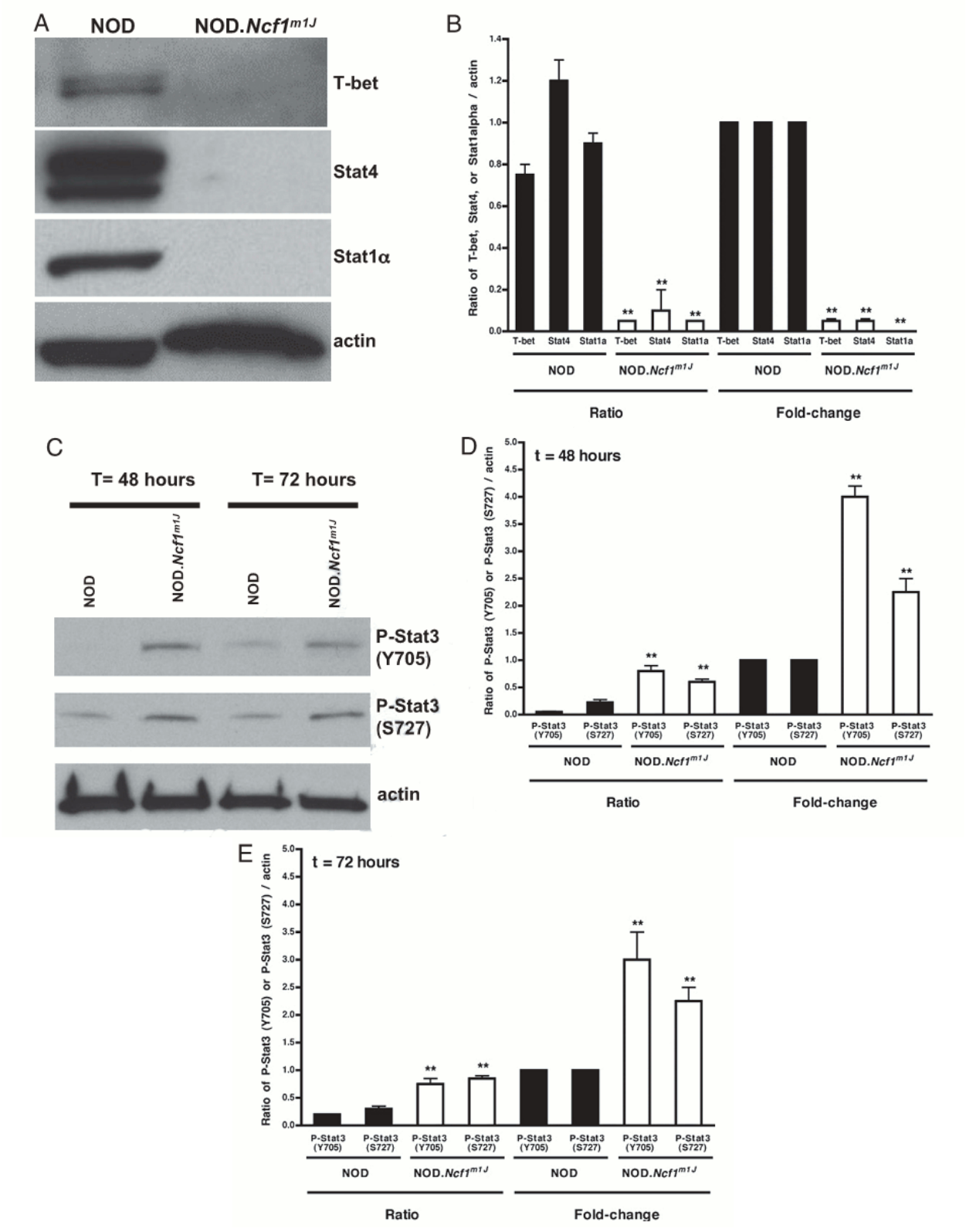

Figure 17: NOD-*Ncf1*^{m1J} T cells do not express Th1 lineage-specific transcription factors upon polyclonal stimulation. (A) Immunoblot analysis of whole-cell lysates (20 μg protein) of negatively selected

purified NOD and NOD-*Ncf1*^{m1J} T cells after anti-CD3 and anti-CD28 stimulation for 72 h for T-bet, STAT4 and STAT1α. Actin was also probed to confirm equal protein loading on the gels. STAT3 activation was assessed by using phospho-specific STAT3 Abs (Y705 and S727) in an immunoblot analysis of anti-CD3- and anti-CD28-stimulated NOD and NOD-*Ncf1*^{m1J} T cells for 48 and 72 h. Actin was also probed to confirm equal protein loading on the gels (C). Cumulative data from 3 independent experiments employing Image J software (NIH) were used to determine the area under the curve values for T-bet, STAT4, STAT1α, P-STAT3 (Y705), P-STAT3 (S727), and actin controls. The data are expressed both as the ratio of T-bet, STAT4, or STAT1α to actin or P-STAT3 (Y705) and P-STAT3 (S727) to actin (D,E) and as the change after NOD T cell samples were normalized to a value of 1. **p<0.01 versus NOD T cells.

4.4.2 NOD.*Ncf1*^{m1J} macrophages exhibit a decrease in pro-inflammatory cytokine and chemokine synthesis after innate immune activation

The generation of innate immune-derived proinflammatory cytokines is a redox-sensitive process that is highly dependent on the intra- and intercellular signaling capacities of ROS (200, 202, 207, 267) and necessary for the generation of an efficient Th1 adaptive immune effector response (200, 202, 207, 267-269). We have previously shown that macrophage NOX effector function is required for T1D onset **(Fig. 10)** and for BDC2.5 CD4$^+$ T cell-mediated diabetes induction **(Fig. 12B)**. To determine whether the *Ncf1*^{m1J} mutation in NOD-*Ncf1*^{m1J} bone marrow-derived macrophages had an effect on skewing the NOD T cell response from a Th1- to a Th17-like phenotype, the innate immune response and the synthesis of proinflammatory cytokines from NOD-*Ncf1*^{m1J} bone marrow-derived macrophages was analyzed after LPS stimulation. To determine if the truncated form of p47^{phox} inherently induced the unfolded protein response (UPR) to affect macrophage activation, markers indicative of the UPR (BIP, CHOP, and XBP1 splicing) were evaluated by qRT-PCR. No differences in expression or

splicing were observed with control and LPS-stimulated NOD and NOD-*Ncf1*^{m1J} macrophages (data not shown), eliminating endoplasmic reticulum stress as a mechanism for the heightened IL-23 production. NOD-*Ncf1*^{m1J} macrophages demonstrated decreases of 1.5-fold in TNFα, 3-fold in IL-1β, 2-fold in IL-12 p70, but no difference in NO_2^- expression after LPS stimulation in comparison to NOD macrophages **(Figure 18A-D)**. In contrast, LPS-stimulated NOD-*Ncf1*^{m1J} macrophages did exhibit increases in IL-12 p40 (3-fold), G-CSF (2-fold), and IL-6 (2-fold) cytokine synthesis as compared with NOD macrophages **(Figure 18E-G)**. Because IL-12 p40 levels in NOD-*Ncf1*^{m1J} macrophages increased 3-fold **(Figure 18E)**, but IL-12 p70 levels decreased 2-fold **(Figure 18C)** in comparison to NOD macrophages, we hypothesize that the increased IL-12 p40 subunit may heterodimerize with IL-12 p19 to generate IL-23. IL-23 synthesis in LPS-stimulated NOD and NOD-*Ncf1*^{m1J} macrophages was examined at the protein level. NOD-*Ncf1*^{m1J} macrophages exhibited a 2-fold increase in IL-23 synthesis by ELISA as compared to NOD macrophages **(Figure 18H)**.

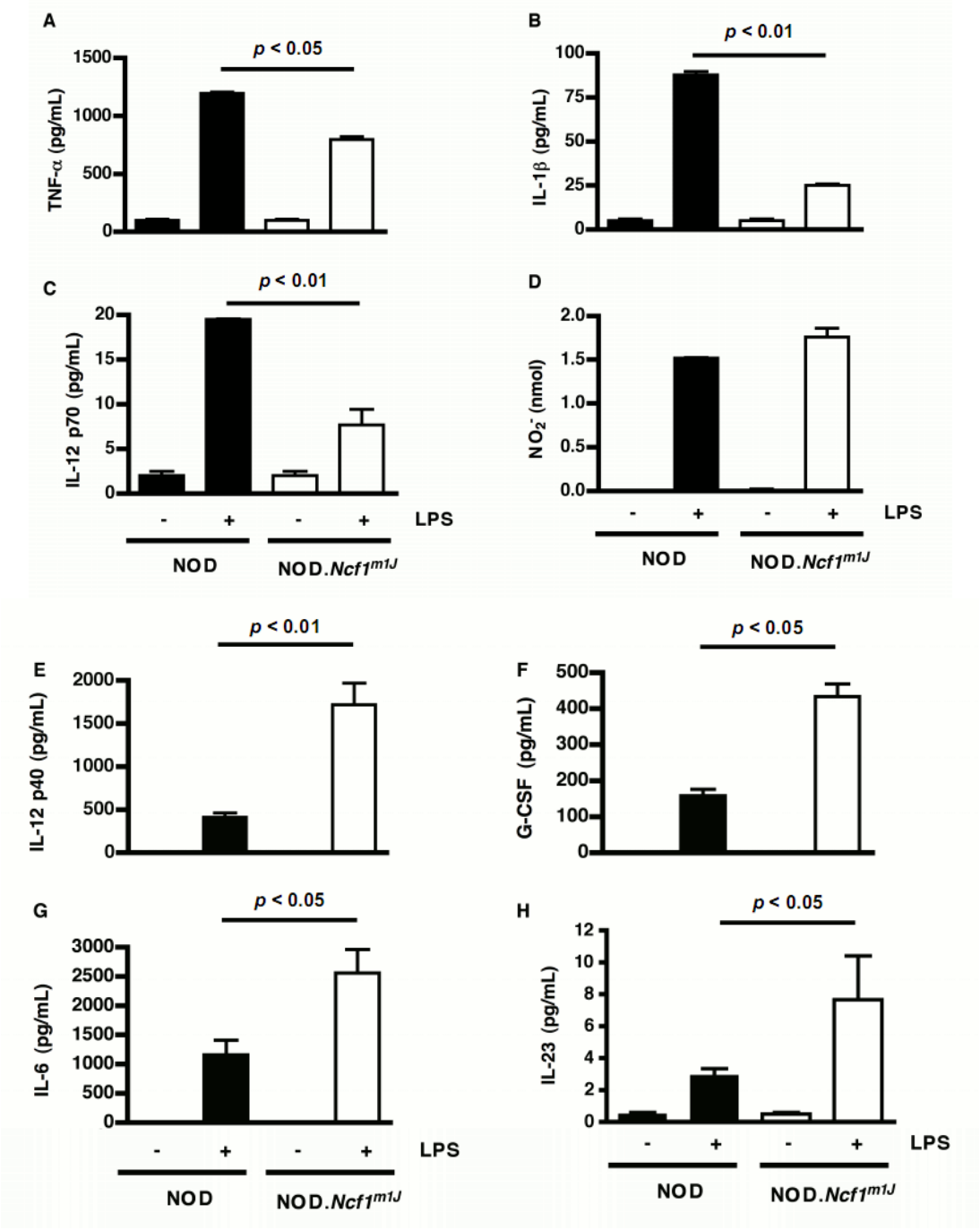

Figure 18: NOD.*Ncf1*^{m1J} macrophages exhibit a skewed Th1 to Th17 pro-inflammatory cytokine response after LPS-stimulation. NOD and NOD.*Ncf1*^{m1J} bone marrow-derived macrophages were stimulated with 1 µg/mL LPS for 4 - 24 hours. Supernatants were harvested and the levels of cytokines and chemokines were measured with cytokine-specific ELISAs and with a Luminex Bio-plex cytokine panel (A-H). Nitrite levels were measured using a Greiss assay. Results are representative of 3 independent experiments done in triplicate.

4.4.3 Modulation of superoxide alters Th17 and Th1 cytokine responses after immunization

To determine if a Th17 response in NOD-*Ncf1*^{m1J} T cells was also occurring in response to nominal antigen immunization, NOD and NOD-*Ncf1*^{m1J} mice were immunized with HEL and an antigen-recall assay was performed. The role and cell source of superoxide were assessed using a crisscross HEL antigen-recall assay with purified and negatively selected CD4^{+} T cell and APC LN cellular fractions from both HEL-immunized NOD and NOD-*Ncf1*^{m1J} mice. As with the anti-CD3/anti-CD28 responses detailed above **(Figure 15B-K)**, in the recall portion of the assay when NOD T cells and APC were mixed, they exhibited a Th1 cytokine response, whereas the mixture of NOD-*Ncf1*^{m1J} T cells and APC remained Th17 skewed **(Figure 19A-F)**. Interestingly, the development of HEL antigen-specific T cells *in vivo* with both intrinsic and extrinsic source of superoxide, provided stringent commitment towards Th1 memory T cell responses that was unaltered when NOX-deficient APC were used in the recall portion of the experiment. However, HEL antigen-specific NOD-*Ncf1*^{m1J} T cells exhibited both Th1 and Th17 cytokine responses in the presence or absence of extrinsic superoxide, respectively. IFNγ and IL-2 levels in HEL-specific NOD-*Ncf1*^{m1J} T cells were restored to NOX-intact levels when NOD APC provided an extrinsic source of superoxide **(Figure 19A and 19B)**. However, in the absence of an intrinsic source of NOX, NOD-*Ncf1*^{m1J} T cells remained high producers of IL-17 and IL-10 **(Figure 19C and 19E)**. These data provide evidence that the presence and cellular source of superoxide are both key in the type of T helper responses generated during immune responses.

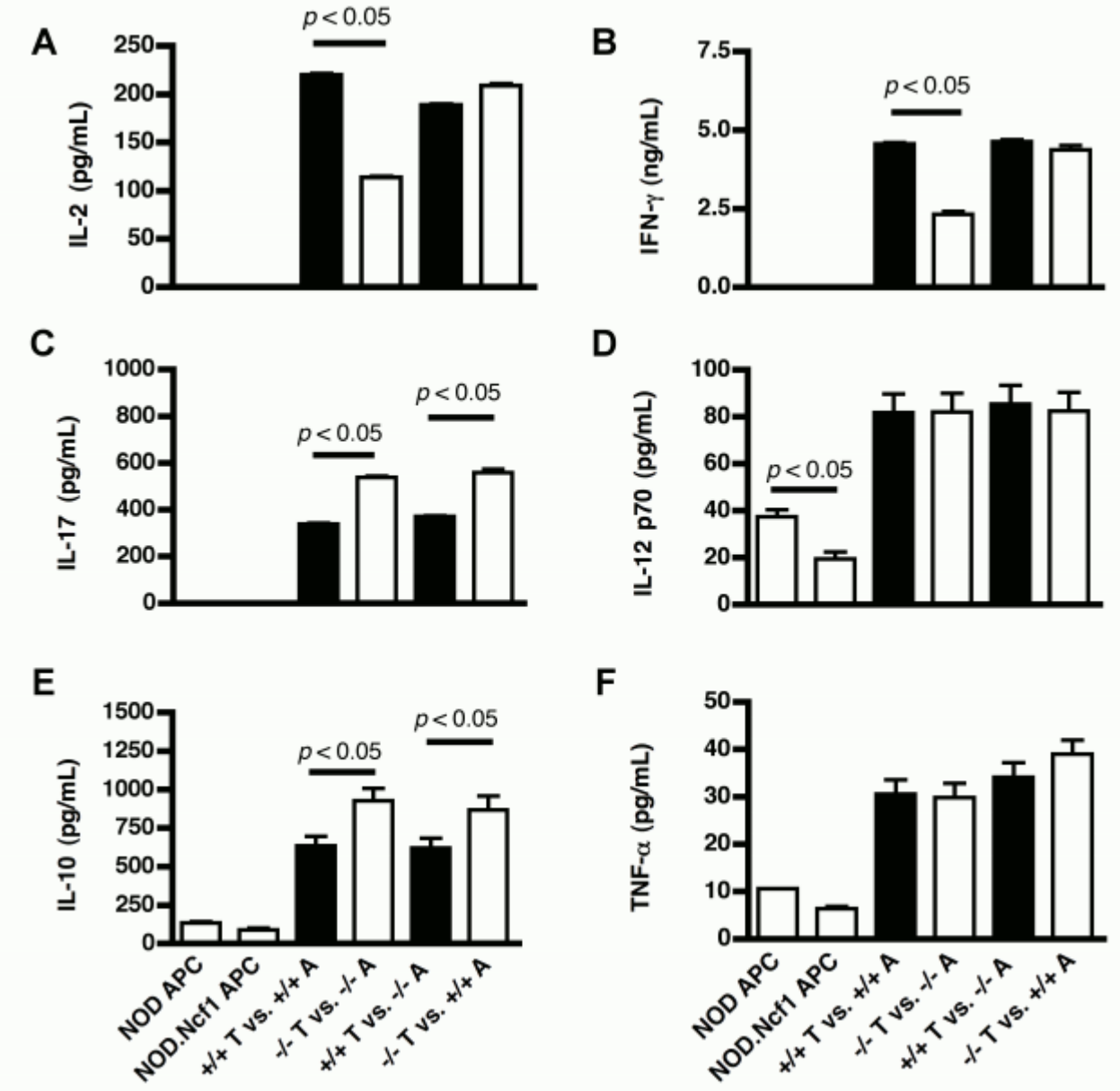

Figure 19: NOD-*Ncf1*^{m1J} mice exhibit both Th17 and Th1 T cell responses after HEL immunization. Antigen-recall crisscross assay with negatively selected and purified T cells and APC from the LN of HEL-immunized NOD and NOD-*Ncf1*^{m1J} mice. T cells (2 x 10^5) and APC (2 x 10^5) were combined in a crisscross fashion with 25 μg HEL and stimulated for 72 h. Supernatants were collected and cytokine synthesis was measured with cytokine-specific ELISAs and a Luminex Bio-plex cytokine panel (A-F). Results are representative of 3 independent experiments.

4.4.4 NOD and NOD.*Ncf1*^{m1J} mice do not differ in levels of T Regulatory (Treg) Cells

Recently, links between Th17 cells and Treg cells have been observed based on their requirement of TGF-β synthesis (270) and the established role of this cytokine in Treg maturation. Subsequently, experiments using combinations of IL-6, IL-21, and IL-23 with TGFβ established the concept that these cytokines influenced T cell progression toward a Th17 or Treg phenotype (271). Since NOD-*Ncf1*^{m1J} mice respond to polyclonal and antigenic stimulation with a Th17-like cytokine profile **(Figures 15, 16, 18, and 19)**, we further examined if these mice also exhibited an increase in Treg cells. Flow cytometry for Treg cells, as defined by the cell-specific markers CD4$^+$CD25$^+$FoxP3$^+$, were compared in NOD-*Ncf1*^{m1J} and NOD mice. We did not observe a difference in absolute numbers of Treg cells **(Figure 20A)** nor in the percentage of Treg cells relative to splenocytes **(Figure 20B)** or CD4$^+$ T cells **(Figure 9B)** between NOD-*Ncf1*^{m1J} and NOD mice.

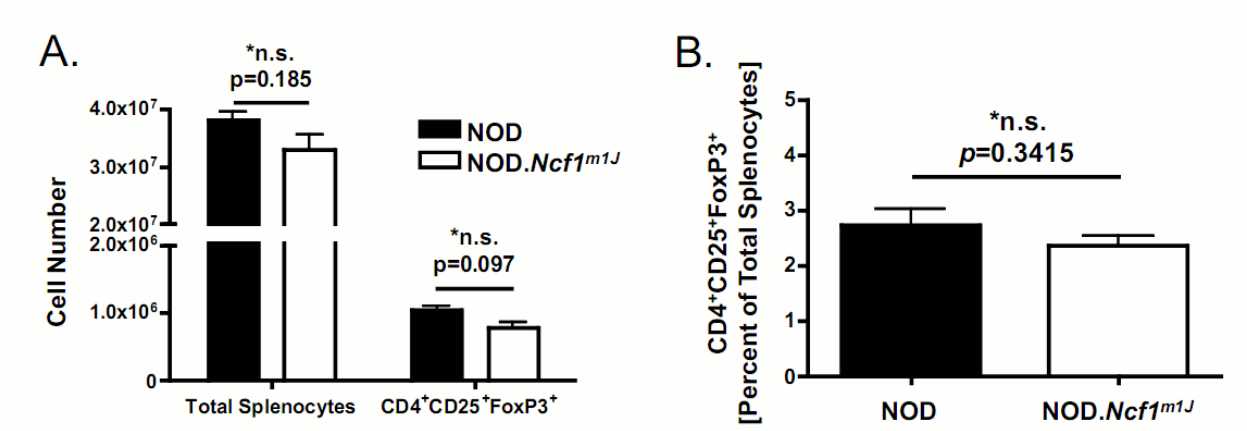

Figure 20: NOD mice with *Ncf1*^{m1J} mutation do not have increased numbers of Treg cells. (A) The total splenocytes and Treg (CD4$^+$CD25$^+$FoxP3$^+$) cell number and (B) percentage of Treg from NOD and NOD-*Ncf1*^{m1J} mice were assessed by flow cytometry. Total splenocytes were counted on Beckman Coulter (Fullerton, CA) counter. Splenocytes were gated on CD4$^+$CD8$^-$T cells, and CD25$^+$FoxP3$^+$ population was selected to determine percentage Treg cells.

4.4.5 NOD.*Ncf1*^{m1J} mice exhibit enhanced sensitivity to MOG_{35-55}-induced Experimental Allergic Encephalomyelitis (EAE).

Th17 cells are essential mediators of autoimmune destruction in multiple sclerosis, enriched in the central nervous system-infiltrates (272), and are highly pathogenic upon adoptive transfer (273). It is important to note that previous research has linked mutations in *Ncf1* to enhanced RA and EAE susceptibility (172, 259), but associations with *Ncf1* polymorphisms and enhanced Th17 responses have not been correlated. We therefore tested for differences in EAE induction between NOD and NOD-*Ncf1*^{m1J} mice by employing an immunization strategy with myelin oligodendrocyte glycoprotein peptide sequence 35-55 (MOG_{35-55}) that was previously demonstrated to elicit a low level of disease incidence in NOD mice (264). Immunization of NOD mice with MOG_{35-55} resulted in low EAE incidence (3/10; **Table 1**) with a mean day of onset at 62 days. In contrast, MOG_{35-55}-immunized NOD-*Ncf1*^{m1J} mice exhibited an extremely accelerated disease with a mean onset of 23 days and 100% incidence **(11/11; Table 1)**.

Table 1. NOD-*Ncf1m1J* mice exhibit enhanced susceptibility to EAE compared to NOD and SJL.

Strain	EAE incidence[a]	Mean Severity	First Day of Onset	Average Age of Onset
SJL	0/9	0	N/A	N/A
NOD	3/10	0.5	51	62 ± 10
NOD-*Ncf1*^{m1J}	11/11[b]	1.8[c]	9	23 ± 18

a - EAE was induced as described in the *Materials and Methods*.

b - EAE incidence compared to NOD $p<0.0001$

c - Mean severity compared to NOD $p=0.0018$

4.5 DISCUSSION

In our previous studies we have demonstrated the importance of ROS in the pathogenesis of T1D (210, 227-229, 232). Whereas elevated ROS-dissipating enzymes protect against beta cell destruction *in vitro*, the transgenic overexpression of antioxidants in beta cells via the rat insulin promoter has been less efficacious in protecting against spontaneous T1D development. Previous studies have demonstrated a role of systemic elevation of ROS dissipation (112, 133, 210, 228, 230, 232) in protection from T1D, yet the effect of altering immune cell ROS production in the context of T1D has not been extensively tested. To address this question, NOD mice containing a mutation in *Ncf1* (NOD-*Ncf1*^{m1J}) that prevents the proper assembly of the NOX complex, resulting in the absence of superoxide synthesis from stimulated neutrophils **(Fig. 8C)**, macrophages **(Fig. 8E)**, and T cells **(Figure 9A)** were generated. Inhibition of NOX activity had a positive impact on diabetes development. NOD-*Ncf1*^{m1J} female mice exhibited a significant reduction (35% in NOD-*Ncf1*^{m1J} versus 85% in NOD; $P<0.0003$) and delay ($P<0.0001$) in autoimmune diabetes development compared to female NOD mice as well as reduced insulitis.

Whereas we have observed reduced autoimmunity in NOD-*Ncf1*^{m1J} mice, the *Ncf1*^{m1J} allele has been characterized previously in murine models of rheumatoid arthritis (RA) and EAE (259). In addition, deactivating mutations in *Ncf1* have been associated with RA in both patients as well as in a rat RA model (171, 274). Likewise, NOD-*Ncf1*^{m1J} mice also exhibited enhanced EAE sensitivity in contrast to the significant reduction in T1D observed in this mutant strain.

There are differences between these diseases, with perhaps the most obvious being the inveterate Th17 responses associated with both EAE and CIA while data extant have positioned T1D as a Th1 mediated disease (255). Based on our results with the NOD-*Ncf1*^{m1J} mouse, we hypothesized that the divergence in onset of autoimmunity in mice with the *Ncf1*^{m1J} mutation results from alterations in the T helper responses that are indicative of T1D (Th1) versus EAE and RA (Th17). The results contained within demonstrate that superoxide is a key mediator of this phenomenon.

In the absence of superoxide generation, the immune system may compensate for impaired neutrophil respiratory burst activity by deviating towards a Th17 phenotype (275). Neutrophils are an essential arm of innate immunity and their main effector mechanism in response to infection is the initiation of a respiratory burst to generate superoxide. IL-17 has no direct chemotactic activity, but it can induce G-CSF, IL-6, and chemokine expression (276, 277) to recruit and activate circulating neutrophils (278). Loss of ROS-mediated inflammation may result in the immune system compensating for this defect by over-expressing signals necessary for neutrophil recruitment via IL-17R-signaling. Recent evidence has demonstrated a role for IL-23 in mobilizing neutrophils when host defenses require superoxide production (275). Therefore, the overproduction of IL-23 in the NOD-*Ncf1*^{m1J} system is likely a result of the absence of superoxide production. These findings provide evidence that the loss of superoxide synthesis will deviate a Th1-prone immune response towards a Th17 cytokine response.

It has been well characterized that NOD mice exhibit numerous T cell immunological defects such as a strong skewed Th1 cytokine response (279), altered secretion of IL-2 (280), and predisposition to heightened IFNγ response compared to C57BL/6 (281). The enhanced Th1 cytokine response in NOD mice may be due to chronic redox signaling mediated by an inherent

altered redox homeostatic state. The cytoplasmic and nuclear redox environment of NOD T cells may facilitate and enhance Th1 proinflammatory cytokine synthesis that is absent in C57BL/6 T cells. The role of NOX inactivity has conflicting interpretations on the C57BL/6 background. Polyclonal-stimulated $CD4^+$ and $CD8^+$ T cells from C57BL/6.p47^{phox} or C57BL/6.gp91^{phox} mice demonstrate elevated IFNγ levels and ERK1/2 phosphorylation in contrast to wild-type T cells. However, C57BL/6 T cells deficient in the GTP-binding protein Rac2, a co-adapter molecule essential for NOX activity (282, 283) exhibited altered T cell activation as evidenced by a 2-3-fold reduction in IFNγ synthesis and decreased ERK1/2 and p38^{MAPK} activation (284, 285). Based on these as well as our previous results, we propose that the introduction of the *Ncf1*^{m1J} mutation in the NOD background lowers the chronic production of ROS, resetting redox homeostasis and signaling in this autoimmune prone strain.

We previously reported that in the absence of a redox-dependent proinflammatory third signal consisting of both ROS and proinflammatory cytokines (TNFα, IL-1β, IL-12 p70), antigen-specific T cells fail to achieve optimal Th1 effector function (202). The NOD-*Ncf1*^{m1J} mouse corroborates these observations due to their inherent inability to generate superoxide and the resulting altered cytokine profile. In our current study, we were able to further define and characterize the importance of proinflammatory third signal synthesis as it pertains to both Th1 and Th17 T cell adaptive immune maturation. Naïve $CD4^+$ T cells from NOD mice elicit a Th1 response synthesizing increased levels of IFN-γ after polyclonal stimulation. However NOD-*Ncf1*^{m1J} naïve T cells had elevated IL-17 demonstrating a Th17 response when ROS production is lacking. Additionally, NOD mice immunized with HEL generated a memory effector Th1 cytokine response (IL-12 p70, IFNγ) whereas NOD-*Ncf1*^{m1J} mice generated a Th17 (IL-17) memory effector cytokine response upon secondary challenge with HEL. In NOX-intact NOD

mice whereby an intrinsic (T cell) and extrinsic (APC) source of superoxide is available, antigen-specific Th1 T cells undergo efficient adaptive immune maturation and effector function. Upon secondary challenge, only a single source of NOX either intrinsically (T cell) or extrinsically (APC) will suffice to mediate an efficient Th1 cytokine response. The memory T cells from the NOD mouse remain committed in a Th1 phenotype; alternatively, the lack of extrinsic superoxide cannot reprogram these cells. Interestingly, the cytokine response of NOD-*Ncf1*^{m1J} T cells from the HEL criss-cross antigen-recall assay could be restored to a Th1 phenotype (IL-12 p70, IFNγ) if an extrinsic source of superoxide (NOD APC) was provided upon secondary challenge. Th17 cells have been noted for their ability to change phenotype. Highly polarized Th17 BDC-2.5 T cells expressing IL-12Rβ2, responded to IL-12 p70, and reverted to a Th1 phenotype after adoptive transfer *in vivo* (286). Further confirming the plasticity of Th17 T cells in T1D, Martin-Orozco *et al.* also demonstrated that Th17-polarized BDC-2.5 T cells converted to IFNγ-producing cells and mediate pancreatic beta cell destruction (287). Th17 T cells may have a role in promoting inflammation, but it is the generation of IFNγ and a Th1 effector response that is ultimately responsible for autoimmune-mediated beta cell death in T1D.

The work presented herein demonstrates the significance and importance of innate and adaptive immune sources of superoxide to mediate efficient Th1 T cell responses. Loss of intrinsic and extrinsic NOX elicited a novel and skewed Th17 lineage commitment program, while suppressing the expression of transcription factors necessary for Th1 T cell development. Alternatively, the presence of superoxide appears to drive commitment to Th1. These *in vitro* responses were confirmed by enhanced susceptibility to EAE in superoxide deficient NOD-*Ncf1*^{m1J} mice while NOX-intact NOD mice were polarized to Th1 and developed T1D. Recent reports have documented that *Tbx21* and *Gata3*, genes for Th1 and Th2 lineage commitment,

respectively, contain both active and repressive histone modifications in all effector T cell subsets that may explain the flexibility of T cells to change phenotypes (288). Whether oxidation of guanine nucleotides to 8-oxo-dG in the promoter elements of *Tbx21, Stat4, Rorc*, and *Stat3* can mediate gene silencing and/or expression similar to histone modifications warrants further study. Furthermore, characterizing the importance of ROS in T cell responses may provide a novel therapeutic target for the treatment of inflammatory-mediated diseases such as T1D, whereas enhancing ROS may skew immune responses that are at the root of multiple sclerosis or rheumatoid arthritis.

5.0 FINE MAPPING OF ALR-DERIVED *SUPPRESSOR OF SUPEROXIDE PRODUCTION* LOCUS ON CHROMOSOME 3

5.1 ABSTRACT

Reactive oxygen species have been proposed to play a role in the pathogenesis of autoimmune type 1 diabetes. Our previous results support this hypothesis by demonstrating that reduction of NADPH Oxidase (NOX) activity by either genetic ablation or heightened antioxidant activity significantly reduces the development of T1D by altering the function of both macrophages and T cells. We previously linked increased SOD1 activity and decreased monocyte ROS with diabetes resistance and decreased autoreactivity in the ALR as well as NOD mice congenic for ALR-derived *Suppressor of Superoxide Production (Susp)* locus. To determine the genetic basis for *Susp* phenotypes we generated reciprocal congenic mouse strains where either the ALR-derived *Susp* region was introgressed into the NOD genetic background or ALR mice carry NOD genome on Chr. 3. These mice were used to map *Susp* to a 20 Mbp interval. However, a dearth of informative markers led to the inability to further positionally clone the phenotype. Due to the extreme genetic similarities of ALR and NOD in the *Susp* region on Chr. 3 we initiated an independent cross to fine map the gene responsible for *Susp*. (ALRxCAST) F1 male mice were backcrossed to ALR females to generate [ALRx(ALRxCAST)F1]BC1 population. Genetic linkage analyses determined that only Chr. 3

was in linkage disequilibrium for *Susp*. Using a total of 464 BC1 mice *Susp* was localized between *D3Mit180* (34,405,650 Mbp) and *D3Mit223* (34,812,804 Mbp) on Chr. 3. This mapping defines a novel candidate region involved in the regulation of SOD1 activity and dimerization stability, resulting in reduced superoxide release via NADPH oxidase activity.

5.2 INTRODUCTION

ROS production via NADPH Oxidase (NOX) by both antigen presenting cells (APC) (153) and T lymphocytes (181) is potentially a major source of free radicals in immune signaling. Genetic ablation of NOX superoxide production in an NOD background provides significant protection from advancing insulitis and diabetes onset (184). As well, antioxidant regulation of free radical production has been associated with T1D resistance (202, 207, 208, 210). Previous genetic mapping studies using T1D-prone NOD with T1D-resistant ALR mice linked resistance against spontaneous autoimmune diabetes, reduced oxidative burst from neutrophils and macrophages, as well as elevated Superoxide Dismutase 1 (SOD1) activity to the *Suppressor of Superoxide Production* (*Susp*) locus on Chr. 3 (112, 230). Congenic replacement of Chr. 3 *Susp* locus in the NOD provided 100% protection from T1D and was associated with decreased autoreactivity of T lymphocytes (Chapter 2). This suggests that *Susp* regulation of SOD1 activity was modifying T1D susceptibility.

The SOD1 enzyme is highly conserved and is ubiquitously expressed (289). Post-translational modifications of SOD1 are essential for enzyme maturation and activation (289-292). Foremost, the binding of zinc and the incorporation of copper facilitated by the copper

chaperone for SOD1 (CCS) are required. Copper loading is accomplished via oxygen-dependent disulfide isomerization, producing disulfide-oxidized SOD1 subunits (293, 294). Two oxidized SOD1 subunits homodimerize to form enzymatically active SOD1 (292, 295). Metal incorporation and dimerization are tightly regulated, however the mechanism controlling these activities are not fully defined. As SOD1 facilitates the dismutation of superoxide to hydrogen peroxide, this scavenging is important to alleviate redox stress during and after inflammatory processes (234, 289, 296). In addition to free radical scavenging, recent studies suggest SOD1 interacts with NOX subunits to regulate superoxide production (297). Characterization of increased SOD1 activity and stability as well as reduced superoxide release in the ALR suggests a novel interaction mediated by a gene candidate for *Susp* is facilitating a post-translational modification of SOD1.

To determine the genetic basis for increased SOD1 activity and stability as well as reduced NOX, (ALRxCAST) F1 male mice were backcrossed to ALR females to generate [ALRx(ALRxCAST)F1]BC1 population. A cohort of 40 BC1 mice, as well as 16 BC1 mice with recombinations on Chr. 3 was assessed for SOD1 activity and respiratory burst. Coupling phenotypic characterization with genotypic profiling analyses determined only Chr. 3 was in linkage disequilibrium. High resolution fine mapping localized ALR-derived *Susp* locus between *D3Mit180* (34,405,650 Mbp) and *D3Mit223* (34,812,804 Mbp) on Chr. 3. To date, this interval contains one known gene, *Sox2*, three predicted genes, and one microRNA, Mir1897. Evaluating the *Susp* interval and these candidates may define allelic or expression differences unique to the ALR that directly or indirectly regulate SOD1 dimerization. This mapping potentially defines a novel candidate involved in the regulation of SOD1 activity and NOX function.

5.3 METHODS

5.3.1 Animals

The ALR-derived *Susp* locus was congenically introgressed into the NOD genome as well as introduction of NOD Chr. 3 region to ALR. NOD mice were mated with male ALR mice, and the subsequent F1 progeny were backcrossed to NOD. Likewise, Fl progeny from ALR female to NOD male matings were backcross to ALR. Selection for either ALR or NOD contributing genome on Chr. 3 and eliminating contamination elsewhere on the genome was achieved through PCR amplification of 76 informative microsatellite primers spanning all Chromosomes and 6 microsatellite primers on Chr. 3. Mice were backcrossed for 10 generations, followed by intercrossing to select NOD mice with ALR homozygous *Susp* locus (NOD-*Susp*) or ALR mice homozygous for NOD genome on Chr. 3 (ALR.NODc3). Mice with various recombinations on Chr. 3 were used for fine mapping analysis.

ALR/LtJ, NOD/ShiLtJ, NOD-*Susp*, ALR.NODc3, as well as [ALRxNOD]F1 hybrid mice were bred and housed in the University of Florida facility under specific pathogen-free conditions. CAST/EiJ were purchased from The Jackson Laboratory (Bar Harbor, ME) and were outcrossed with ALR/LtJ in our facility. [ALRxCAST]F1 hybrid progeny were backcrossed to ALR to generate a first backcross (BC1) generation. All mice were housed in specific pathogen-free facilities and approved by the Institution Animal Care and Use Committee at the University of Florida.

5.3.2 Materials

Dihydrorhodamine 123 (DHR123) was purchased from Invitrogen (Carlsbad, CA). Superoxide Dismutase activity assay kit was purchased from Cayman Chemical (Chantilly, Virginia). All DNA oligonucleotides were obtained from Integrated DNA Technologies, Inc. (Coralville, Iowa). Histopaque-1119 was obtained from Sigma-Aldrich (St. Loius, MO).

5.3.3 Assessment of SOD1 activity

Liver and bone marrow homogenates were prepared in 20 mM HEPES buffer (pH 7.2) with 1 mM EGTA, 210 mM mannitol and 70 mM Sucrose. Protein content was determined using Pierce BCA Protein Assay Kit (Thermo Scientific). SOD1 was extracted using ethanol:chloroform (62.5/37.5 v/v). After centrifugation at 3000 x *g* for 5 min, the aqueous layer contained SOD1 was collected. SOD1 activity was measured with Superoxide Dismutase Assay Kit (Cayman Chemical) following manufacturer's protocol.

5.3.4 Flow cytometric analysis of oxidative burst

Neutrophil and macrophage superoxide production were assayed using FACS as previously described (230). Briefly, bone marrow was isolated and purified using a Histopaque-1119 gradient. Cells were labeled with PerCpCy5.5-labeled anti-Ly6g (Gr1) and APC-labeled anti-CD11b and then loaded with Dihydrorhodamine 123 (DHR 123) for 5 minutes at 37°C. Cells were subjected to flow cytometry prior to stimulation, and then at 5 min intervals after 98

nM PMA stimulation. The ROS driven conversion of DHR 123 to rhodamine was measured using a BD Fortessa and were analyzed with FACSDiva software (BD Biosciences).

5.3.5 Genome Wide Scan using single nucleotide polymorphisms

Backcross mice generated from the mating of (ALRxCAST) F1 to ALR were used for phenotypic analysis of oxidative burst and SOD1 activity as well as genotypic analysis. Genomic DNA was prepared from kidney and genotyped for 73 SNPs spanning all chromosomes by Kbiosciences **(Table 2)**. High resolution coverage of Chr. 3 was obtained by PCR amplification of 10 microsatellite markers **(Table 2)**. Chi square values were calculated using JMP software and considered significant with $p<0.001$.

5.3.6 Candidate gene expression analysis

RNA was isolated from bone marrow and live lysates with TRIzol and cDNA prepared by M-MLV reverse transcriptase kit (Invitrogen). PCR amplification was performed with the following primers: *Gm3143* forward 5'-TCACAGGAAAGATGGCAGTCA-3', reverse 5'-TTGGGCCACAACAGTGAAAG-3'; *Gm6282* forward 5'-ATCCAGTCGCTCAGGTGCT-3', reverse 5'-TGGGAGATGCTGTTCCAAAGT-3'; *Gm7723* forward 5'-GAGCAGGGAAAGTTTGGAGC-3', *Gm7723* 5'-GGTGAAGAGGGGTTGGTGAG-3'; and *Sox2* forward 5'-CGAACTGGAGAAGGGGAGAG-3', reverse 5'-AAGCGTTAATTTGGATGGGA-3'. Amplification products were separated on a 4% agarose gel and visualized with ethidium bromide.

5.3.7 Cytochrome c measurement of oxidative burst

Bone marrow was collected from age-matched female mice and red blood cells were removed on a Histopaque-1119 gradient as previously described (230). Cells (10^5) were pretreated with 2 mM KCN or HBSS for 15 min at room temperature, transferred to HBSS containing 145 μM cytochrome C, and were stimulated with PMA (98 nM) at 37°C. Reduction of cytochrome C was measured at 550 nm at 1 min intervals for 45 min. The maximum rate of reduction was calculated by linear regression analysis. Purified SOD1 (0.5 U/mL) was used to confirm specificity of superoxide production.

5.3.8 Statistics

GraphPad Prism (GraphPad Software, Inc, (La Jolla, CA)] was used for calculating statistical differences. Significance between mean values was determined using the Student's *t* test or One-way ANOVA test, with $p < 0.05$ considered significant. Kaplan-Meier survival analysis was used to evaluate diabetes onset.

5.4 RESULTS

5.4.1 Genetic analysis and fine mapping of *Susp* locus on Chr. 3.

Previous segregation analysis localized reduced superoxide production in the ALR to a locus on Chr. 3 termed *Susp* (112, 230), controlling increased SOD1 activity and decreased NOX

function. This locus overlapped with an independently mapped ALR-derived T1D protective locus, suggesting *Susp* may contribute to diabetes resistance by modifying ROS production (230). To evaluate the role of the Chr. 3 locus, NOD-*Susp* mice were generated by introducing ALR Chr. 3 genome into the NOD background (NOD-*Susp*), as well as the reciprocal congenic by introgressing of NOD Chr. 3 genome to the ALR (ALR.NODc3). During the development of the congenic mice progeny were screened on Chr. 3 to map recombinations, followed by phenotypic analyses of oxidative burst and SOD1 activity. Coupling phenotypic profile **(Fig. 21A-B, showing most informative mice)** with genotyping information a physical location between microsatellite markers *D3Mit167* (32.1 Mbp) and *D3Mit64* (49.9 Mbp) was defined **(Fig. 21C)**. Further recombination boundary discrimination was limited due to the lack of additional informative microsatellites. In fact, in the region on Chr. 3 NOD and ALR have few, if any, polymorphisms. To identify informative polymorphisms comparing ALR to NOD the Jax Diversity array was run. Analyses did not provide additional polymorphisms comparing NOD and ALR **(Fig. 22)** and served to confirm the haploidentity throughout this region on Chr. 3. However, the diversity array analysis comparing ALR to CAST identified high degree of genetic diversity **(Fig. 22)**. CAST strain also elicits a robust oxidative burst and demonstrates low SOD1 activity compared to the ALR **(Fig. 23)**. Therefore, to obtain high resolution fine mapping, the ALR was mated to CAST, followed by backcrossing F1 progeny to ALR.

Genome-wide linkage analysis was performed using a cohort of 40 BC1 mice. Backcross mice were assessed for oxidative burst and SOD1 activity compared to parental controls. Genomic DNA was analyzed for 73 informative SNPs spanning all chromosomes, with only Chr. 3 in linkage disequilibrium with *Susp* **(Table 2)**, with the peak at *D3Mit168* **(Fig. 24)**. An additional 490 backcross mice were screened for recombinations on Chr. 3, identifying 16 mice

that exhibited meioses within the *Susp* interval. Genotypic profiling and phenotypic analyses of these mice allowed for high resolution mapping on Chr. 3, localizing *Susp* to the 407,297 bp region between *D3Mit180* (34.4 Mbp) and *D3Mit223* (34.81 Mbp).

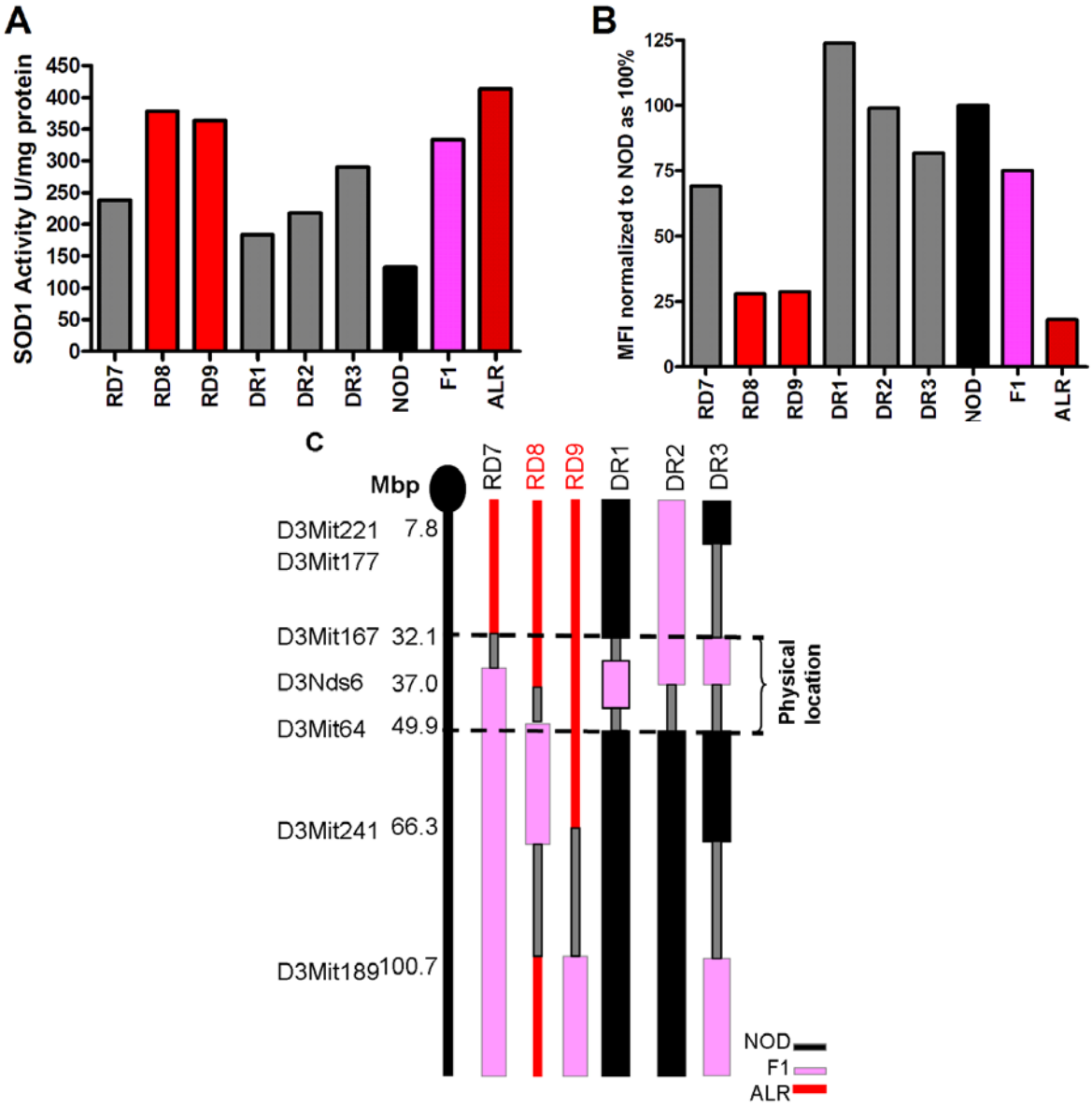

Figure 21: Fine Mapping of NOD-*Susp* and ALR.NODc3 recombinant mice. Evaluation of phenotypic profile of (A) liver-homogenate SOD1 activity and (B) macrophage respiratory burst after PMA stimulation. Superoxide production was measured by monitoring the conversion of DHR123 via flow cytometry.

Mean fluorescence intensity (MFI) at 30 min post-PMA is normalized to NOD as 100%. (C) Genotyping of microsatellite markers on Chr. 3 defines the physical location of *Susp*. Represented are the most informative mice, defining the boundaries of the physical location. Regions of unknown genetic inheritance in grey.

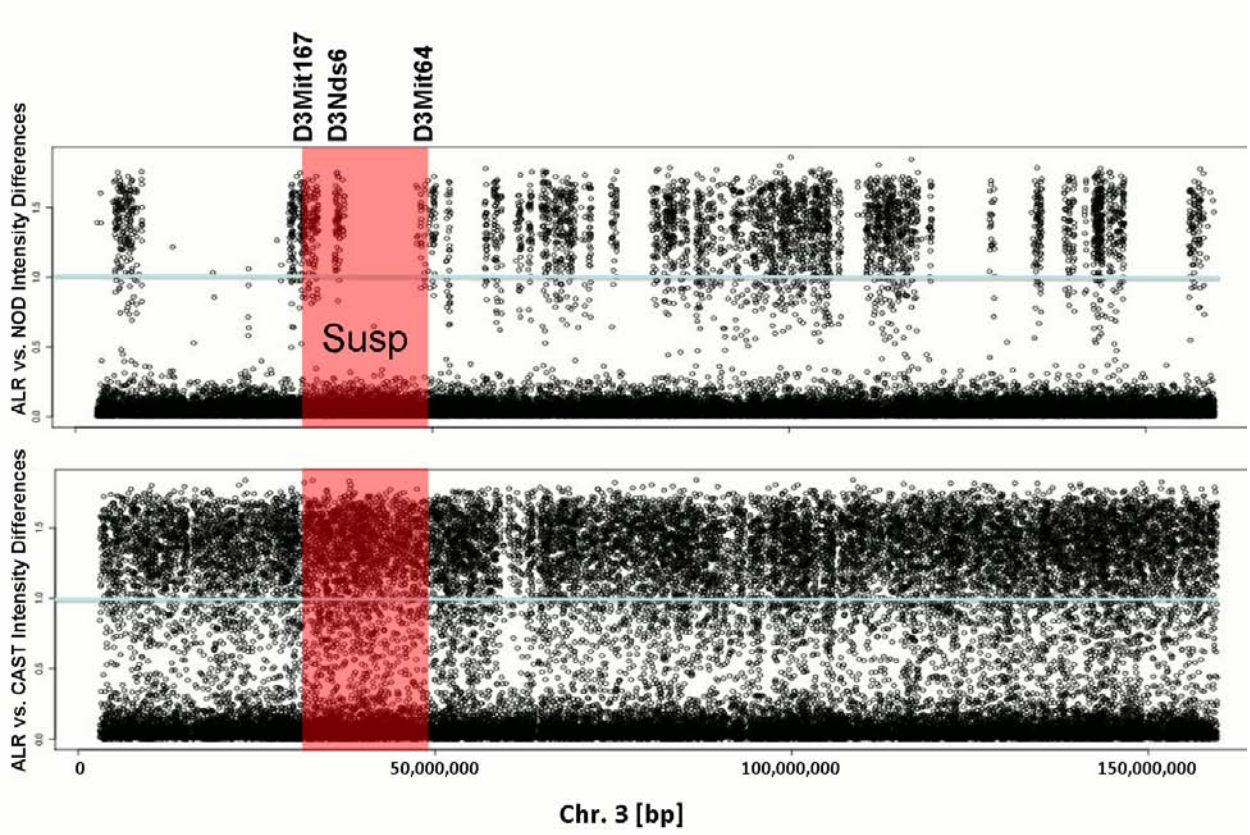

Figure 22: Diversity array of Single Nucleotide Polymorphisms (SNP) across Chr. 3 comparing ALR to CAST and NOD. SNPs determined as the measured intensity difference (y-axis) in nucleotide base at a given position across Chr. 3 (x-axis), with a difference above 1 (blue line) considered as polymorphic.

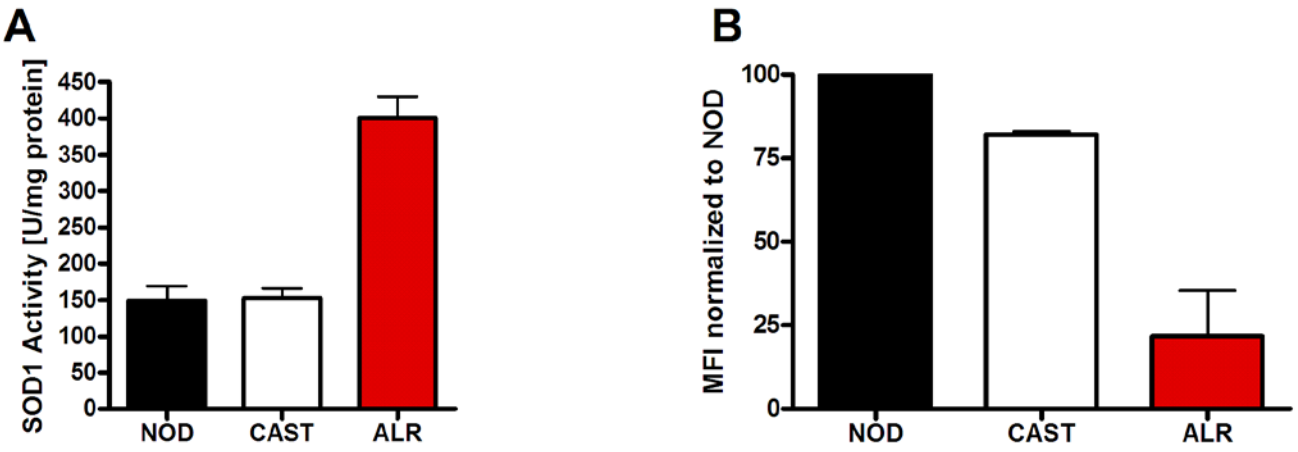

Figure 23: Phenotypic profile of CAST mice. (A) Liver SOD1 activity of CAST compared to NOD and ALR. (B) Superoxide production was measured by monitoring the conversion of DHR123 via flow cytometry. Mean fluorescence intensity at 30 min post PMA is normalized to NOD as 100%.

Table 2: Linkage of SNP and microsatellites in [ALRx(ALRxCAST)F1]BC1 mice. Mice were phenotypes for SOD1 activity and NOX respiratory burst. Mice were characterized as ALR-like with high SOD1 activity (>300U/mg protein) and low NOX (MFI <50% of control) or CAST-like. All mice exhibited the inverse correlation of SOD1 and NOX activities. Marker positions in base pairs were obtained from The Jackson Laboratory Mouse Genome Informatics Database.

		BC1 High SOD/Low NOX		**BC1 Low SOD/High NOX**		***P* value**	**X^2**
Locus	base pair	**R**	**FI**	**R**	**FI**		
01-008110094-M	8,110,094	12	8	9	15	0.1353	2.231
01-062173915-M	62,173,915	10	11	10	16	0.5279	0.398
01-114000704-M	114,000,704	11	10	9	17	0.2202	1.503
01-147325075-M	147,325,075	12	9	6	16	0.0454	4.002
01-193173300-M	193,173,300	14	6	11	12	0.1389	2.19
02-025336678-N	25,336,678	9	12	13	12	0.536	0.383
02-080232231-M	80,232,231	12	9	11	15	0.311	1.027
02-119060027-N	119,060,027	16	6	11	14	0.025	5.022
02-172943830-M	172,943,830	12	8	11	14	0.2848	1.144
03-009298864-M	**9,298,864**	**18**	**9**	**2**	**23**	**0.0001**	**20.983**
D3Mit167	**32,170,748**	**22**	**5**	**0**	**27**	**0.0001**	**47.122**

D3Mit240	**32,529,024**	**23**	**4**	**0**	**23**	**0.0001**	**51.018**
D3Mit181	**32,965,530**	**26**	**1**	**0**	**24**	**0.0001**	**66.232**
03-034069633-M	**34,069,633**	**25**	**1**	**0**	**26**	**0.0001**	**66.232**
D3Mit180	**34,405,650**	**25**	**1**	**0**	**27**	**0.0001**	**66.232**
D3Mit168	**34,539,623**	**27**	**0**	**0**	**27**	**0.0001**	**74.86**
D3Mit223	**34,812,804**	**27**	**0**	**1**	**26**	**0.0001**	**66.232**
03-036328929-N	**36,328,929**	**24**	**0**	**2**	**24**	**0.0001**	**60.305**
D3Nds6	**37,018,998**	**26**	**1**	**1**	**25**	**0.0001**	**51.973**
D3Nds43		**25**	**2**	**2**	**21**	**0.0001**	**46.342**
D3Mit295	**38,827,463**	**23**	**4**	**4**	**19**	**0.0001**	**29.556**
D3Mit307	**39,437,974**	**22**	**5**	**4**	**23**	**0.0001**	**26.259**
03-043110442-M	**43,110,442**	**20**	**6**	**3**	**23**	**0.0001**	**24.706**
D3Mit65	**50,488,800**	**19**	**8**	**5**	**22**	**0.0001**	**15.501**
03-074327277-M	**74,327,277**	**18**	**8**	**4**	**22**	**0.0001**	**16.43**
03-100489838-M	100,489,838	18	8	8	18	0.005	7.894
03-131286062-N	131,286,062	15	11	10	16	0.1639	1.938
03-155372777-M	155,372,777	16	10	16	10	1	0
04-014657884-N	14,657,884	10	11	13	13	0.871	0.026
04-053894587-M	53,894,587	7	14	12	13	0.3125	1.02
04-103038694-M	103,038,694	6	15	11	15	0.3273	0.96
04-151168886-M	151,168,886	8	13	15	11	0.1799	1.799
05-113995253-M	113,995,253	11	10	10	16	0.3396	0.912
05-125054661-M	125,054,661	13	8	12	14	0.2806	1.164
05-137165117-N	137,165,117	14	7	12	14	0.1573	2
05-150172420-M	150,172,420	13	8	11	15	0.1799	1.799
06-006933444-M	6,933,444	12	9	10	15	0.2453	1.35
06-064751205-M	64,751,205	13	7	13	13	0.3071	1.043
06-109051116-M	109,051,116	10	10	16	10	0.4339	0.612
07-006208019-M	6,208,019	11	10	16	11	0.6338	0.227
07-043206744-N	43,206,744	14	7	13	11	0.3918	0.733
07-093235239-M	93,235,239	12	9	16	9	0.6352	0.225
07-135024189-M	135,024,189	12	8	14	11	0.7871	0.073
08-007750917-N	7,750,917	9	12	9	17	0.5636	0.333
D8Mit293	148,932,688					0.35	0.873
08-088042210-M	88,042,210	10	11	8	17	0.2794	1.17
08-126038064-N	126,038,064	9	12	13	12	0.536	0.383
09-003938578-M	3,938,578	9	12	12	14	0.8211	0.051
09-052894456-M	52,894,456	9	12	10	16	0.7602	0.093
09-115037423-M	115,037,423	13	8	11	14	0.2244	1.476

10-018064293-M	18,064,293	13	8	13	13	0.4134	0.669
10-089875395-N	89,875,395	13	8	13	12	0.499	0.457
10-128874353-N	128,874,353	9	12	11	14	0.9379	0.006
11-011378766-M	11,378,766	10	10	10	16	0.3396	0.912
11-066278669-N	66,278,669	9	12	16	10	0.2009	1.636
11-115546745-M	115,546,745	10	10	12	12	1	0
12-009581325-M	9,581,325	11	8	13	13	0.5997	0.276
12-053361254-M	53,361,254	13	8	11	11	0.4313	0.619
12-107541607-M	107,541,607	10	9	12	13	0.7608	0.093
13-009820324-M	9,820,324	9	10	8	16	0.35	0.873
13-062804732-M	62,804,732	10	10	8	19	0.1556	2.016
13-105849719-M	105,849,719	11	9	11	14	0.4629	0.539
14-013002953-M	13,002,953	13	8	10	15	0.1372	2.209
14-062668837-N	62,668,837	9	12	14	12	0.4531	0.563
14-112544301-N	112,544,301	9	12	14	11	0.3738	0.791
15-006448712-N	6,448,712	11	9	13	13	0.7364	0.113
15-055111506-N	55,111,506	12	9	13	13	0.6253	0.238
15-103221933-M	103,221,933	11	10	11	14	0.5707	0.322
16-005644892-N	5,644,892	10	11	12	14	0.9203	0.01
16-031980782-C	31,980,782	10	11	10	15	0.6036	0.27
16-090091107-C	90,091,107	9	12	10	16	0.7602	0.093
16-091028945-C	91,028,945	9	12	9	17	0.5636	0.333
16-096070057-C	96,070,057	9	12	10	16	0.5636	0.333
17-004147924-M	4,147,924	10	11	12	13	0.9794	0.001
17-031242489-M	31,242,489	11	10	12	14	0.6711	0.18
17-034146583-M	34,146,583	10	11	12	14	0.9203	0.01
17-092673068-N	92,673,068	12	9	14	12	0.8211	0.051
18-006845916-M	6,845,916	9	12	13	13	0.6253	0.238
18-063800148-N	63,800,148	8	13	14	12	0.2806	1.164
19-007376322-N	7,376,322	8	13	17	10	0.0856	2.954
19-057152618-M	57,152,618	12	9	14	12	0.8211	0.051
X-035414447-M	35,414,447	11	8	13	11	0.8068	0.06
X-121648292-M	121,648,292	10	11	14	11	0.8061	0.06

X^2 values are considered significant at $p<0.001$

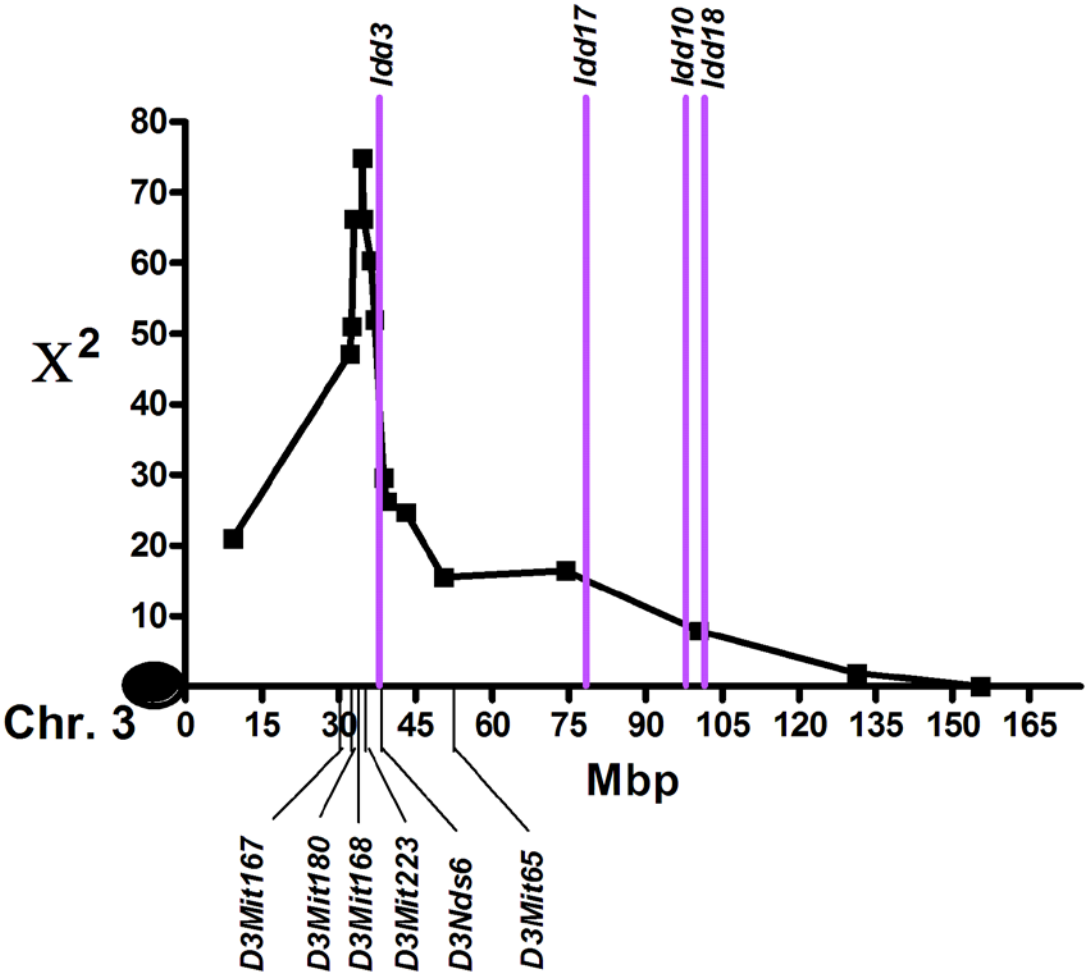

Figure 24: Map position of ALR-derived *Susp* locus on Chr. 3. Genetic linkage analysis using [(ALRxCAST)F1xALR]BC1 mice assessed for SOD1 activity and respiratory burst. Linkage was determined with 56 BC1 mice using χ^2 analysis (JMP, Cary, NC) with *P*-value less than 0.001 considered significant.

5.4.2 Evaluation of genes within the *Susp* interval

High resolution fine mapping localized *Susp* between markers *D3Mit180* (34,405,650 Mbp) and *D3Mit223* (34,812,804 Mbp) on Chr. 3 **(Table 2)** with peak Chi square value at

D3Mit168. PCR was performed to determine liver and bone marrow expression of the known gene, *Sox2*, and predicted genes, Gm3143, Gm6282, and Gm7723. Neither *Sox2* nor the predicted genes were expressed in either tissue from NOD and ALR (Data not shown), eliminating these as potential candidates. Contained within this interval is a microRNA Mir1897, which is currently being evaluated for polymorphisms unique to ALR.

5.4.3 Assessment of respiratory burst in SOD$^{-/-}$ mice

Previous reports suggest a regulatory role for SOD1 by binding to NOX complex subunits (297). Measuring superoxide release in bone marrow from B6-SOD1$^{-/-}$ knock out mice demonstrated a robust respiratory burst after PMA stimulation, even higher than full inhibition of SOD1 with KCN in B6 bone marrow **(Fig. 25)**. These data suggest that the physical presence of SOD1, even without dismutation activity, regulates NOX function.

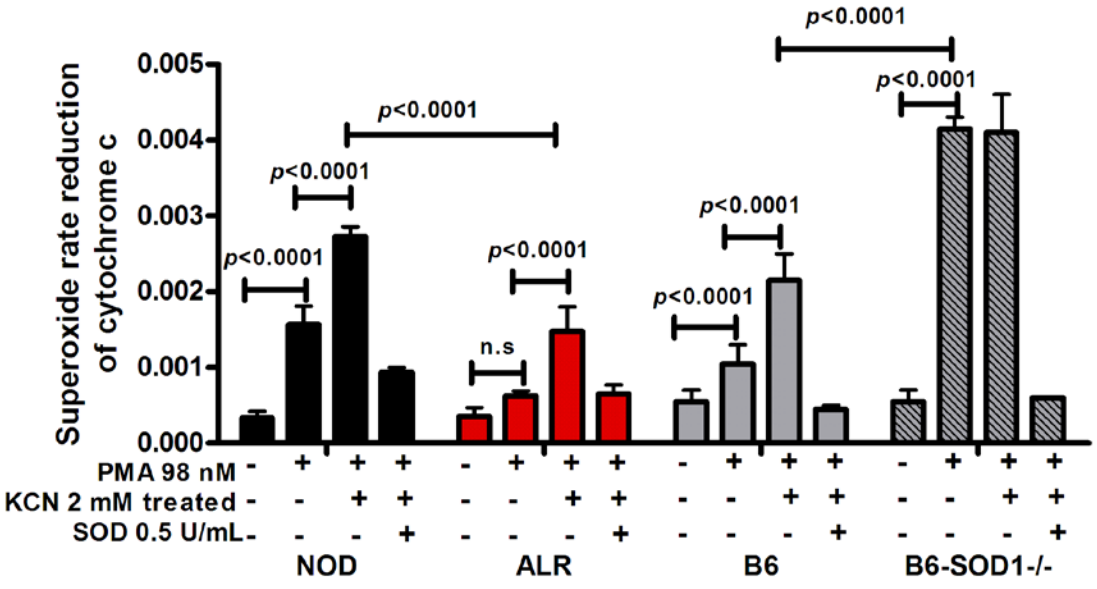

Figure 25: Superoxide release after KCN inhibition of SOD1 and PMA stimulation. Bone marrow cells from NOD, ALR, B6 and B6-SOD-/- mice were pretreated with 2 mM KCN to inhibit SOD1 activity. Cells

were stimulated with PMA and the release of superoxide was measured by rate cytochrome c reduction. Purified SOD1 was added to confirm specificity of superoxide production.

5.5 DISCUSSION

Previous segregation analysis localized reduced superoxide production in the ALR to a locus on Chr. 3 termed *Susp* (230). This locus overlapped with an independently mapped ALR-derived T1D protective locus, suggesting *Susp* may contribute to diabetes resistance in the ALR. Introduction of the ALR-derived *Susp* locus to the NOD background provided full protection from T1D and insulitis **(Fig. 4)** and a loss of diabetogenic reactivity of NOD-*Susp* $CD4^+$ T cells in susceptible hosts **(Fig. 5C)**. The reduction in neutrophil, macrophage, and $CD4^+$ T cell ROS production after stimulation is associated with increased activity of SOD1 **(Fig. 6)**.

We have previously shown that reduction of superoxide production by macrophages and T cells has a profound impact on cytokine synthesis and T lymphocyte lineage commitment (184, 202). Likewise, antioxidant regulation of free radicals also modifies macrophage and T cell reactivity (208, 210). In order to define the modification to SOD1 and the resulting modulation of immune effector function inherent to ALR, genome wide analyses were performed to fine map *Susp*. Through the use of [ALRx(ALRxCAST)F1]BC1 mice ALR-derived *Susp* locus was mapped between *D3Mit180* (34,405,650 Mbp) and *D3Mit223* (34,812,804 Mbp) on Chr. 3 **(Table 2)** with peak Chi square value at *D3Mit168*. Described to date in this region is one known gene, *Sox2,* three predicted genes, and one microRNA, Mir1897. *Sox2* and the three predicted genes were not expressed in liver or bone marrow cDNA as determined by PCR, eliminating these as candidates. Evaluating the microRNA and further

sequencing of the *Susp* interval may define allelic or expression differences unique to the ALR that directly or indirectly regulate SOD1 dimerization.

Evaluation of SOD1 from ALR did not define any polymorphisms in cDNA sequence, expression, or protein content **(Fig. 2)** compared to control strains that would account for increased activity. ALR and NOD-*Susp* SOD1 dimer activity under reducing conditions was enhanced **(Fig. 2)**, suggesting a post-translational modification was increasing enzyme stability. Inhibiting SOD1 with KCN was able to restore superoxide release after stimulation **(Fig. 3B)**; confirming elevated dismutation modified immune cell effector function. However, ALR and NOD-*Susp* superoxide release after KCN inhibition of SOD1 was not restored to the same levels as NOD, suggesting further regulation of NOX activity. Recent data suggests that SOD1 interactions with NOX complex subunits, including Rac1, provide physical control of superoxide production (297). Measuring superoxide release in bone marrow from B6-SOD1$^{-/-}$ knock out mice demonstrated a robust respiratory burst after PMA stimulation, even higher than full inhibition of SOD1 with KCN in B6 bone marrow **(Fig. 25)**. These data suggest that the physical presence of SOD1, even without dismutation activity, regulates NOX function.

Enhanced stability of ALR SOD1 dimer may also provide enhanced physical association with NOX-regulating compounds. There are several reports that describe a regulatory role of various proteins contributing to SOD1 binding and stability (138, 298, 299). Post-translational modifications are required for the assembly and maturation of active SOD1 enzyme, including incorporation of zinc and copper (138). While regulation of copper loading by the copper chaperone for SOD1 (CCS) (298) is described, mechanisms regulating dimerization are not well defined. Recently, a novel interaction of copper metabolism Murr1 domain containing 1 (COMMD1) with SOD1 was associated with regulation of enzyme maturation and dissipation

(299). A candidate gene or microRNA in the *Susp* interval may directly or indirectly modify dimer stabilization and binding, resulting in increased free radical scavenging and regulation of NOX. The alterations in redox balance may then modify free radical signaling and immune cell activity during inflammatory processes **(Fig 26)**.

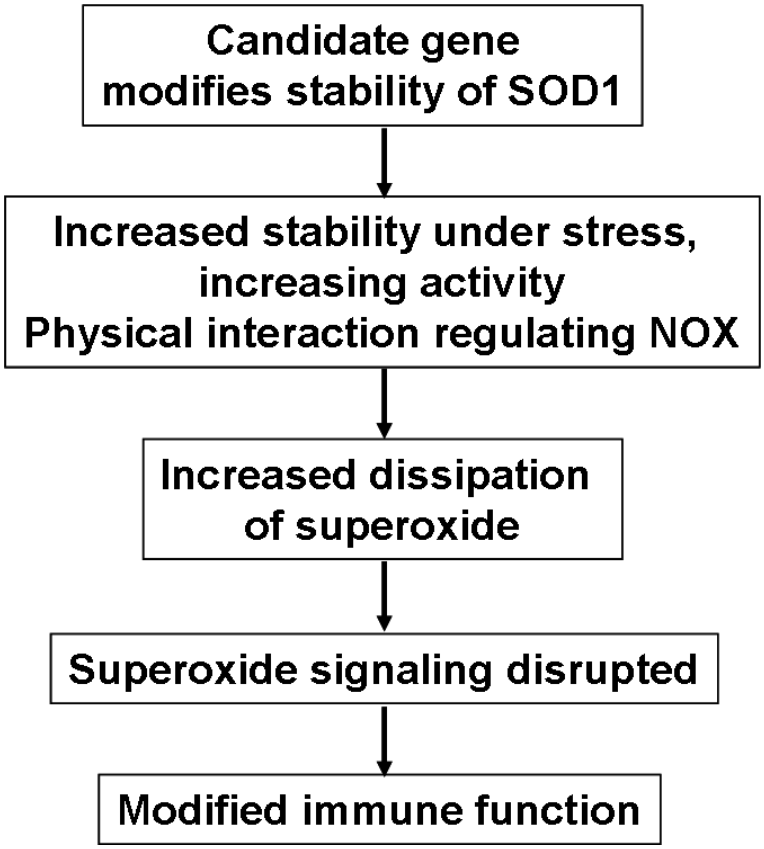

Figure 26: Schematic of proposed model of *Susp* contributions to free radical dissipation, redox signaling, and immune cell function.

6.0 CONCLUSION AND SIGNIFICANCE

Type 1A diabetes (T1D) is an autoimmune disease typically diagnosed in children and adolescents. According to the American Diabetes Association National Fact Sheet (2007), approximately 1% of the US population has T1D, with an incidence that is increasing at a rate of 3% per year. Despite advances in insulin-replacement therapy and blood glucose monitoring, there is no cure for T1D. Additionally, patients are at increased risk of severe complications associated with poor glycemic control, including cardiovascular disease, blindness, neuropathy, and nephropathy.

While previous reports suggested that antioxidant scavenging protected beta cells against free radical-mediated damage, the data presented here suggest that modulation of ROS had profound effects on the activity of autoimmune effectors. Specifically, the work herein describes a critical role for ROS signaling in the development of proinflammatory T lymphocyte responses. Two models were used to define the role of leukocyte-produced superoxide in the development of T1D: the NOD-*Ncf1*^{m1J}, with a genetic ablation of NOX function, and the NOD-*Susp*, congenic for the ALR-derived allele associated with increased free radical scavenging.

In both models, the inhibition of NOX function significantly reduced the development of T1D. This was coupled with reduced severity of insulitic infiltration, suggesting that ROS production may play a role in the migration and/or accumulation of autoreactive effectors. Despite previous reports that antioxidant therapy could protect beta cells from ROS-mediated

damage *in vitro*, the transgenic over-expression of antioxidants in beta cells via the rat insulin promoter has been less efficacious in preventing spontaneous T1D development (225, 237, 238). Rather, systemic elevation of antioxidants has more consistent results for protection of islets from damage (202, 210, 232, 239). Concordantly, islets from NOD-*Susp* congenic mice did not exhibit full protection from proinflammatory mediators, suggesting that elevated SOD1 in the pancreata was not providing the majority of T1D resistance. When assessing immune function, T cells from NOD-*Susp* mice failed to induce T1D in a susceptible host. Likewise, splenocytes and purified T cells from NOD-*Ncf1*^{m1J}mice exhibited delayed transfer of T1D. Taken together, these data highlight an essential role for ROS production in the development of efficient T lymphocyte autoreactive effector function.

Characterization of NOD-*Ncf1*^{m1J} macrophage and T cell responses identified a skewed phenotype favoring Th17 lineage commitment, as opposed to the proinflammatory Th1 profile typical of NOD. Th1 associated cytokine synthesis could be recovered as long as either APC or T cells were competent ROS producers during antigen recall. Interestingly, NOX-deficient T cells maintained elevated IL-17 and IL-10 production, suggesting *in vivo* imprinting for cytokine production. These data suggest that ROS may provide transcriptional regulation during T cell development and activation. Preliminary data with ALR splenocytes suggest a similar skewing of the immune response. Now that the *Susp* locus has been mapped to a ~407,000 bp interval, production of congenic mice based on this region can identify a candidate gene and mechanism accounting for the increased SOD1 activity and stability. Additionally, the role of *Susp* in modifying T cell effector function can be defined. These data suggest that redox-sensitive genetic regulatory elements are critical in the development of T helper lineage commitment.

Further identification of these targets may define mechanisms important in the aberrant immune response in mouse and human autoimmune conditions.

The primary goals of ongoing research of T1D in the NOD mouse are to determine factors that contribute to and drive autoimmune pathogenesis, to develop ways to intervene and/or reverse the course of beta cell loss and ultimately to apply these therapeutics to cure and prevent human T1D. Therapies to modulate tolerance to autoantigens, such as insulin, have been tested in NOD (300-302) and human patients (303). Treatments to modulate the immune response through the administration of anti-CD3 in mice (304-307) and humans (308), as well as anti-thymocyte globulin (ATG) (309) have also been investigated. While such treatments are effective in the mouse, responses in human patients have so far been underwhelming (308). This demonstrates the need for improved translation of dosing and timing requirements from mouse to human patients. Additionally, the identification and evaluation of subgroups to determine which regimens are the most successful stratified by biological markers and disease state may positively affect trial outcomes.

Much of the work in the NOD demonstrates that diabetes is a multigenic, multifaceted disease; there are most likely many genetic and immunological dysfunctions that, when combined with environmental factors, influence disease pathogenesis. Investigation of T cell activation demonstrates that many conditions can affect activation status, including redox status. Cytokine production and mechanisms of killing involve multiple pathways with overlap and redundancy, suggesting that therapeutics targeting these products will require a combination of approaches. It is important to note that there are hundreds of therapies that can prevent and dozens that can reverse T1D in the NOD (reviewed in (95, 303)). Failures in translation may prove useful in exposing both the similarities and differences between diabetes in mouse and

man. These observations also reinforce the need to standardize characterization of disease state, assessment of biological targets, and outcome of therapies in the NOD. Timing and dosing thresholds for effective prevention or reversal are critical. Similarly, standardized definitions of biomarker positivity, such as autoantibody titer, C-peptide, and markers of immune modulation during the course of treatment are needed to assist researchers in comparing successes and failures within and between laboratories and to assist in the translation of these data to human T1D trials. As the pathology of many diseases in humans, particularly autoimmune diabetes, is multifaceted and complex, therapies will most likely require a combined approach. Clinical trials are underway to assess the safety and effectiveness of immune suppression and alteration of APC function, including tolerizing DC populations and depletion of B cells with rituximab. However, immune suppression is far from ideal, as it is associated with various risks and complications. Defining redox-sensitive targets that modulate immune reactivity may provide further methods of regulating T cell reactivity. Therefore, combined therapy may provide sufficient tailoring of the immune response without rigorous immunosuppression.

BIBLIOGRAPHY

References

1. Malaisse, W., D. Hager, and L. Orci. 1972. The stimulus-secretion coupling of glucose-induced insulin release. IX. The participation of the beta cell web. *Diabetes* 21:594-604.
2. Kowluru, A. 2010. Small G proteins in islet beta-cell function. *Endocr Rev* 31:52-78.
3. Newgard, C., D. Lu, M. Jensen, J. Schissler, A. Boucher, S. Burgess, and A. Sherry. 2002. Stimulus/secretion coupling factors in glucose-stimulated insulin secretion: insights gained from a multidisciplinary approach. *Diabetes* 51 Suppl 3:S389-393.
4. Eisenbarth, G. 1986. Type I diabetes mellitus. A chronic autoimmune disease. *N Engl J Med* 314:1360-1368.
5. Bouma, G., J. Coppens, S. Mourits, T. Nikolic, S. Sozzani, H. Drexhage, and M. Versnel. 2005. Evidence for an enhanced adhesion of DC to fibronectin and a role of CCL19 and CCL21 in the accumulation of DC around the pre-diabetic islets in NOD mice. *Eur J Immunol* 35:2386-2396.
6. Delovitch, T., and B. Singh. 1997. The nonobese diabetic mouse as a model of autoimmune diabetes: immune dysregulation gets the NOD. *Immunity* 7:727-738.
7. Willcox, A., S. Richardson, A. Bone, A. Foulis, and N. Morgan. 2009. Analysis of islet inflammation in human type 1 diabetes. *Clin Exp Immunol* 155:173-181.
8. Foulis, A. K., C. N. Liddle, M. A. Farquharson, J. A. Richmond, and R. S. Weir. 1986. The histopathology of the pancreas in type 1 (insulin-dependent) diabetes mellitus: a 25-year review of deaths in patients under 20 years of age in the United Kingdom. *Diabetologia* 29:267-274.
9. Hanafusa, T., and A. Imagawa. 2008. Insulitis in human type 1 diabetes. *Annals of the New York Academy of Sciences* 1150:297-299.
10. Makino, S., K. Kunimoto, Y. Muraoka, Y. Mizushima, K. Katagiri, and Y. Tochino. 1980. Breeding of a non-obese, diabetic strain of mice. *Jikken dobutsu* 29:1-13.
11. Kikutani, H., and S. Makino. 1992. The murine autoimmune diabetes model: NOD and related strains. *Adv Immunol* 51:285-322.
12. Atkinson, M. A., and E. H. Leiter. 1999. The NOD mouse model of type 1 diabetes: as good as it gets? *Nature medicine* 5:601-604.
13. Roep, B. O., and M. Atkinson. 2004. Animal models have little to teach us about type 1 diabetes: 1. In support of this proposal. *Diabetologia* 47:1650-1656.
14. Roep, B. O., M. Atkinson, and M. von Herrath. 2004. Satisfaction (not) guaranteed: re-evaluating the use of animal models of type 1 diabetes. *Nature reviews* 4:989-997.

15. Yang, Y., and P. Santamaria. 2003. Dissecting autoimmune diabetes through genetic manipulation of non-obese diabetic mice. *Diabetologia* 46:1447-1464.
16. Wicker, L. S., J. Clark, H. I. Fraser, V. E. Garner, A. Gonzalez-Munoz, B. Healy, S. Howlett, K. Hunter, D. Rainbow, R. L. Rosa, L. J. Smink, J. A. Todd, and L. B. Peterson. 2005. Type 1 diabetes genes and pathways shared by humans and NOD mice. *Journal of autoimmunity* 25 Suppl:29-33.
17. Wicker, L. S., B. J. Miller, L. Z. Coker, S. E. McNally, S. Scott, Y. Mullen, and M. C. Appel. 1987. Genetic control of diabetes and insulitis in the nonobese diabetic (NOD) mouse. *The Journal of experimental medicine* 165:1639-1654.
18. Sawyer, D., G. Donowitz, and G. Mandell. 1989. Polymorphonuclear neutrophils: an effective antimicrobial force. *Rev Infect Dis* 11 Suppl 7:S1532-1544.
19. Modi, W., M. Dean, H. Seuanez, N. Mukaida, K. Matsushima, and S. O'Brien. 1990. Monocyte-derived neutrophil chemotactic factor (MDNCF/IL-8) resides in a gene cluster along with several other members of the platelet factor 4 gene superfamily. *Hum Genet* 84:185-187.
20. Ryder, M. 2010. Comparison of neutrophil functions in aggressive and chronic periodontitis. *Periodontol 2000* 53:124-137.
21. McEver, R. 2010. Rolling back neutrophil adhesion. *Nat Immunol* 11:282-284.
22. Mazaki, Y. 2006. [Directional sensing and superoxide production in neutrophils]. *Tanpakushitsu Kakusan Koso* 51:727-732.
23. Calderon, B., A. Suri, X. Pan, J. Mills, and E. Unanue. 2008. IFN-gamma-dependent regulatory circuits in immune inflammation highlighted in diabetes. *J Immunol* 181:6964-6974.
24. Calderon, B., A. Suri, and E. Unanue. 2006. In CD4+ T-cell-induced diabetes, macrophages are the final effector cells that mediate islet beta-cell killing: studies from an acute model. *Am J Pathol* 169:2137-2147.
25. Barnett, J., and K. Brundage. 2010. Evaluating macrophages in immunotoxicity testing. *Methods Mol Biol* 598:75-94.
26. Jansen, A., F. Homo-Delarche, H. Hooijkaas, P. Leenen, M. Dardenne, and H. Drexhage. 1994. Immunohistochemical characterization of monocytes-macrophages and dendritic cells involved in the initiation of the insulitis and beta-cell destruction in NOD mice. *Diabetes* 43:667-675.
27. Lee, K. U., K. Amano, and J. W. Yoon. 1988. Evidence for initial involvement of macrophage in development of insulitis in NOD mice. *Diabetes* 37:989-991.
28. Jun, H. S., C. S. Yoon, L. Zbytnuik, N. van Rooijen, and J. W. Yoon. 1999. The role of macrophages in T cell-mediated autoimmune diabetes in nonobese diabetic mice. *The Journal of experimental medicine* 189:347-358.
29. Clare-Salzler, M. J., J. Brooks, A. Chai, K. Van Herle, and C. Anderson. 1992. Prevention of diabetes in nonobese diabetic mice by dendritic cell transfer. *The Journal of clinical investigation* 90:741-748.
30. Lo, J., and M. J. Clare-Salzler. 2006. Dendritic cell subsets and type I diabetes: focus upon DC-based therapy. *Autoimmunity reviews* 5:419-423.
31. Papaccio, G., F. Nicoletti, F. A. Pisanti, K. Bendtzen, and M. Galdieri. 2000. Prevention of spontaneous autoimmune diabetes in NOD mice by transferring in vitro antigen-pulsed syngeneic dendritic cells. *Endocrinology* 141:1500-1505.

32. Bromley, S., W. Burack, K. Johnson, K. Somersalo, T. Sims, C. Sumen, M. Davis, A. Shaw, P. Allen, and M. Dustin. 2001. The immunological synapse. *Annu Rev Immunol* 19:375-396.
33. Dorhoi, A., and S. Kaufmann. 2009. Fine-tuning of T cell responses during infection. *Curr Opin Immunol* 21:367-377.
34. Lehuen, A., J. Diana, P. Zaccone, and A. Cooke. 2010. Immune cell crosstalk in type 1 diabetes. *Nat Rev Immunol* 10:501-513.
35. Hall, J., and A. Rosen. 2010. Type I interferons: crucial participants in disease amplification in autoimmunity. *Nat Rev Rheumatol* 6:40-49.
36. Romagnani, S. 2006. Regulation of the T cell response. *Clin Exp Allergy* 36:1357-1366.
37. Pasquali, L., N. Giannoukakis, and M. Trucco. 2008. Induction of immune tolerance to facilitate beta cell regeneration in type 1 diabetes. *Advanced drug delivery reviews* 60:106-113.
38. Kyewski, B., and J. Derbinski. 2004. Self-representation in the thymus: an extended view. *Nat Rev Immunol* 4:688-698.
39. Su, M., and M. Anderson. 2004. Aire: an update. *Curr Opin Immunol* 16:746-752.
40. Peterson, P., and L. Peltonen. 2005. Autoimmune polyendocrinopathy syndrome type 1 (APS1) and AIRE gene: new views on molecular basis of autoimmunity. *J Autoimmun* 25 Suppl:49-55.
41. Park, Y. 2007. Functional evaluation of the type 1 diabetes (T1D) susceptibility candidate genes. *Diabetes Res Clin Pract* 77 Suppl 1:S110-115.
42. Videbaek, N., S. Harach, J. Phillips, P. Hutchings, P. Ozegbe, B. Michelsen, and A. Cooke. 2003. An islet-homing NOD CD8+ cytotoxic T cell clone recognizes GAD65 and causes insulitis. *J Autoimmun* 20:97-109.
43. Tisch, R., X. Yang, S. Singer, R. Liblau, L. Fugger, and H. McDevitt. 1993. Immune response to glutamic acid decarboxylase correlates with insulitis in non-obese diabetic mice. *Nature* 366:72-75.
44. Tian, J., M. Atkinson, M. Clare-Salzler, A. Herschenfeld, T. Forsthuber, P. Lehmann, and D. Kaufman. 1996. Nasal administration of glutamate decarboxylase (GAD65) peptides induces Th2 responses and prevents murine insulin-dependent diabetes. *J Exp Med* 183:1561-1567.
45. McDevitt, H. 2004. Specific antigen vaccination to treat autoimmune disease. *Proc Natl Acad Sci U S A* 101 Suppl 2:14627-14630.
46. Ma, S., Y. Huang, Z. Yin, R. Menassa, J. Brandle, and A. Jevnikar. 2004. Induction of oral tolerance to prevent diabetes with transgenic plants requires glutamic acid decarboxylase (GAD) and IL-4. *Proc Natl Acad Sci U S A* 101:5680-5685.
47. Anderson, M., and J. Bluestone. 2005. The NOD mouse: a model of immune dysregulation. *Annu Rev Immunol* 23:447-485.
48. Zhang, L., M. Nakayama, and G. Eisenbarth. 2008. Insulin as an autoantigen in NOD/human diabetes. *Curr Opin Immunol* 20:111-118.
49. Wegmann, D., M. Norbury-Glaser, and D. Daniel. 1994. Insulin-specific T cells are a predominant component of islet infiltrates in pre-diabetic NOD mice. *Eur J Immunol* 24:1853-1857.
50. French, M., J. Allison, D. Cram, H. Thomas, M. Dempsey-Collier, A. Silva, H. Georgiou, T. Kay, L. Harrison, and A. Lew. 1997. Transgenic expression of mouse proinsulin II prevents diabetes in nonobese diabetic mice. *Diabetes* 46:34-39.

51. Fan, Y., W. A. Rudert, M. Grupillo, J. He, G. Sisino, and M. Trucco. 2009. Thymus-specific deletion of insulin induces autoimmune diabetes. *The EMBO journal* 28:2812-2824.
52. Vafiadis, P., S. T. Bennett, J. A. Todd, J. Nadeau, R. Grabs, C. G. Goodyer, S. Wickramasinghe, E. Colle, and C. Polychronakos. 1997. Insulin expression in human thymus is modulated by INS VNTR alleles at the IDDM2 locus. *Nature genetics* 15:289-292.
53. Pugliese, A., M. Zeller, A. J. Fernandez, L. Zalcberg, R. Bartlett, C. Ricordi, M. Pietropaolo, G. Eisenbarth, S. Bennett, and D. Patel. 1997. The insulin gene is transcribed in the human thymus and transcription levels correlated with allelic variation at the INS VNTR-IDDM2 susceptibility locus for type 1 diabetes. *Nat Genet* 15:293-297.
54. Geenen, V. 2006. Thymus-dependent T cell tolerance of neuroendocrine functions: principles, reflections, and implications for tolerogenic/negative self-vaccination. *Annals of the New York Academy of Sciences* 1088:284-296.
55. Chentoufi, A. A., and C. Polychronakos. 2002. Insulin expression levels in the thymus modulate insulin-specific autoreactive T-cell tolerance: the mechanism by which the IDDM2 locus may predispose to diabetes. *Diabetes* 51:1383-1390.
56. Nakayama, M., N. Abiru, H. Moriyama, N. Babaya, E. Liu, D. Miao, L. Yu, D. R. Wegmann, J. C. Hutton, J. F. Elliott, and G. S. Eisenbarth. 2005. Prime role for an insulin epitope in the development of type 1 diabetes in NOD mice. *Nature* 435:220-223.
57. Tait, K. F., J. E. Collins, J. M. Heward, I. Eaves, H. Snook, J. A. Franklyn, A. H. Barnett, J. A. Todd, M. Maranian, A. Compston, S. Sawcer, and S. C. Gough. 2004. Evidence for a Type 1 diabetes-specific mechanism for the insulin gene-associated IDDM2 locus rather than a general influence on autoimmunity. *Diabet Med* 21:267-270.
58. Cloutier, J. F., and A. Veillette. 1999. Cooperative inhibition of T-cell antigen receptor signaling by a complex between a kinase and a phosphatase. *The Journal of experimental medicine* 189:111-121.
59. Hasegawa, K., F. Martin, G. Huang, D. Tumas, L. Diehl, and A. C. Chan. 2004. PEST domain-enriched tyrosine phosphatase (PEP) regulation of effector/memory T cells. *Science (New York, N.Y* 303:685-689.
60. Bottini, N., L. Musumeci, A. Alonso, S. Rahmouni, K. Nika, M. Rostamkhani, J. MacMurray, G. F. Meloni, P. Lucarelli, M. Pellecchia, G. S. Eisenbarth, D. Comings, and T. Mustelin. 2004. A functional variant of lymphoid tyrosine phosphatase is associated with type I diabetes. *Nature genetics* 36:337-338.
61. Dultz, G., N. Matheis, M. Dittmar, B. Rohrig, K. Bender, and G. J. Kahaly. 2009. The protein tyrosine phosphatase non-receptor type 22 C1858T polymorphism is a joint susceptibility locus for immunthyroiditis and autoimmune diabetes. *Thyroid* 19:143-148.
62. Smyth, D., J. D. Cooper, J. E. Collins, J. M. Heward, J. A. Franklyn, J. M. Howson, A. Vella, S. Nutland, H. E. Rance, L. Maier, B. J. Barratt, C. Guja, C. Ionescu-Tirgoviste, D. A. Savage, D. B. Dunger, B. Widmer, D. P. Strachan, S. M. Ring, N. Walker, D. G. Clayton, R. C. Twells, S. C. Gough, and J. A. Todd. 2004. Replication of an association between the lymphoid tyrosine phosphatase locus (LYP/PTPN22) with type 1 diabetes, and evidence for its role as a general autoimmunity locus. *Diabetes* 53:3020-3023.
63. Höglund, P., J. Mintern, C. Waltzinger, W. Heath, C. Benoist, and D. Mathis. 1999. Initiation of autoimmune diabetes by developmentally regulated presentation of islet cell antigens in the pancreatic lymph nodes. *J Exp Med* 189:331-339.

64. Zhang, Y., B. O'Brien, J. Trudeau, R. Tan, P. Santamaria, and J. Dutz. 2002. In situ beta cell death promotes priming of diabetogenic CD8 T lymphocytes. *J Immunol* 168:1466-1472.
65. Gagnerault, M., J. Luan, C. Lotton, and F. Lepault. 2002. Pancreatic lymph nodes are required for priming of beta cell reactive T cells in NOD mice. *J Exp Med* 196:369-377.
66. Streeter, P., E. Berg, B. Rouse, R. Bargatze, and E. Butcher. 1988. A tissue-specific endothelial cell molecule involved in lymphocyte homing. *Nature* 331:41-46.
67. Yang, X., H. Sytwu, H. McDevitt, and S. Michie. 1997. Involvement of beta 7 integrin and mucosal addressin cell adhesion molecule-1 (MAdCAM-1) in the development of diabetes in obese diabetic mice. *Diabetes* 46:1542-1547.
68. Wang, B., A. Gonzalez, C. Benoist, and D. Mathis. 1996. The role of CD8+ T cells in the initiation of insulin-dependent diabetes mellitus. *Eur J Immunol* 26:1762-1769.
69. Liblau, R., F. Wong, L. Mars, and P. Santamaria. 2002. Autoreactive CD8 T cells in organ-specific autoimmunity: emerging targets for therapeutic intervention. *Immunity* 17:1-6.
70. Kägi, D., B. Odermatt, P. Seiler, R. Zinkernagel, T. Mak, and H. Hengartner. 1997. Reduced incidence and delayed onset of diabetes in perforin-deficient nonobese diabetic mice. *J Exp Med* 186:989-997.
71. Itoh, N., A. Imagawa, T. Hanafusa, M. Waguri, K. Yamamoto, H. Iwahashi, M. Moriwaki, H. Nakajima, J. Miyagawa, M. Namba, S. Makino, S. Nagata, N. Kono, and Y. Matsuzawa. 1997. Requirement of Fas for the development of autoimmune diabetes in nonobese diabetic mice. *J Exp Med* 186:613-618.
72. Amrani, A., J. Verdaguer, B. Anderson, T. Utsugi, S. Bou, and P. Santamaria. 1999. Perforin-independent beta-cell destruction by diabetogenic CD8(+) T lymphocytes in transgenic nonobese diabetic mice. *J Clin Invest* 103:1201-1209.
73. Allison, J., and A. Strasser. 1998. Mechanisms of beta cell death in diabetes: a minor role for CD95. *Proc Natl Acad Sci U S A* 95:13818-13822.
74. Dudek, N., H. Thomas, L. Mariana, R. Sutherland, J. Allison, E. Estella, E. Angstetra, J. Trapani, P. Santamaria, A. Lew, and T. Kay. 2006. Cytotoxic T-cells from T-cell receptor transgenic NOD8.3 mice destroy beta-cells via the perforin and Fas pathways. *Diabetes* 55:2412-2418.
75. Verdaguer, J., D. Schmidt, A. Amrani, B. Anderson, N. Averill, and P. Santamaria. 1997. Spontaneous autoimmune diabetes in monoclonal T cell nonobese diabetic mice. *J Exp Med* 186:1663-1676.
76. Christianson, S., L. Shultz, and E. Leiter. 1993. Adoptive transfer of diabetes into immunodeficient NOD-scid/scid mice. Relative contributions of CD4+ and CD8+ T-cells from diabetic versus prediabetic NOD.NON-Thy-1a donors. *Diabetes* 42:44-55.
77. de Jersey, J., S. Snelgrove, S. Palmer, S. Teteris, A. Mullbacher, J. Miller, and R. Slattery. 2007. Beta cells cannot directly prime diabetogenic CD8 T cells in nonobese diabetic mice. *Proc Natl Acad Sci U S A* 104:1295-1300.
78. O'Neill, S., E. Liu, and J. Cambier. 2009. Change you can B(cell)eive in: recent progress confirms a critical role for B cells in type 1 diabetes. *Curr Opin Endocrinol Diabetes Obes* 16:293-298.
79. Atkinson, M., and G. Eisenbarth. 2001. Type 1 diabetes: new perspectives on disease pathogenesis and treatment. *Lancet* 358:221-229.

80. Cameron, M., G. Arreaza, L. Waldhauser, J. Gauldie, and T. Delovitch. 2000. Immunotherapy of spontaneous type 1 diabetes in nonobese diabetic mice by systemic interleukin-4 treatment employing adenovirus vector-mediated gene transfer. *Gene Ther* 7:1840-1846.
81. Goudy, K., S. Song, C. Wasserfall, Y. Zhang, M. Kapturczak, A. Muir, M. Powers, M. Scott-Jorgensen, M. Campbell-Thompson, J. Crawford, T. Ellis, T. Flotte, and M. Atkinson. 2001. Adeno-associated virus vector-mediated IL-10 gene delivery prevents type 1 diabetes in NOD mice. *Proc Natl Acad Sci U S A* 98:13913-13918.
82. Goudy, K., B. Burkhardt, C. Wasserfall, S. Song, M. Campbell-Thompson, T. Brusko, M. Powers, M. Clare-Salzler, E. Sobel, T. Ellis, T. Flotte, and M. Atkinson. 2003. Systemic overexpression of IL-10 induces CD4+CD25+ cell populations in vivo and ameliorates type 1 diabetes in nonobese diabetic mice in a dose-dependent fashion. *J Immunol* 171:2270-2278.
83. King, C., J. Davies, R. Mueller, M. Lee, T. Krahl, B. Yeung, E. O'Connor, and N. Sarvetnick. 1998. TGF-beta1 alters APC preference, polarizing islet antigen responses toward a Th2 phenotype. *Immunity* 8:601-613.
84. Fiorentino, D., M. Bond, and T. Mosmann. 1989. Two types of mouse T helper cell. IV. Th2 clones secrete a factor that inhibits cytokine production by Th1 clones. *J Exp Med* 170:2081-2095.
85. Gazzinelli, R., I. Oswald, S. James, and A. Sher. 1992. IL-10 inhibits parasite killing and nitrogen oxide production by IFN-gamma-activated macrophages. *J Immunol* 148:1792-1796.
86. Marchant, A., C. Bruyns, P. Vandenabeele, M. Ducarme, C. Gérard, A. Delvaux, D. De Groote, D. Abramowicz, T. Velu, and M. Goldman. 1994. Interleukin-10 controls interferon-gamma and tumor necrosis factor production during experimental endotoxemia. *Eur J Immunol* 24:1167-1171.
87. de Waal Malefyt, R., J. Haanen, H. Spits, M. Roncarolo, A. te Velde, C. Figdor, K. Johnson, R. Kastelein, H. Yssel, and J. de Vries. 1991. Interleukin 10 (IL-10) and viral IL-10 strongly reduce antigen-specific human T cell proliferation by diminishing the antigen-presenting capacity of monocytes via downregulation of class II major histocompatibility complex expression. *J Exp Med* 174:915-924.
88. de Waal Malefyt, R., J. Abrams, B. Bennett, C. Figdor, and J. de Vries. 1991. Interleukin 10(IL-10) inhibits cytokine synthesis by human monocytes: an autoregulatory role of IL-10 produced by monocytes. *J Exp Med* 174:1209-1220.
89. Fiorentino, D., A. Zlotnik, P. Vieira, T. Mosmann, M. Howard, K. Moore, and A. O'Garra. 1991. IL-10 acts on the antigen-presenting cell to inhibit cytokine production by Th1 cells. *J Immunol* 146:3444-3451.
90. Gombert, J., A. Herbelin, E. Tancrède-Bohin, M. Dy, C. Carnaud, and J. Bach. 1996. Early quantitative and functional deficiency of NK1+-like thymocytes in the NOD mouse. *Eur J Immunol* 26:2989-2998.
91. Hammond, K., L. Poulton, L. Palmisano, P. Silveira, D. Godfrey, and A. Baxter. 1998. alpha/beta-T cell receptor (TCR)+CD4-CD8- (NKT) thymocytes prevent insulin-dependent diabetes mellitus in nonobese diabetic (NOD)/Lt mice by the influence of interleukin (IL)-4 and/or IL-10. *J Exp Med* 187:1047-1056.
92. Irie, J., and W. Ridgway. 2005. A modular theory of autoimmunity. *Keio J Med* 54:121-126.

93. Mueller, R., L. Bradley, T. Krahl, and N. Sarvetnick. 1997. Mechanism underlying counterregulation of autoimmune diabetes by IL-4. *Immunity* 7:411-418.
94. Balasa, B., K. Van Gunst, N. Jung, D. Balakrishna, P. Santamaria, T. Hanafusa, N. Itoh, and N. Sarvetnick. 2000. Islet-specific expression of IL-10 promotes diabetes in nonobese diabetic mice independent of Fas, perforin, TNF receptor-1, and TNF receptor-2 molecules. *J Immunol* 165:2841-2849.
95. von Herrath, M., and G. T. Nepom. 2009. Animal models of human type 1 diabetes. *Nature immunology* 10:129-132.
96. Yu, L., and G. Eisenbarth. 2004. Humoral autoimmunity. *Adv Exp Med Biol* 552:247-267.
97. Forsgren, S., A. Andersson, V. Hillörn, A. Söderström, and D. Holmberg. 1991. Immunoglobulin-mediated prevention of autoimmune diabetes in the non-obese diabetic (NOD) mouse. *Scand J Immunol* 34:445-451.
98. Serreze, D., H. Chapman, D. Varnum, M. Hanson, P. Reifsnyder, S. Richard, S. Fleming, E. Leiter, and L. Shultz. 1996. B lymphocytes are essential for the initiation of T cell-mediated autoimmune diabetes: analysis of a new "speed congenic" stock of NOD.Ig mu null mice. *J Exp Med* 184:2049-2053.
99. Akashi, T., S. Nagafuchi, K. Anzai, S. Kondo, D. Kitamura, S. Wakana, J. Ono, M. Kikuchi, Y. Niho, and T. Watanabe. 1997. Direct evidence for the contribution of B cells to the progression of insulitis and the development of diabetes in non-obese diabetic mice. *Int Immunol* 9:1159-1164.
100. Serreze, D., S. Fleming, H. Chapman, S. Richard, E. Leiter, and R. Tisch. 1998. B lymphocytes are critical antigen-presenting cells for the initiation of T cell-mediated autoimmune diabetes in nonobese diabetic mice. *J Immunol* 161:3912-3918.
101. Falcone, M., J. Lee, G. Patstone, B. Yeung, and N. Sarvetnick. 1998. B lymphocytes are crucial antigen-presenting cells in the pathogenic autoimmune response to GAD65 antigen in nonobese diabetic mice. *J Immunol* 161:1163-1168.
102. Noorchashm, H., Y. Lieu, N. Noorchashm, S. Rostami, S. Greeley, A. Schlachterman, H. Song, L. Noto, A. Jevnikar, C. Barker, and A. Naji. 1999. I-Ag7-mediated antigen presentation by B lymphocytes is critical in overcoming a checkpoint in T cell tolerance to islet beta cells of nonobese diabetic mice. *J Immunol* 163:743-750.
103. Hussain, S., K. Salojin, and T. Delovitch. 2004. Hyperresponsiveness, resistance to B-cell receptor-dependent activation-induced cell death, and accumulation of hyperactivated B-cells in islets is associated with the onset of insulitis but not type 1 diabetes. *Diabetes* 53:2003-2011.
104. Silveira, P., H. Chapman, J. Stolp, E. Johnson, S. Cox, K. Hunter, L. Wicker, and D. Serreze. 2006. Genes within the Idd5 and Idd9/11 diabetes susceptibility loci affect the pathogenic activity of B cells in nonobese diabetic mice. *J Immunol* 177:7033-7041.
105. Mariño, E., M. Batten, J. Groom, S. Walters, D. Liuwantara, F. Mackay, and S. Grey. 2008. Marginal-zone B-cells of nonobese diabetic mice expand with diabetes onset, invade the pancreatic lymph nodes, and present autoantigen to diabetogenic T-cells. *Diabetes* 57:395-404.
106. Barrett, J. C., D. G. Clayton, P. Concannon, B. Akolkar, J. D. Cooper, H. A. Erlich, C. Julier, G. Morahan, J. Nerup, C. Nierras, V. Plagnol, F. Pociot, H. Schuilenburg, D. J. Smyth, H. Stevens, J. A. Todd, N. M. Walker, and S. S. Rich. 2009. Genome-wide

association study and meta-analysis find that over 40 loci affect risk of type 1 diabetes. *Nature genetics*.

107. Sato, A. K., T. Sturniolo, F. Sinigaglia, and L. J. Stern. 1999. Substitution of aspartic acid at beta57 with alanine alters MHC class II peptide binding activity but not protein stability: HLA-DQ (alpha1*0201, beta1*0302) and (alpha1*0201, beta1*0303). *Human immunology* 60:1227-1236.
108. Antoniou, A. N., J. Elliott, E. Rosmarakis, and P. J. Dyson. 1998. MHC class II Ab diabetogenic residue 57 Asp/non-Asp dimorphism influences T-cell recognition and selection. *Immunogenetics* 47:218-225.
109. Howson, J. M., N. M. Walker, D. Clayton, and J. A. Todd. 2009. Confirmation of HLA class II independent type 1 diabetes associations in the major histocompatibility complex including HLA-B and HLA-A. *Diabetes, obesity & metabolism* 11 Suppl 1:31-45.
110. Bennett, S. T., A. J. Wilson, L. Esposito, N. Bouzekri, D. E. Undlien, F. Cucca, L. Nistico, R. Buzzetti, E. Bosi, F. Pociot, J. Nerup, A. Cambon-Thomsen, A. Pugliese, J. P. Shield, P. A. McKinney, S. C. Bain, C. Polychronakos, and J. A. Todd. 1997. Insulin VNTR allele-specific effect in type 1 diabetes depends on identity of untransmitted paternal allele. The IMDIAB Group. *Nature genetics* 17:350-352.
111. Prochazka, M., E. H. Leiter, D. V. Serreze, and D. L. Coleman. 1987. Three recessive loci required for insulin-dependent diabetes in nonobese diabetic mice. *Science (New York, N.Y* 237:286-289.
112. Mathews, C. E., R. T. Graser, R. J. Bagley, J. W. Caldwell, R. Li, G. A. Churchill, D. V. Serreze, and E. H. Leiter. 2003. Genetic analysis of resistance to Type-1 Diabetes in ALR/Lt mice, a NOD-related strain with defenses against autoimmune-mediated diabetogenic stress. *Immunogenetics* 55:491-496.
113. McAleer, M. A., P. Reifsnyder, S. M. Palmer, M. Prochazka, J. M. Love, J. B. Copeman, E. E. Powell, N. R. Rodrigues, J. B. Prins, D. V. Serreze, and et al. 1995. Crosses of NOD mice with the related NON strain. A polygenic model for IDDM. *Diabetes* 44:1186-1195.
114. Yui, M. A., K. Muralidharan, B. Moreno-Altamirano, G. Perrin, K. Chestnut, and E. K. Wakeland. 1996. Production of congenic mouse strains carrying NOD-derived diabetogenic genetic intervals: an approach for the genetic dissection of complex traits. *Mamm Genome* 7:331-334.
115. Acha-Orbea, H., and H. O. McDevitt. 1987. The first external domain of the nonobese diabetic mouse class II I-A beta chain is unique. *Proceedings of the National Academy of Sciences of the United States of America* 84:2435-2439.
116. Ridgway, W. M., M. Fasso, and C. G. Fathman. 1999. A new look at MHC and autoimmune disease. *Science (New York, N.Y* 284:749, 751.
117. Tisch, R., and H. McDevitt. 1996. Insulin-dependent diabetes mellitus. *Cell* 85:291-297.
118. Wong, F. S., and L. Wen. 2004. What can the HLA transgenic mouse tell us about autoimmune diabetes? *Diabetologia* 47:1476-1487.
119. Rajagopalan, G., Y. C. Kudva, L. Chen, L. Wen, and C. S. David. 2003. Autoimmune diabetes in HLA-DR3/DQ8 transgenic mice expressing the co-stimulatory molecule B7-1 in the beta cells of islets of Langerhans. *International immunology* 15:1035-1044.
120. Wen, L., F. S. Wong, J. Tang, N. Y. Chen, M. Altieri, C. David, R. Flavell, and R. Sherwin. 2000. In vivo evidence for the contribution of human histocompatibility

leukocyte antigen (HLA)-DQ molecules to the development of diabetes. *The Journal of experimental medicine* 191:97-104.

121. Jarchum, I., J. C. Baker, T. Yamada, T. Takaki, M. P. Marron, D. V. Serreze, and T. P. DiLorenzo. 2007. In vivo cytotoxicity of insulin-specific CD8+ T-cells in HLA-A*0201 transgenic NOD mice. *Diabetes* 56:2551-2560.
122. Marron, M. P., R. T. Graser, H. D. Chapman, and D. V. Serreze. 2002. Functional evidence for the mediation of diabetogenic T cell responses by HLA-A2.1 MHC class I molecules through transgenic expression in NOD mice. *Proceedings of the National Academy of Sciences of the United States of America* 99:13753-13758.
123. Hattori, M., E. Yamato, N. Itoh, H. Senpuku, T. Fujisawa, M. Yoshino, M. Fukuda, E. Matsumoto, T. Toyonaga, I. Nakagawa, M. Petruzzelli, A. McMurray, H. Weiner, T. Sagai, K. Moriwaki, T. Shiroishi, R. Maron, and T. Lund. 1999. Cutting edge: homologous recombination of the MHC class I K region defines new MHC-linked diabetogenic susceptibility gene(s) in nonobese diabetic mice. *J Immunol* 163:1721-1724.
124. Pomerleau, D. P., R. J. Bagley, D. V. Serreze, C. E. Mathews, and E. H. Leiter. 2005. Major histocompatibility complex-linked diabetes susceptibility in NOD/Lt mice: subcongenic analysis localizes a component of Idd16 at the H2-D end of the diabetogenic H2(g7) complex. *Diabetes* 54:1603-1606.
125. Brims, D. R., J. Qian, I. Jarchum, L. Mikesh, E. Palmieri, U. A. Ramagopal, V. N. Malashkevich, R. J. Chaparro, T. Lund, M. Hattori, J. Shabanowitz, D. F. Hunt, S. G. Nathenson, S. C. Almo, and T. P. Dilorenzo. Predominant occupation of the class I MHC molecule H-2Kwm7 with a single self-peptide suggests a mechanism for its diabetes-protective effect. *International immunology* 22:191-203.
126. Hamilton-Williams, E. E., D. V. Serreze, B. Charlton, E. A. Johnson, M. P. Marron, A. Mullbacher, and R. M. Slattery. 2001. Transgenic rescue implicates beta2-microglobulin as a diabetes susceptibility gene in nonobese diabetic (NOD) mice. *Proceedings of the National Academy of Sciences of the United States of America* 98:11533-11538.
127. Kissler, S., P. Stern, K. Takahashi, K. Hunter, L. B. Peterson, and L. S. Wicker. 2006. In vivo RNA interference demonstrates a role for Nramp1 in modifying susceptibility to type 1 diabetes. *Nature genetics* 38:479-483.
128. Araki, M., D. Chung, S. Liu, D. B. Rainbow, G. Chamberlain, V. Garner, K. M. Hunter, L. Vijayakrishnan, L. B. Peterson, M. Oukka, A. H. Sharpe, R. Sobel, V. K. Kuchroo, and L. S. Wicker. 2009. Genetic evidence that the differential expression of the ligand-independent isoform of CTLA-4 is the molecular basis of the Idd5.1 type 1 diabetes region in nonobese diabetic mice. *J Immunol* 183:5146-5157.
129. Mathews, C. E., E. H. Leiter, O. Spirina, Y. Bykhovskaya, A. M. Gusdon, S. Ringquist, and N. Fischel-Ghodsian. 2005. mt-Nd2 Allele of the ALR/Lt mouse confers resistance against both chemically induced and autoimmune diabetes. *Diabetologia* 48:261-267.
130. Uchigata, Y., T. Okada, J. S. Gong, Y. Yamada, Y. Iwamoto, and M. Tanaka. 2002. A mitochondrial genotype associated with the development of autoimmune-related type 1 diabetes. *Diabetes care* 25:2106.
131. Gusdon, A. M., T. V. Votyakova, and C. E. Mathews. 2008. mt-Nd2a suppresses reactive oxygen species production by mitochondrial complexes I and III. *The Journal of biological chemistry* 283:10690-10697.

132. Gusdon, A. M., T. V. Votyakova, I. J. Reynolds, and C. E. Mathews. 2007. Nuclear and mitochondrial interaction involving mt-Nd2 leads to increased mitochondrial reactive oxygen species production. *The Journal of biological chemistry* 282:5171-5179.
133. Chen, J., A. M. Gusdon, T. C. Thayer, and C. E. Mathews. 2008. Role of increased ROS dissipation in prevention of T1D. *Annals of the New York Academy of Sciences* 1150:157-166.
134. Chen, J., Y. Lu, C. H. Lee, R. Li, E. H. Leiter, and C. E. Mathews. 2008. Commonalities of genetic resistance to spontaneous autoimmune and free radical--mediated diabetes. *Free radical biology & medicine* 45:1263-1270.
135. Chen, A., C. Davies, M. De Lin, and B. Fermor. 2008. Oxidative DNA damage in osteoarthritic porcine articular cartilage. *J Cell Physiol* 217:828-833.
136. Evans, M., M. Dizdaroglu, and M. Cooke. 2004. Oxidative DNA damage and disease: induction, repair and significance. *Mutat Res* 567:1-61.
137. Xie, L., X. Zhu, Y. Hu, T. Li, Y. Gao, Y. Shi, and S. Tang. 2008. Mitochondrial DNA oxidative damage triggering mitochondrial dysfunction and apoptosis in high glucose-induced HRECs. *Invest Ophthalmol Vis Sci* 49:4203-4209.
138. Miao, L., and D. St Clair. 2009. Regulation of superoxide dismutase genes: implications in disease. *Free Radic Biol Med* 47:344-356.
139. Sun, Y., and L. Oberley. 1996. Redox regulation of transcriptional activators. *Free Radic Biol Med* 21:335-348.
140. Babior, B., R. Kipnes, and J. Curnutte. 1973. Biological defense mechanisms. The production by leukocytes of superoxide, a potential bactericidal agent. *J Clin Invest* 52:741-744.
141. Rossi, F., and M. Zatti. 1964. Biochemical aspects of phagocytosis in polymorphonuclear leucocytes. NADH and NADPH oxidation by the granules of resting and phagocytizing cells. *Experientia* 20:21-23.
142. Nauseef, W. 2008. Biological roles for the NOX family NADPH oxidases. *J Biol Chem* 283:16961-16965.
143. Vignais, P. 2002. The superoxide-generating NADPH oxidase: structural aspects and activation mechanism. *Cell Mol Life Sci* 59:1428-1459.
144. El-Benna, J., P. Dang, and M. Gougerot-Pocidalo. 2008. Priming of the neutrophil NADPH oxidase activation: role of p47phox phosphorylation and NOX2 mobilization to the plasma membrane. *Semin Immunopathol* 30:279-289.
145. Sheppard, F., M. Kelher, E. Moore, N. McLaughlin, A. Banerjee, and C. Silliman. 2005. Structural organization of the neutrophil NADPH oxidase: phosphorylation and translocation during priming and activation. *J Leukoc Biol* 78:1025-1042.
146. Silliman, C. 1999. Transfusion-related acute lung injury. *Transfus Med Rev* 13:177-186.
147. Silliman, C., D. Ambruso, and L. Boshkov. 2005. Transfusion-related acute lung injury. *Blood* 105:2266-2273.
148. Kwong, C., H. Malech, D. Rotrosen, and T. Leto. 1993. Regulation of the human neutrophil NADPH oxidase by rho-related G-proteins. *Biochemistry* 32:5711-5717.
149. Wyman, T., C. Dinarello, A. Banerjee, F. Gamboni-Robertson, A. Hiester, K. England, M. Kelher, and C. Silliman. 2002. Physiological levels of interleukin-18 stimulate multiple neutrophil functions through p38 MAP kinase activation. *J Leukoc Biol* 72:401-409.

150. Wyman, T., A. Bjornsen, D. Elzi, C. Smith, K. England, M. Kelher, and C. Silliman. 2002. A two-insult in vitro model of PMN-mediated pulmonary endothelial damage: requirements for adherence and chemokine release. *Am J Physiol Cell Physiol* 283:C1592-1603.
151. Kelher, M., D. Ambruso, D. Elzi, S. Anderson, A. Paterson, G. Thurman, and C. Silliman. 2003. Formyl-Met-Leu-Phe induces calcium-dependent tyrosine phosphorylation of Rel-1 in neutrophils. *Cell Calcium* 34:445-455.
152. Aiboshi, J., E. Moore, D. Ciesla, and C. Silliman. 2001. Blood transfusion and the two-insult model of post-injury multiple organ failure. *Shock* 15:302-306.
153. Babior, B. 1992. The respiratory burst oxidase. *Adv Enzymol Relat Areas Mol Biol* 65:49-95.
154. Rodaway, A., C. Teahan, C. Casimir, A. Segal, and D. Bentley. 1990. Characterization of the 47-kilodalton autosomal chronic granulomatous disease protein: tissue-specific expression and transcriptional control by retinoic acid. *Mol Cell Biol* 10:5388-5396.
155. Yuzawa, S., N. Suzuki, Y. Fujioka, K. Ogura, H. Sumimoto, and F. Inagaki. 2004. A molecular mechanism for autoinhibition of the tandem SH3 domains of p47phox, the regulatory subunit of the phagocyte NADPH oxidase. *Genes Cells* 9:443-456.
156. Ponting, C. 1996. Novel domains in NADPH oxidase subunits, sorting nexins, and PtdIns 3-kinases: binding partners of SH3 domains? *Protein Sci* 5:2353-2357.
157. Finan, P., Y. Shimizu, I. Gout, J. Hsuan, O. Truong, C. Butcher, P. Bennett, M. Waterfield, and S. Kellie. 1994. An SH3 domain and proline-rich sequence mediate an interaction between two components of the phagocyte NADPH oxidase complex. *J Biol Chem* 269:13752-13755.
158. Hiroaki, H., T. Ago, T. Ito, H. Sumimoto, and D. Kohda. 2001. Solution structure of the PX domain, a target of the SH3 domain. *Nat Struct Biol* 8:526-530.
159. Zhan, Y., J. Virbasius, X. Song, D. Pomerleau, and G. Zhou. 2002. The p40phox and p47phox PX domains of NADPH oxidase target cell membranes via direct and indirect recruitment by phosphoinositides. *J Biol Chem* 277:4512-4518.
160. Ago, T., R. Takeya, H. Hiroaki, F. Kuribayashi, T. Ito, D. Kohda, and H. Sumimoto. 2001. The PX domain as a novel phosphoinositide- binding module. *Biochem Biophys Res Commun* 287:733-738.
161. Leto, T., A. Adams, and I. de Mendez. 1994. Assembly of the phagocyte NADPH oxidase: binding of Src homology 3 domains to proline-rich targets. *Proc Natl Acad Sci U S A* 91:10650-10654.
162. Sumimoto, H., Y. Kage, H. Nunoi, H. Sasaki, T. Nose, Y. Fukumaki, M. Ohno, S. Minakami, and K. Takeshige. 1994. Role of Src homology 3 domains in assembly and activation of the phagocyte NADPH oxidase. *Proc Natl Acad Sci U S A* 91:5345-5349.
163. Dang, P., A. Cross, and B. Babior. 2001. Assembly of the neutrophil respiratory burst oxidase: a direct interaction between p67PHOX and cytochrome b558. *Proc Natl Acad Sci U S A* 98:3001-3005.
164. DeLeo, F., J. Renee, S. McCormick, M. Nakamura, M. Apicella, J. Weiss, and W. Nauseef. 1998. Neutrophils exposed to bacterial lipopolysaccharide upregulate NADPH oxidase assembly. *J Clin Invest* 101:455-463.
165. Thrasher, A., N. Keep, F. Wientjes, and A. Segal. 1994. Chronic granulomatous disease. *Biochim Biophys Acta* 1227:1-24.

166. Jendrossek, V., A. Ritzel, B. Neubauer, S. Heyden, and M. Gahr. 1997. An in-frame triplet deletion within the gp91-phox gene in an adult X-linked chronic granulomatous disease patient with residual NADPH-oxidase activity. *Eur J Haematol* 58:78-85.
167. Rae, J., P. Newburger, M. Dinauer, D. Noack, P. Hopkins, R. Kuruto, and J. Curnutte. 1998. X-Linked chronic granulomatous disease: mutations in the CYBB gene encoding the gp91-phox component of respiratory-burst oxidase. *Am J Hum Genet* 62:1320-1331.
168. Roesler, J., J. Curnutte, J. Rae, D. Barrett, P. Patino, S. Chanock, and A. Goerlach. 2000. Recombination events between the p47-phox gene and its highly homologous pseudogenes are the main cause of autosomal recessive chronic granulomatous disease. *Blood* 95:2150-2156.
169. Moltyaner, Y., W. Geerts, D. Chamberlain, P. Heyworth, D. Noack, J. Rae, J. Doyle, and G. Downey. 2003. Underlying chronic granulomatous disease in a patient with bronchocentric granulomatosis. *Thorax* 58:1096-1098.
170. Mardiney, M. r., S. Jackson, S. Spratt, F. Li, S. Holland, and H. Malech. 1997. Enhanced host defense after gene transfer in the murine p47phox-deficient model of chronic granulomatous disease. *Blood* 89:2268-2275.
171. Olofsson, P., J. Holmberg, J. Tordsson, S. Lu, B. Akerström, and R. Holmdahl. 2003. Positional identification of Ncf1 as a gene that regulates arthritis severity in rats. *Nat Genet* 33:25-32.
172. Hultqvist, M., P. Olofsson, J. Holmberg, B. Bäckström, J. Tordsson, and R. Holmdahl. 2004. Enhanced autoimmunity, arthritis, and encephalomyelitis in mice with a reduced oxidative burst due to a mutation in the Ncf1 gene. *Proc Natl Acad Sci U S A* 101:12646-12651.
173. van der Veen, R., T. Dietlin, F. Hofman, L. Pen, B. Segal, and S. Holland. 2000. Superoxide prevents nitric oxide-mediated suppression of helper T lymphocytes: decreased autoimmune encephalomyelitis in nicotinamide adenine dinucleotide phosphate oxidase knockout mice. *J Immunol* 164:5177-5183.
174. Grankvist, K., S. Marklund, and I. Täljedal. 1981. CuZn-superoxide dismutase, Mn-superoxide dismutase, catalase and glutathione peroxidase in pancreatic islets and other tissues in the mouse. *Biochem J* 199:393-398.
175. Lenzen, S., J. Drinkgern, and M. Tiedge. 1996. Low antioxidant enzyme gene expression in pancreatic islets compared with various other mouse tissues. *Free Radic Biol Med* 20:463-466.
176. Griffiths, H. 2005. ROS as signalling molecules in T cells--evidence for abnormal redox signalling in the autoimmune disease, rheumatoid arthritis. *Redox Rep* 10:273-280.
177. Lander, H., A. Milbank, J. Tauras, D. Hajjar, B. Hempstead, G. Schwartz, R. Kraemer, U. Mirza, B. Chait, S. Burk, and L. Quilliam. 1996. Redox regulation of cell signalling. *Nature* 381:380-381.
178. Corbett, J., and M. McDaniel. 1992. Does nitric oxide mediate autoimmune destruction of beta-cells? Possible therapeutic interventions in IDDM. *Diabetes* 41:897-903.
179. Tirosh, O., A. Aronis, and J. Melendez. 2003. Mitochondrial state 3 to 4 respiration transition during Fas-mediated apoptosis controls cellular redox balance and rate of cell death. *Biochem Pharmacol* 66:1331-1334.
180. Phillips, D., and H. Griffiths. 2003. Ceramide induces a loss in cytosolic peroxide levels in mononuclear cells. *Biochem J* 375:567-579.

181. Jackson, S., S. Devadas, J. Kwon, L. Pinto, and M. Williams. 2004. T cells express a phagocyte-type NADPH oxidase that is activated after T cell receptor stimulation. *Nat Immunol* 5:818-827.
182. Devadas, S., L. Zaritskaya, S. Rhee, L. Oberley, and M. Williams. 2002. Discrete generation of superoxide and hydrogen peroxide by T cell receptor stimulation: selective regulation of mitogen-activated protein kinase activation and fas ligand expression. *J Exp Med* 195:59-70.
183. van Reyk, D., N. King, M. Dinauer, and N. Hunt. 2001. The intracellular oxidation of 2',7'-dichlorofluorescin in murine T lymphocytes. *Free Radic Biol Med* 30:82-88.
184. Tse, H., T. Thayer, C. Steele, C. Cuda, L. Morel, J. Piganelli, and C. Mathews. 2010. NADPH Oxidase Deficiency Regulates Th Lineage Commitment and Modulates Autoimmunity. *J Immunol*.
185. Jackson, M., S. Papa, J. Bolaños, R. Bruckdorfer, H. Carlsen, R. Elliott, J. Flier, H. Griffiths, S. Heales, B. Holst, M. Lorusso, E. Lund, J. Øivind Moskaug, U. Moser, M. Di Paola, M. Polidori, A. Signorile, W. Stahl, J. Viña-Ribes, and S. Astley. 2002. Antioxidants, reactive oxygen and nitrogen species, gene induction and mitochondrial function. *Mol Aspects Med* 23:209-285.
186. Peterson, J., L. Herzenberg, K. Vasquez, and C. Waltenbaugh. 1998. Glutathione levels in antigen-presenting cells modulate Th1 versus Th2 response patterns. *Proc Natl Acad Sci U S A* 95:3071-3076.
187. Finkel, T. 2001. Reactive oxygen species and signal transduction. *IUBMB Life* 52:3-6.
188. Finkel, T. 1999. Signal transduction by reactive oxygen species in non-phagocytic cells. *J Leukoc Biol* 65:337-340.
189. Reth, M. 2002. Hydrogen peroxide as second messenger in lymphocyte activation. *Nat Immunol* 3:1129-1134.
190. Gamaley, I., and I. Klyubin. 1999. Roles of reactive oxygen species: signaling and regulation of cellular functions. *Int Rev Cytol* 188:203-255.
191. Bootman, M., T. Collins, C. Peppiatt, L. Prothero, L. MacKenzie, P. De Smet, M. Travers, S. Tovey, J. Seo, M. Berridge, F. Ciccolini, and P. Lipp. 2001. Calcium signalling--an overview. *Semin Cell Dev Biol* 12:3-10.
192. Huyer, G., S. Liu, J. Kelly, J. Moffat, P. Payette, B. Kennedy, G. Tsaprailis, M. Gresser, and C. Ramachandran. 1997. Mechanism of inhibition of protein-tyrosine phosphatases by vanadate and pervanadate. *J Biol Chem* 272:843-851.
193. Nordberg, J., and E. Arnér. 2001. Reactive oxygen species, antioxidants, and the mammalian thioredoxin system. *Free Radic Biol Med* 31:1287-1312.
194. Schreck, R., P. Rieber, and P. Baeuerle. 1991. Reactive oxygen intermediates as apparently widely used messengers in the activation of the NF-kappa B transcription factor and HIV-1. *EMBO J* 10:2247-2258.
195. Yamagishi, S., Y. Inagaki, K. Nakamura, and T. Imaizumi. 2004. Azelnidipine, a newly developed long-acting calcium antagonist, inhibits tumor necrosis factor-alpha-induced interleukin-8 expression in endothelial cells through its anti-oxidative properties. *J Cardiovasc Pharmacol* 43:724-730.
196. Chen, X., Q. Zhang, R. Zhao, and R. Medford. 2004. Superoxide, H2O2, and iron are required for TNF-alpha-induced MCP-1 gene expression in endothelial cells: role of Rac1 and NADPH oxidase. *Am J Physiol Heart Circ Physiol* 286:H1001-1007.

197. Batista, F., D. Iber, and M. Neuberger. 2001. B cells acquire antigen from target cells after synapse formation. *Nature* 411:489-494.
198. Rutault, K., C. Alderman, B. Chain, and D. Katz. 1999. Reactive oxygen species activate human peripheral blood dendritic cells. *Free Radic Biol Med* 26:232-238.
199. Zola, H. 1997. The development of antibody responses in the infant. *Immunol Cell Biol* 75:587-590.
200. Karin, M. 1998. The NF-kappa B activation pathway: its regulation and role in inflammation and cell survival. *Cancer J Sci Am* 4 Suppl 1:S92-99.
201. Suzuki, Y., H. Forman, and A. Sevanian. 1997. Oxidants as stimulators of signal transduction. *Free Radic Biol Med* 22:269-285.
202. Tse, H., M. Milton, S. Schreiner, J. Profozich, M. Trucco, and J. Piganelli. 2007. Disruption of innate-mediated proinflammatory cytokine and reactive oxygen species third signal leads to antigen-specific hyporesponsiveness. *J Immunol* 178:908-917.
203. Kabe, Y., K. Ando, S. Hirao, M. Yoshida, and H. Handa. 2005. Redox regulation of NF-kappaB activation: distinct redox regulation between the cytoplasm and the nucleus. *Antioxid Redox Signal* 7:395-403.
204. Gloire, G., and J. Piette. 2009. Redox regulation of nuclear post-translational modifications during NF-kappaB activation. *Antioxid Redox Signal* 11:2209-2222.
205. Gloire, G., S. Legrand-Poels, and J. Piette. 2006. NF-kappaB activation by reactive oxygen species: fifteen years later. *Biochem Pharmacol* 72:1493-1505.
206. Pani, G., R. Colavitti, S. Borrello, and T. Galeotti. 2000. Endogenous oxygen radicals modulate protein tyrosine phosphorylation and JNK-1 activation in lectin-stimulated thymocytes. *Biochem J* 347 Pt 1:173-181.
207. Tse, H., M. Milton, and J. Piganelli. 2004. Mechanistic analysis of the immunomodulatory effects of a catalytic antioxidant on antigen-presenting cells: implication for their use in targeting oxidation-reduction reactions in innate immunity. *Free Radic Biol Med* 36:233-247.
208. Sklavos, M., H. Tse, and J. Piganelli. 2008. Redox modulation inhibits CD8 T cell effector function. *Free Radic Biol Med* 45:1477-1486.
209. Piganelli, J., and C. Mathews. 2007. Autoreactive T-cell responses: new technology in pursuit of an old nemesis. *Pediatr Diabetes* 8:249-251.
210. Piganelli, J., S. Flores, C. Cruz, J. Koepp, I. Batinic-Haberle, J. Crapo, B. Day, R. Kachadourian, R. Young, B. Bradley, and K. Haskins. 2002. A metalloporphyrin-based superoxide dismutase mimic inhibits adoptive transfer of autoimmune diabetes by a diabetogenic T-cell clone. *Diabetes* 51:347-355.
211. Los, M., H. Schenk, K. Hexel, P. Baeuerle, W. Dröge, and K. Schulze-Osthoff. 1995. IL-2 gene expression and NF-kappa B activation through CD28 requires reactive oxygen production by 5-lipoxygenase. *EMBO J* 14:3731-3740.
212. Boehme, S., and M. Lenardo. 1993. Propriocidal apoptosis of mature T lymphocytes occurs at S phase of the cell cycle. *Eur J Immunol* 23:1552-1560.
213. Weber, G., S. Abromson-Leeman, and H. Cantor. 1995. A signaling pathway coupled to T cell receptor ligation by MMTV superantigen leading to transient activation and programmed cell death. *Immunity* 2:363-372.
214. Cauley, L., E. Miller, M. Yen, and S. Swain. 2000. Superantigen-induced CD4 T cell tolerance mediated by myeloid cells and IFN-gamma. *J Immunol* 165:6056-6066.

215. Sandstrom, P., M. Mannie, and T. Buttke. 1994. Inhibition of activation-induced death in T cell hybridomas by thiol antioxidants: oxidative stress as a mediator of apoptosis. *J Leukoc Biol* 55:221-226.
216. Hildeman, D., T. Mitchell, J. Kappler, and P. Marrack. 2003. T cell apoptosis and reactive oxygen species. *J Clin Invest* 111:575-581.
217. McLaughlin, K., B. Osborne, and R. Goldsby. 1996. The role of oxygen in thymocyte apoptosis. *Eur J Immunol* 26:1170-1174.
218. Caldwell, C., H. Kojima, D. Lukashev, J. Armstrong, M. Farber, S. Apasov, and M. Sitkovsky. 2001. Differential effects of physiologically relevant hypoxic conditions on T lymphocyte development and effector functions. *J Immunol* 167:6140-6149.
219. Hohmeier, H., A. Thigpen, V. Tran, R. Davis, and C. Newgard. 1998. Stable expression of manganese superoxide dismutase (MnSOD) in insulinoma cells prevents IL-1beta-induced cytotoxicity and reduces nitric oxide production. *J Clin Invest* 101:1811-1820.
220. Lortz, S., M. Tiedge, T. Nachtwey, A. Karlsen, J. Nerup, and S. Lenzen. 2000. Protection of insulin-producing RINm5F cells against cytokine-mediated toxicity through overexpression of antioxidant enzymes. *Diabetes* 49:1123-1130.
221. Kubisch, H., J. Wang, R. Luche, E. Carlson, T. Bray, C. Epstein, and J. Phillips. 1994. Transgenic copper/zinc superoxide dismutase modulates susceptibility to type I diabetes. *Proc Natl Acad Sci U S A* 91:9956-9959.
222. Lizard, G., S. Gueldry, O. Sordet, S. Monier, A. Athias, C. Miguet, G. Bessede, S. Lemaire, E. Solary, and P. Gambert. 1998. Glutathione is implied in the control of 7-ketocholesterol-induced apoptosis, which is associated with radical oxygen species production. *FASEB J* 12:1651-1663.
223. Saitoh, M., H. Nishitoh, M. Fujii, K. Takeda, K. Tobiume, Y. Sawada, M. Kawabata, K. Miyazono, and H. Ichijo. 1998. Mammalian thioredoxin is a direct inhibitor of apoptosis signal-regulating kinase (ASK) 1. *EMBO J* 17:2596-2606.
224. Matsuda, M., H. Masutani, H. Nakamura, S. Miyajima, A. Yamauchi, S. Yonehara, A. Uchida, K. Irimajiri, A. Horiuchi, and J. Yodoi. 1991. Protective activity of adult T cell leukemia-derived factor (ADF) against tumor necrosis factor-dependent cytotoxicity on U937 cells. *J Immunol* 147:3837-3841.
225. Hotta, M., F. Tashiro, H. Ikegami, H. Niwa, T. Ogihara, J. Yodoi, and J. Miyazaki. 1998. Pancreatic beta cell-specific expression of thioredoxin, an antioxidative and antiapoptotic protein, prevents autoimmune and streptozotocin-induced diabetes. *J Exp Med* 188:1445-1451.
226. Graser, R., C. Mathews, E. Leiter, and D. Serreze. 1999. MHC characterization of ALR and ALS mice: respective similarities to the NOD and NON strains. *Immunogenetics* 49:722-726.
227. Mathews, C., and E. Leiter. 1999. Constitutive differences in antioxidant defense status distinguish alloxan-resistant and alloxan-susceptible mice. *Free Radic Biol Med* 27:449-455.
228. Mathews, C., W. Suarez-Pinzon, J. Baust, K. Strynadka, E. Leiter, and A. Rabinovitch. 2005. Mechanisms underlying resistance of pancreatic islets from ALR/Lt mice to cytokine-induced destruction. *J Immunol* 175:1248-1256.
229. Mathews, C., and E. Leiter. 1999. Resistance of ALR/Lt islets to free radical-mediated diabetogenic stress is inherited as a dominant trait. *Diabetes* 48:2189-2196.

230. Mathews, C., B. Dunn, M. Hannigan, C. Huang, and E. Leiter. 2002. Genetic control of neutrophil superoxide production in diabetes-resistant ALR/Lt mice. *Free Radic Biol Med* 32:744-751.
231. Kawasaki, E., N. Abiru, and K. Eguchi. 2004. Prevention of type 1 diabetes: from the view point of beta cell damage. *Diabetes Res Clin Pract* 66 Suppl 1:S27-32.
232. Mathews, C., R. Graser, A. Savinov, D. Serreze, and E. Leiter. 2001. Unusual resistance of ALR/Lt mouse beta cells to autoimmune destruction: role for beta cell-expressed resistance determinants. *Proc Natl Acad Sci U S A* 98:235-240.
233. Ino, T., Y. Kawamoto, K. Sato, K. Nishikawa, A. Yamada, K. Ishibashi, and F. Sekiguchi. 1991. Selection of mouse strains showing high and low incidences of alloxan-induced diabetes. *Jikken Dobutsu* 40:61-67.
234. Beauchamp, C., and I. Fridovich. 1971. Superoxide dismutase: improved assays and an assay applicable to acrylamide gels. *Anal Biochem* 44:276-287.
235. Gotoh, M., T. Maki, T. Kiyoizumi, S. Satomi, and A. Monaco. 1985. An improved method for isolation of mouse pancreatic islets. *Transplantation* 40:437-438.
236. Graser, R., T. DiLorenzo, F. Wang, G. Christianson, H. Chapman, D. Roopenian, S. Nathenson, and D. Serreze. 2000. Identification of a CD8 T cell that can independently mediate autoimmune diabetes development in the complete absence of CD4 T cell helper functions. *J Immunol* 164:3913-3918.
237. Chen, H., X. Li, and P. Epstein. 2005. MnSOD and catalase transgenes demonstrate that protection of islets from oxidative stress does not alter cytokine toxicity. *Diabetes* 54:1437-1446.
238. Li, X., H. Chen, and P. Epstein. 2006. Metallothionein and catalase sensitize to diabetes in nonobese diabetic mice: reactive oxygen species may have a protective role in pancreatic beta-cells. *Diabetes* 55:1592-1604.
239. Piganelli, J., T. Martin, and K. Haskins. 1998. Splenic macrophages from the NOD mouse are defective in the ability to present antigen. *Diabetes* 47:1212-1218.
240. Daley, J., A. Thomay, M. Connolly, J. Reichner, and J. Albina. 2008. Use of Ly6G-specific monoclonal antibody to deplete neutrophils in mice. *J Leukoc Biol* 83:64-70.
241. Szkudelski, T. 2001. The mechanism of alloxan and streptozotocin action in B cells of the rat pancreas. *Physiol Res* 50:537-546.
242. Morgan, D., H. Oliveira-Emilio, D. Keane, A. Hirata, M. Santos da Rocha, S. Bordin, R. Curi, P. Newsholme, and A. Carpinelli. 2007. Glucose, palmitate and pro-inflammatory cytokines modulate production and activity of a phagocyte-like NADPH oxidase in rat pancreatic islets and a clonal beta cell line. *Diabetologia* 50:359-369.
243. Newsholme, P., D. Morgan, E. Rebelato, H. Oliveira-Emilio, J. Procopio, R. Curi, and A. Carpinelli. 2009. Insights into the critical role of NADPH oxidase(s) in the normal and dysregulated pancreatic beta cell. *Diabetologia* 52:2489-2498.
244. Oliveira, H., R. Verlengia, C. Carvalho, L. Britto, R. Curi, and A. Carpinelli. 2003. Pancreatic beta-cells express phagocyte-like NAD(P)H oxidase. *Diabetes* 52:1457-1463.
245. Lee, K., M. Kim, K. Amano, C. Pak, M. Jaworski, J. Mehta, and J. Yoon. 1988. Preferential infiltration of macrophages during early stages of insulitis in diabetes-prone BB rats. *Diabetes* 37:1053-1058.
246. Lee, K., C. Pak, K. Amano, and J. Yoon. 1988. Prevention of lymphocytic thyroiditis and insulitis in diabetes-prone BB rats by the depletion of macrophages. *Diabetologia* 31:400-402.

247. Oschilewski, U., U. Kiesel, and H. Kolb. 1985. Administration of silica prevents diabetes in BB-rats. *Diabetes* 34:197-199.
248. Cantor, J., and K. Haskins. 2007. Recruitment and activation of macrophages by pathogenic CD4 T cells in type 1 diabetes: evidence for involvement of CCR8 and CCL1. *J Immunol* 179:5760-5767.
249. Nikolic, T., S. Geutskens, N. van Rooijen, H. Drexhage, and P. Leenen. 2005. Dendritic cells and macrophages are essential for the retention of lymphocytes in (peri)-insulitis of the nonobese diabetic mouse: a phagocyte depletion study. *Lab Invest* 85:487-501.
250. Hillebrands, J., N. van der Werf, F. Klatter, C. Bruggeman, and J. Rozing. 2003. Role of peritoneal macrophages in cytomegalovirus-induced acceleration of autoimmune diabetes in BB-rats. *Clin Dev Immunol* 10:133-139.
251. Hirasawa, K., S. Tsutsui, M. Takeda, M. Mizutani, S. Itagaki, and K. Doi. 1996. Depletion of Mac1-positive macrophages protects DBA/2 mice from encephalomyocarditis virus-induced myocarditis and diabetes. *J Gen Virol* 77 (Pt 4):737-741.
252. Hutchings, P., H. Rosen, L. O'Reilly, E. Simpson, S. Gordon, and A. Cooke. 1990. Transfer of diabetes in mice prevented by blockade of adhesion-promoting receptor on macrophages. *Nature* 348:639-642.
253. DiLorenzo, T., S. Lieberman, T. Takaki, S. Honda, H. Chapman, P. Santamaria, D. Serreze, and S. Nathenson. 2002. During the early prediabetic period in NOD mice, the pathogenic CD8(+) T-cell population comprises multiple antigenic specificities. *Clin Immunol* 105:332-341.
254. Oliveira-Marques, V., H. Marinho, L. Cyrne, and F. Antunes. 2009. Role of hydrogen peroxide in NF-kappaB activation: from inducer to modulator. *Antioxid Redox Signal* 11:2223-2243.
255. Katz, J., C. Benoist, and D. Mathis. 1995. T helper cell subsets in insulin-dependent diabetes. *Science* 268:1185-1188.
256. Tse, H., S. Josephy, E. Chan, D. Fouts, and A. Cooper. 2002. Activation of the mitogen-activated protein kinase signaling pathway is instrumental in determining the ability of Mycobacterium avium to grow in murine macrophages. *J Immunol* 168:825-833.
257. Snelgrove, R., L. Edwards, A. Rae, and T. Hussell. 2006. An absence of reactive oxygen species improves the resolution of lung influenza infection. *Eur J Immunol* 36:1364-1373.
258. Snelgrove, R., L. Edwards, A. Williams, A. Rae, and T. Hussell. 2006. In the absence of reactive oxygen species, T cells default to a Th1 phenotype and mediate protection against pulmonary Cryptococcus neoformans infection. *J Immunol* 177:5509-5516.
259. Hultqvist, M., and R. Holmdahl. 2005. Ncf1 (p47phox) polymorphism determines oxidative burst and the severity of arthritis in rats and mice. *Cell Immunol* 233:97-101.
260. Olofsson, P., and R. Holmdahl. 2003. Positional cloning of Ncf1--a piece in the puzzle of arthritis genetics. *Scand J Immunol* 58:155-164.
261. Langrish, C., Y. Chen, W. Blumenschein, J. Mattson, B. Basham, J. Sedgwick, T. McClanahan, R. Kastelein, and D. Cua. 2005. IL-23 drives a pathogenic T cell population that induces autoimmune inflammation. *J Exp Med* 201:233-240.
262. Martinon, F., X. Chen, A. Lee, and L. Glimcher. 2010. TLR activation of the transcription factor XBP1 regulates innate immune responses in macrophages. *Nat Immunol* 11:411-418.

263. Greve, B., L. Vijayakrishnan, A. Kubal, R. Sobel, L. Peterson, L. Wicker, and V. Kuchroo. 2004. The diabetes susceptibility locus Idd5.1 on mouse chromosome 1 regulates ICOS expression and modulates murine experimental autoimmune encephalomyelitis. *J Immunol* 173:157-163.
264. Ichikawa, M., C. Koh, A. Inoue, J. Tsuyusaki, M. Yamazaki, Y. Inaba, Y. Sekiguchi, M. Itoh, H. Yagita, and A. Komiyama. 2000. Anti-IL-12 antibody prevents the development and progression of multiple sclerosis-like relapsing--remitting demyelinating disease in NOD mice induced with myelin oligodendrocyte glycoprotein peptide. *J Neuroimmunol* 102:56-66.
265. Mathur, A., H. Chang, D. Zisoulis, G. Stritesky, Q. Yu, J. O'Malley, R. Kapur, D. Levy, G. Kansas, and M. Kaplan. 2007. Stat3 and Stat4 direct development of IL-17-secreting Th cells. *J Immunol* 178:4901-4907.
266. Yang, X., A. Panopoulos, R. Nurieva, S. Chang, D. Wang, S. Watowich, and C. Dong. 2007. STAT3 regulates cytokine-mediated generation of inflammatory helper T cells. *J Biol Chem* 282:9358-9363.
267. Torres, M., and H. Forman. 2003. Redox signaling and the MAP kinase pathways. *Biofactors* 17:287-296.
268. Curtsinger, J., C. Schmidt, A. Mondino, D. Lins, R. Kedl, M. Jenkins, and M. Mescher. 1999. Inflammatory cytokines provide a third signal for activation of naive CD4+ and CD8+ T cells. *J Immunol* 162:3256-3262.
269. Pape, K., A. Khoruts, A. Mondino, and M. Jenkins. 1997. Inflammatory cytokines enhance the in vivo clonal expansion and differentiation of antigen-activated CD4+ T cells. *J Immunol* 159:591-598.
270. Veldhoen, M., R. Hocking, C. Atkins, R. Locksley, and B. Stockinger. 2006. TGFbeta in the context of an inflammatory cytokine milieu supports de novo differentiation of IL-17-producing T cells. *Immunity* 24:179-189.
271. Zhou, L., J. Lopes, M. Chong, I. Ivanov, R. Min, G. Victora, Y. Shen, J. Du, Y. Rubtsov, A. Rudensky, S. Ziegler, and D. Littman. 2008. TGF-beta-induced Foxp3 inhibits T(H)17 cell differentiation by antagonizing RORgammat function. *Nature* 453:236-240.
272. Tzartos, J., M. Friese, M. Craner, J. Palace, J. Newcombe, M. Esiri, and L. Fugger. 2008. Interleukin-17 production in central nervous system-infiltrating T cells and glial cells is associated with active disease in multiple sclerosis. *Am J Pathol* 172:146-155.
273. Jäger, A., V. Dardalhon, R. Sobel, E. Bettelli, and V. Kuchroo. 2009. Th1, Th17, and Th9 effector cells induce experimental autoimmune encephalomyelitis with different pathological phenotypes. *J Immunol* 183:7169-7177.
274. Bäckdahl, L., J. Guo, M. Jagodic, K. Becanovic, B. Ding, T. Olsson, and J. Lorentzen. 2009. Definition of arthritis candidate risk genes by combining rat linkage-mapping results with human case-control association data. *Ann Rheum Dis* 68:1925-1932.
275. Dietlin, T., D. Cua, K. Burke, B. Lund, and R. van der Veen. 2009. Role of IL-23 in mobilization of immunoregulatory nitric oxide- or superoxide-producing Gr-1+ cells from bone marrow. *Free Radic Biol Med* 47:357-363.
276. Fossiez, F., O. Djossou, P. Chomarat, L. Flores-Romo, S. Ait-Yahia, C. Maat, J. Pin, P. Garrone, E. Garcia, S. Saeland, D. Blanchard, C. Gaillard, B. Das Mahapatra, E. Rouvier, P. Golstein, J. Banchereau, and S. Lebecque. 1996. T cell interleukin-17 induces stromal cells to produce proinflammatory and hematopoietic cytokines. *J Exp Med* 183:2593-2603.

277. Wuyts, W., B. Vanaudenaerde, L. Dupont, D. Van Raemdonck, M. Demedts, and G. Verleden. 2005. Interleukin-17--induced interleukin-8 release in human airway smooth muscle cells: role for mitogen-activated kinases and nuclear factor-kappaB. *J Heart Lung Transplant* 24:875-881.
278. Laan, M., Z. Cui, H. Hoshino, J. Lötvall, M. Sjöstrand, D. Gruenert, B. Skoogh, and A. Lindén. 1999. Neutrophil recruitment by human IL-17 via C-X-C chemokine release in the airways. *J Immunol* 162:2347-2352.
279. Liblau, R., S. Singer, and H. McDevitt. 1995. Th1 and Th2 CD4+ T cells in the pathogenesis of organ-specific autoimmune diseases. *Immunol Today* 16:34-38.
280. Serreze, D., and E. Leiter. 1988. Defective activation of T suppressor cell function in nonobese diabetic mice. Potential relation to cytokine deficiencies. *J Immunol* 140:3801-3807.
281. Koarada, S., Y. Wu, and W. Ridgway. 2001. Increased entry into the IFN-gamma effector pathway by CD4+ T cells selected by I-Ag7 on a nonobese diabetic versus C57BL/6 genetic background. *J Immunol* 167:1693-1702.
282. Knaus, U., P. Heyworth, T. Evans, J. Curnutte, and G. Bokoch. 1991. Regulation of phagocyte oxygen radical production by the GTP-binding protein Rac 2. *Science* 254:1512-1515.
283. Roberts, A., C. Kim, L. Zhen, J. Lowe, R. Kapur, B. Petryniak, A. Spaetti, J. Pollock, J. Borneo, G. Bradford, S. Atkinson, M. Dinauer, and D. Williams. 1999. Deficiency of the hematopoietic cell-specific Rho family GTPase Rac2 is characterized by abnormalities in neutrophil function and host defense. *Immunity* 10:183-196.
284. Li, B., H. Yu, W. Zheng, R. Voll, S. Na, A. Roberts, D. Williams, R. Davis, S. Ghosh, and R. Flavell. 2000. Role of the guanosine triphosphatase Rac2 in T helper 1 cell differentiation. *Science* 288:2219-2222.
285. Yu, H., D. Leitenberg, B. Li, and R. Flavell. 2001. Deficiency of small GTPase Rac2 affects T cell activation. *J Exp Med* 194:915-926.
286. Bending, D., H. De La Peña, M. Veldhoen, J. Phillips, C. Uyttenhove, B. Stockinger, and A. Cooke. 2009. Highly purified Th17 cells from BDC2.5NOD mice convert into Th1-like cells in NOD/SCID recipient mice. *J Clin Invest*.
287. Martin-Orozco, N., Y. Chung, S. Chang, Y. Wang, and C. Dong. 2009. Th17 cells promote pancreatic inflammation but only induce diabetes efficiently in lymphopenic hosts after conversion into Th1 cells. *Eur J Immunol* 39:216-224.
288. Wilson, C., E. Rowell, and M. Sekimata. 2009. Epigenetic control of T-helper-cell differentiation. *Nat Rev Immunol* 9:91-105.
289. Fridovich, I. 1986. Superoxide dismutases. *Adv Enzymol Relat Areas Mol Biol* 58:61-97.
290. Casareno, R., D. Waggoner, and J. Gitlin. 1998. The copper chaperone CCS directly interacts with copper/zinc superoxide dismutase. *J Biol Chem* 273:23625-23628.
291. Culotta, V., L. Klomp, J. Strain, R. Casareno, B. Krems, and J. Gitlin. 1997. The copper chaperone for superoxide dismutase. *J Biol Chem* 272:23469-23472.
292. Furukawa, Y., and T. O'Halloran. 2006. Posttranslational modifications in Cu,Zn-superoxide dismutase and mutations associated with amyotrophic lateral sclerosis. *Antioxid Redox Signal* 8:847-867.
293. Arnesano, F., L. Banci, I. Bertini, M. Martinelli, Y. Furukawa, and T. O'Halloran. 2004. The unusually stable quaternary structure of human Cu,Zn-superoxide dismutase 1 is controlled by both metal occupancy and disulfide status. *J Biol Chem* 279:47998-48003.

294. Ding, F., and N. Dokholyan. 2008. Dynamical roles of metal ions and the disulfide bond in Cu, Zn superoxide dismutase folding and aggregation. *Proc Natl Acad Sci U S A* 105:19696-19701.
295. Culotta, V., M. Yang, and T. O'Halloran. 2006. Activation of superoxide dismutases: putting the metal to the pedal. *Biochim Biophys Acta* 1763:747-758.
296. McCord, J., and I. Fridovich. 1969. Superoxide dismutase. An enzymic function for erythrocuprein (hemocuprein). *J Biol Chem* 244:6049-6055.
297. Harraz, M., J. Marden, W. Zhou, Y. Zhang, A. Williams, V. Sharov, K. Nelson, M. Luo, H. Paulson, C. Schöneich, and J. Engelhardt. 2008. SOD1 mutations disrupt redox-sensitive Rac regulation of NADPH oxidase in a familial ALS model. *J Clin Invest* 118:659-670.
298. Proescher, J., M. Son, J. Elliott, and V. Culotta. 2008. Biological effects of CCS in the absence of SOD1 enzyme activation: implications for disease in a mouse model for ALS. *Hum Mol Genet* 17:1728-1737.
299. Vonk, W., C. Wijmenga, R. Berger, B. van de Sluis, and L. Klomp. 2010. Cu,Zn superoxide dismutase maturation and activity are regulated by COMMD1. *J Biol Chem* 285:28991-29000.
300. Harrison, L., M. Dempsey-Collier, D. Kramer, and K. Takahashi. 1996. Aerosol insulin induces regulatory CD8 gamma delta T cells that prevent murine insulin-dependent diabetes. *J Exp Med* 184:2167-2174.
301. Zhang, Z., L. Davidson, G. Eisenbarth, and H. Weiner. 1991. Suppression of diabetes in nonobese diabetic mice by oral administration of porcine insulin. *Proc Natl Acad Sci U S A* 88:10252-10256.
302. Atkinson, M., N. Maclaren, and R. Luchetta. 1990. Insulitis and diabetes in NOD mice reduced by prophylactic insulin therapy. *Diabetes* 39:933-937.
303. Shoda, L., D. Young, S. Ramanujan, C. Whiting, M. Atkinson, J. Bluestone, G. Eisenbarth, D. Mathis, A. Rossini, S. Campbell, R. Kahn, and H. Kreuwel. 2005. A comprehensive review of interventions in the NOD mouse and implications for translation. *Immunity* 23:115-126.
304. Hayward, A., and M. Shreiber. 1989. Neonatal injection of CD3 antibody into nonobese diabetic mice reduces the incidence of insulitis and diabetes. *J Immunol* 143:1555-1559.
305. Chatenoud, L., E. Thervet, J. Primo, and J. Bach. 1992. [Remission of established disease in diabetic NOD mice induced by anti-CD3 monoclonal antibody]. *C R Acad Sci III* 315:225-228.
306. Chatenoud, L., E. Thervet, J. Primo, and J. Bach. 1994. Anti-CD3 antibody induces long-term remission of overt autoimmunity in nonobese diabetic mice. *Proc Natl Acad Sci U S A* 91:123-127.
307. Mottram, P., L. Murray-Segal, W. Han, J. Maguire, and A. Stein-Oakley. 2002. Remission and pancreas isograft survival in recent onset diabetic NOD mice after treatment with low-dose anti-CD3 monoclonal antibodies. *Transpl Immunol* 10:63-72.
308. Keymeulen, B., E. Vandemeulebroucke, A. Ziegler, C. Mathieu, L. Kaufman, G. Hale, F. Gorus, M. Goldman, M. Walter, S. Candon, L. Schandene, L. Crenier, C. De Block, J. Seigneurin, P. De Pauw, D. Pierard, I. Weets, P. Rebello, P. Bird, E. Berrie, M. Frewin, H. Waldmann, J. Bach, D. Pipeleers, and L. Chatenoud. 2005. Insulin needs after CD3-antibody therapy in new-onset type 1 diabetes. *N Engl J Med* 352:2598-2608.

309. Parker, M., S. Xue, J. Alexander, C. Wasserfall, M. Campbell-Thompson, M. Battaglia, S. Gregori, C. Mathews, S. Song, M. Troutt, S. Eisenbeis, J. Williams, D. Schatz, M. Haller, and M. Atkinson. 2009. Immune depletion with cellular mobilization imparts immunoregulation and reverses autoimmune diabetes in nonobese diabetic mice. *Diabetes* 58:2277-2284.